Analysis and Filtering of Time-Varying Signals

by

Marwan Bikdash

Thesis submitted to the Faculty of the

Virginia Polytechnic Institute and State University

in partial fulfillment of the requirements for the degree of

Master of Science

in

Electrical Engineering

APPROVED:

Kai-Bor Yu, Chairman

A. A. (Louis) Beex

Ioannis M. Besieris

June, 1988

Blacksburg, Virginia

Analysis and Filtering of Time-Varying Signals

by

Marwan Bikdash

Kai-Bor Yu, Chairman

Electrical Engineering

(ABSTRACT)

The characterization, analysis and filtering of a slowly time-varying (STV) deterministic signal are considered. A STV signal is characterized as a sophisticated signal whose windowed sections are elementary signals. Mixed time-frequency representations (MTFRs) such as the Wigner distribution (WD), the Pseudo-Wigner distribution (PWD), the Short-time Fourier transform (STFT) and the optimally smoothed Wigner distribution (OSWD) used in analyzing STV signals are analyzed and compared. The OSWD is shown to perform satisfactorily even if the signals are amplitude modulated. The OSWD is shown to yield the exact instantaneous frequency for STV signals having quadratic phase, and to have a minimal and meaningful Bandwidth (BW) that does not depend on the slope of the instantaneous frequency curve in the time-frequency plane, unlike the BW of the spectrogram. We also present some contributions to the ongoing debate addressing the issue of choosing the MTFR that is best suited to the analysis of STV signals. Using analytical and experimental results, the performances of the different MTFRs are compared, and the conditions under which a given MTFR performs better are considered.

The filtering of a signal from a noise-corrupted measurement, and the decomposition of a STV signal into its components in the presence of noise, are considered. These two related problems have been solved through masking the MTFRs of the measured signal. This approach has been successfully used in the case of the WD, PWD and the STFT. We propose extending the use of this approach to the OSWD. An equivalent time-domain implementation based on linear shift-variant (LSV) filters is derived and fully analyzed. It is based on the concept of local nonstationarity cancellation. The proposed filter is shown to have a superior performance when compared to the filter based on masking the STFT. The sensitivity of the

filter is studied. The filter ability to suppress white noise and to decompose a STV signal into its components is analyzed and illustrated.

Acknowledgements

My foremost gratitude goes to my advisor Dr. Kai-Bor Yu, for his guidance, patience and support. Sincere thanks are extended to the members of my committee, Dr. I.M. Besieris and Dr. A.A. Beex. A special acknowledgement is dedicated to my parents and brothers for their deep love and caring. I would also like to thank all my friends in Hillcrest for the good time we had together. Special thanks are due to two special friends, Raouf and Kathy Raouf, whose styles and personalities have been most inspiring.

Table of Contents

List of Illustrations

1.0 Introduction

A typical problem in signal processing consists of filtering a desired deterministic signal in the presence of noise or signal interference. In the case where the signals are time-invariant or stationary in nature, that is, when the spectral contents of the signals are invariant with time, the problem is typically solved in three steps: analysis of the signal spectral characteristics, specification of the filter characteristics, and finally, a practical implementation obtained through some approximation process. These steps are in general quite well understood [P2], [P1], [O2], [R1].

In the analysis step, the Fourier transform (FT) is used to characterize the spectral content of the signal. In the case where the signal is bandlimited, one possible characterization is in terms of the frequency region of support (ROS).

In the second step, the information obtained in the analysis is used to specify a filter that eliminates the undesired signals. Ideally, in the case where the desired and undesired signals have disjoint frequency supports, the desired signal is passed through the specified filter without any distortion. The specification is usually laid down in the frequency domain since such a specification is both mathematically tractable and physically meaningful. The specified ideal filter may not, however, be in a form that is practically implementable or even physically realizable.

In the implementation step, an easily implementable filter (e.g. digital nonrecursive filter) whose characteristics best approximate those of the specified filter is sought.

In many signal processing applications such as seismic data processing [B6], [B2], modeling of the vocal tract in a speech analysis and synthesis system, [P7], or in the analysis of weakly nonlinear systems with parameteric excitations [N1], the signals of interest are nonstationary or time-varying, in the sense that their spectral content varies considerably with time. In this case, the three-step procedure has to be modified to accommodate the time-varying signal characteristics.

Characterization of Slowly Time-Varying (STV) signals

The concept of time-varying deterministic signals is frequently introduced in conjunction with the concept of mixed time-frequency representation (MTFRs) of signals. A time-varying signal is a signal whose MTFR exhibits a "time-varying pattern" in the time-frequency plane [C1], [K1]. Claasen et al. [C4] defined a stationary deterministic signal as a signal that can be expressed as an infinite but countable sum of sinusoids. The signal is stationary in the sense that different windowed sections of the signal have similar spectral properties if the window is long enough. A sinusoidally frequency modulated (SFM) signal is stationary in this sense, although it is intuitively a time-varying signal.

Bouachache and Flandrin [B1] studied the manifolds of the WD of time-varying signals, and noted that if the time-bandwidth product (TBP) of the signal is large, the time-varying signals can be characterized by simple curves in the time-frequency plane. The TBP has a lower bound given by the uncertainty principle of signal analysis [P2]. Signals with large TBP are called sophisticated, and signals with a small TBP product are called elementary or simple [P2]. Bouachache and Flandrin [B1] argued that signals with large TBP can be written in the form $x(t) = a(t)e^{j\phi(t)}$ where $a(t)$ is a slowly varying envelope and $\phi(t)$ is a rapidly-varying phase.

Kodera et al. [K1] considered time-varying quasi-monochromatic signals whose amplitude and instantaneous frequency change slowly with time. They noted that the energy

of a monochromatic signal is concentrated along a slowly varying curve in the time-frequency plane. This curve can be estimated using the instantaneous frequency or the group delay of the signal. In this sense, a quasi-monochromatic signal is 'slowly time-varying'. Kodera et al. noted that if the TBP of the signal is large, then the instantaneous frequency and group delay of the signal are practically the same. They also argued that if the TBP is small (approximately equal to the TBP lower bound), then the notions of instantaneous frequency and group delay are not useful. The above discussion suggests that STV signals cannot have a small TBP. In Chapter 2, we elaborate on this concept; we also consider two classical examples of time-varying signals, the linear chirp signal (LCS) and the sinusoidally frequency modulated (SFM) signal, and show that these signals are sophisticated, i.e., have a large TBP. We also show that windowed sections of these signals have a reduced BW and hence a reduced TBP.

Analysis of STV signals

An extension of the Fourier analysis techniques to time-varying signals is mixed time-frequency representations (MTFRs) of signals. MTFRs have received a lot of attention in recent years; examples include the Wigner distribution (WD) [C1], [C2], [C3], the short-time Fourier transform (STFT) [P8], [R1], and their modifications, such as the modified STFT [K2], [K1], the optimally smoothed WD (OSWD) [A1], and others [C3].

MTFRs can be classified into two categories. The first is based on a 'short-time' approach such as the STFT. Using short duration windows, the time-varying signal is divided into a series of overlapping windowed signals which are approximately elementary (having a small TBP). This approach is quite simple to implement, but is known to suffer from a basic problem concerning the time duration of the analysis window and resulting in an unavoidable tradeoff between time and frequency resolutions: short duration windows tend to conserve the time-varying character of the signal but cannot provide frequency representations with high resolution, while long-duration windows tend to average the time-varying character of a signal.

The second category includes global representations such as the Ambiguity function, the WD and the Rihaczeck function [C3]. These global MTFRs do not suffer from the stationarity versus frequency resolution tradeoff inherent in the short-time approach. However, they suffer from several other drawbacks, such as computational complexity and presence of negatively-valued cross-terms. Moreover, Global MTFRs tend to represent multicomponent signals with complicated patterns. Although these MTFRs are more difficult to use in practice, they possess many interesting properties, and hence, are useful as analytical tools.

A hybrid approach is frequently adopted. It attempts to conserve as much as possible of the properties of the global MTFRs, while maintaining a reasonable computational complexity and a simple representation of multicomponent signals. The PWD and the OSWD are two examples of hybrid MTFRs which can be thought of as smoothed versions of the WD. The PWD can be obtained from the WD via a smoothing operation in the frequency direction [C1], [C2]. The OSWD [A1] can be obtained from the WD via a two-dimensional smoothing in both time and frequency directions.

The OSWD was recently proposed in [A1]. It was required to be positive, and to have the sharpest (minimum bandwidth) representation of the constant envelope signal $x(t) = e^{j\phi(t)}$ whose phase $\phi(t)$ is locally quadratic. It was shown [A1] that the OSWD can be computed as a spectrogram using an analysis window that is signal-dependent, complex and highly oscillatory. This is in contrast with the spectrogram analysis windows conventionally used, which are real, positive, symmetric and low-pass, such as the Hamming or the Gaussian window. In fact, the OSWD analysis window proposed in [A1] is obtained from a conventional window via a quadratic phase modulation. The fact that the OSWD is a spectrogram computed with a particular though unconventional window poses the following question: does the OSWD have all the properties of the spectrogram? If not, then which of the properties of the spectrogram do not hold? In particular, does the OSWD suffer from the frequency vs. time resolution tradeoff problem? Can the OSWD yield the instantaneous frequency correctly? These questions will be addressed in Section 3.5.2.1.

In Section 3.5.2.2. and 3.5.3., we study the BW of the OSWD and compare it to that of the spectrogram. We attempt to show that the OSWD gives a more meaningful time-varying BW, with possible application in the filtering of a time-varying signal. A useful description of such a signal is given in terms of the region of support (ROS) of one of its MTFRs. Huang and Aggarwal [H3] have shown that knowledge of the ROS of the spectrogram of a desired signal can be used to design a linear shift-variant (LSV) filter capable of isolating the desired signal and suppressing the corrupting noise. The ROS can be described in terms of the instantaneous frequency of the signal and its time-varying BW. Unfortunately, when the observed or measured signal is composed of many components and is corrupted with noise, the problem of identifying the ROS of each component becomes difficult. This is due to the fact that the ROS of the different components may overlap [G2].

To illustrate the properties of the different MTFRs, we study the MTFR of two time-varying signals, the LCS and the SFM signal. The expressions of the WD and the PWD of the LCS were derived in [C1]. The spectrogram and the OSWD were derived in [K1] and [A1] respectively. In these papers, the WD, the PWD and the spectrogram were compared. The comparison favored the WD and the PWD. No comparison to the OSWD is available. In Section 3.6, we rederive expressions of the MTFRs of the LCS, and write them in a way that allows easy comparison. A more general example, namely the SFM signal, is also considered. The ROS of the different MTFRs are then studied and compared.

In Section 3.7, we conduct a comparative study designed to answer the following question: Which MTFR can characterize the ROS of the different signal components more successfully? Several issues should be considered. These include frequency resolution, time resolution, the ability to accurately estimate the instantaneous frequency and BW of a single component, positivity, the ease with which patterns can be recognized in the time-frequency plane, computational complexity and storage requirements. Some of these issues have been addressed in [C3], [K1], [G2] and [B1], but no decisive conclusion has been reached, especially in the context of decomposing a STV signal into its components. We pay special

attention to the effect of changing the length of the analysis window of the PWD, the spectrogram and the OSWD.

Filtering of STV signals

Filtering of the desired signal components can be carried out in the time-frequency plane. The MTFR of the measured signal is multiplied by a masking function in order to isolate the MTFR of the desired signal component. The masking function is usually defined using the ROS of the MTFR of the desired signal. A synthesis procedure is then applied to the modified MTFR to obtain the desired signal. The modified MTFR is usually not a valid one and a projection into the space of valid MTFRs is required [S1]. The masking function approach depends heavily on which MTFR is used and on the way the masking function is defined. In [B5] and [Y1], this approach is applied to the WD and the PWD, while in [H3] it was applied to the STFT. Due to the existence of cross-terms, application of the masking function approach to the WD or the PWD is usually difficult or unsatisfactory, especially if the measured signal is multicomponent. Application of this approach to the STFT is easier, but can be difficult or unsatisfactory when the BW of the spectrogram of one signal component is excessively large, or when the ROS of the different signal components overlap.

The above approach admits an alternative formulation in the time-domain. The procedure consists of using the time-varying parameters such as the instantaneous frequency and the instantaneous bandwidth to directly specify and design a digital linear shift-variant (LSV) filter. The filter can be specified in the form of its shift-variant impulse response, or in the form of its shift-variant system response (consisting of samples of Green's function) [P8]. The filter can also be specified in terms of the corresponding Generalized frequency functions [H3], [Z1]. Clarke [C5], determined the impulse response of a LSV filter in the time domain, using the autocorrelations and crosscorrelation of the signal and the noise. Huang and Aggarwal [H3] showed that the filter based on masking the STFT can be equivalently implemented in the time-domain, by convolving the input signal with the filter impulse response. They noted however that this implementation can be computationally inefficient.

Consequently, a more efficient implementation based on interpolation was derived [H3]. Huang and Aggarwal [H4] showed that if the system response has a degenerate form, the LSV filter can be implemented very efficiently as a shift-variant difference equation. The above result was generalized to the nondegenerate case by applying a singular value decomposition to an arbitrary system response [H1]. Huang and Aggarwal [H2], compared the filter proposed by Clarke [C5], to LSV filters specified in the frequency domain, specifically to the STFT masking filters. They found that the latter are easier to implement, and are more efficient computationally. They also showed that, if the time-varying signal is corrupted with noise, a time-varying Wiener filter can be specified, based on a short-time spectrum of the signal. Further improvements in the efficiency and storage requirements of LSV filters have been discussed in [P5], [P4] and [O1].

In this thesis, we apply the masking function filtering approach to the optimal STFT (OSTFT), the STFT obtained using the analysis window of the OSWD. This filtering operation is expected to be superior to the filtering approach based on masking the spectrogram, because the BW of the OSWD is often much smaller than that of the spectrogram. As is illustrated in Chapter 3, the ROS of the spectrograms of two signals can be overlapping, while the ROS of the correspondsing OSWDs are not. The specification and analysis of this filtering operation is the main theme of Chapter 4, in which the proposed filter is derived and studied in the time-domain. The proposed filter is based on local nonstationarity cancellation (LNC); i.e., the filter attempts to locally cancel the time-varying character of the signal, hence reducing the LSV filtering problem to a sequence of local linear shift-invariant (LSI) filtering problems. The effect of using erroneous estimates of the instantaneous frequency and its derivative is studied. The conditions under which two signal components can be separated without errors are also considered.

Overview of the thesis

In Chapter 2, a review of some basic concepts such as modulation theory and the theory of sophisticated signals is included. A characterization of STV signals is attempted in terms

of the time-bandwidth products of the signal and of its windowed sections. Linear chirp signals and sinusoidally frequency modulated signals are considered as examples.

In Chapter 3, several MTFRs are studied. Some new properties of the OSWD are shown. The WD, PWD, STFT and OSWD of the LCS and SFM signal are then computed and compared. Several issues about the usefulness of the different MTFRs are addressed and illustrated. Conclusions are drawn.

In Chapter 4, LSV filters are defined and studied. The conventional approach to specifying a LSV filter based on the ROS of the STFT is shown. The modified approach based on LNC is then derived both as a special case of the general masking function approach and independently. The proposed filter is analyzed; its robustness and its performance in suppressing random noise and separating different signal components are analyzed and illustrated.

2.0 Slowly time-varying signals

This chapter reviews some basic concepts in signal analysis that will prove to be useful in the subsequent discussions. These include amplitude and frequency modulated signals, instantaneous frequency, BandWidth (BW), and the Uncertainty Principle. This chapter also considers slowly time-varying (STV) signals and the effect of windowing on such signals. Two examples of STV signals, the linear chirp (LC) signal and the sinusoidally frequency modulated signal, are studied in detail. These signals are shown to have a large time-bandwidth product (TBP), while their windowed sections have a small TBP.

2.1 *Bandwidth, duration and the Uncertainty Principle*

2.1.1 Bandwidth of a lowpass signal

The BandWidth (BW) of a signal is a measure of the width of the frequency support of its FT. Unless otherwise indicated, we associate the BW of a signal with its support over the positive frequencies only.

The root mean square (RMS) bandwidth is defined as

$$RMS \quad B_a = \left[\frac{\frac{1}{2\pi}\int_0^\infty \omega^2 |A(\omega)|^2 d\omega}{\frac{1}{2\pi}\int_0^\infty |A(\omega)|^2 d\omega} \right]^{1/2} \tag{2.1.1}$$

If the signal $a(t)$ is real, then $|A(\omega)| = |A(-\omega)|$, and the same value for the RMS BW is obtained if one substitutes $\int_{-\infty}^{\infty}$ for $\int_0^\infty$ in the above equation.

An alternative and more practical characterization of BW is the p-percent BW B^p satisfying

$$\frac{1}{2\pi}\int_0^{B^p} |A(\omega)|^2 d\omega = p \ \frac{1}{2\pi}\int_0^\infty |A(\omega)|^2 d\omega \tag{2.1.2}$$

where $0 \leq p \leq 1$. For $p = 0.95$, 95 percent of the total signal energy is located in the frequency interval $(-B^p, B^p)$. The p-percent BW gives a flexible and practical description of the signal BW.

2.1.2 Bandwidth of bandpass signals

The above definitions can be easily extended to the case of bandpass signals. Consider the real bandpass signal $x(t)$ derived from the lowpass signal $a(t)$ via the transformation

$$x(t) = a(t)\cos(\omega_0 t + \phi_0) \quad , \quad \omega_0 > B_a \tag{2.1.3}$$

Clearly,

$$B_x = 2B_a \tag{2.1.4}$$

The modulation of $a(t)$ by a constant frequency carrier does not change the BW of the lowpass signal $a(t)$ except by a factor of 2. The RMS BW is defined for a bandpass signal as

$$RMS \quad B_a = \left[\frac{\frac{1}{2\pi}\int_0^\infty (\omega - \omega_0)^2 |X(\omega)|^2 d\omega}{\frac{1}{2\pi}\int_0^\infty |X(\omega)|^2 d\omega} \right]^{1/2} \tag{2.1.5}$$

The p-percent bandwidth B^p is now defined as

$$\frac{1}{2\pi}\int_{\omega_0 - B^p/2}^{\omega_0 + B^p/2} |X(\omega)|^2 d\omega = p\,\frac{1}{2\pi}\int_0^\infty |X(\omega)|^2 d\omega \tag{2.1.6}$$

Not all bandpass signals are given by Eq. (2.1.3). In general, one needs to calculate the BW of the bandpass signal around a "center" frequency ω_0. The center frequency ω_0 can be taken to be that frequency that minimizes the bandwidth given in Eq. (2.1.5) or in Eq. (2.1.6). In this sense, the center frequency gives the frequency around which most of the energy of the signal is concentrated. If the RMS definition is used, the center frequency is given by

$$\omega_0 = \left[\frac{\frac{1}{2\pi}\int_0^\infty \omega |X(\omega)|^2 d\omega}{\frac{1}{2\pi}\int_0^\infty |X(\omega)|^2 d\omega} \right]^{1/2} \tag{2.1.7}$$

2.1.3 Duration

The duration of the signal is a measure of the time support of the signal. Duration is the time-domain dual of the frequency-domain BW. Hence, arguments parallel to those used in the previous sections can be used. Of special interest is the RMS duration given by

$$T_x^2 = \frac{\int_{-\infty}^\infty (t - t_0)^2 |x(t)|^2 dt}{\int_{-\infty}^\infty |x(t)|^2 dt} \tag{2.1.8}$$

where t_0 is the "center" time of the signal,

$$t_0 = \frac{\int_{-\infty}^\infty t |x(t)|^2 dt}{\int_{-\infty}^\infty |x(t)|^2 dt} \tag{2.1.9}$$

A p-percent duration is defined as the time interval over which p-percent of the signal energy is located.

2.1.4 Uncertainty Principle

The duration and BW of a signal are inversely related. For example, very short signals have a large BW, and vice versa. An important figure describing a signal $x(t)$ is its time-bandwidth product (TBP) defined as

$$\Pi_x = T_x B_x \tag{2.1.10}$$

where T_x and B_x represent the duration and BW of $x(t)$ respectively. An important result known as the Uncertainty Principle [P2] gives a lower bound on the RMS value of the TBP.

Theorem Consider an energy signal $x(t)$ whose RMS duration and BW are given by T_x and B_x as defined in Eq. (2.1.8) and (2.1.5) with $t_0 = 0$. If the signal satisfies the relation $\sqrt{t}\,x(t) \to 0$ as $|t| \to \infty$, then

$$\Pi_x = T_x B_x \geq \frac{1}{2} \tag{2.1.11}$$

The equality holds only if the signal is Gaussian; i.e., $x(t) = e^{-\zeta t^2}$. The proof can be found in [P2].

This principle shows that signals cannot be time-limited and band-limited simultaneously. In short-time analysis, this fact manifests itself as a tradeoff between frequency resolution and time resolution. If $x(t)$ represents a window of duration T then its BW, and hence its frequency resolution, is at least of the order of $\frac{1}{T}$. To achieve a desirable frequency resolution δ_f, one must use a window of total length $2T_{min}$ where

$$T_{min} > \frac{1}{\delta_f} \tag{2.1.12}$$

2.1.4.1 *Elementary and sophisticated signals*

Signals having a RMS TBP close to $\frac{1}{2}$ are called *elementary signals* [P2]. Although a lower bound exists for the TBP, no upper bound exists. Signals with arbitrarily large TBP can be found or constructed [P2]. Such signals are called *sophisticated signals* [P2].

2.2 *Amplitude and frequency modulation*

Amplitude and frequency modulation are useful concepts in the field of communication systems. These phenomena have been observed in many physical systems. It has been argued that many biological systems use frequency modulation to encode information [M1]. This section reviews some of the concepts of modulation theory. These will be used later to qualitatively describe some aspects of time-varying signals.

2.2.1 Amplitude modulated signals

Consider a real lowpass signal $a(t)$ bandlimited to B_a. It can represent the impulse response of a lowpass filter. Since a(t) is real, the FT $A(\omega)$ of a(t) possesses conjugate symmetry about $\omega = 0$; i.e., $A^*(-\omega) = A(\omega)$. Form the signal

$$\tilde{x}(t) = a(t)e^{j\omega_0 t + j\phi_0} \tag{2.2.1}$$

where ω_0 and ϕ_0 are constants, and $\omega_0 > B_a$. The FT of the signal $\tilde{x}(t)$ is given by

$$\tilde{X}(\omega) = \left|\tilde{X}(\omega)\right| e^{j\Phi(\omega)} = A(\omega - \omega_0)e^{j\phi_0} \tag{2.2.2}$$

The signal $x(t) = Re\,\tilde{x}(t) = a(t)\cos(\omega_0 t + \phi_0)$ consists of an amplitude modulated (AM) signal [S3], where the carrier $\cos\omega_0 t$ is amplitude modulated by the information carrying signal $a(t)$. Its Bandwidth (BW) is unchanged except for a factor of 2. AM signals can be demodulated using coherent demodulation or envelope detection to yield the signal $a(t)$ [S3].

2.2.1.1 *Effect of amplitude modulation on bandwidth*

Consider the modulated signal $x(t) = a(t)m(t)$. It is of interest to determine the relationship between the BW of $x(t)$ and the BWs of $a(t)$ and $m(t)$. The FT $X(\omega)$ of $x(t)$ is given by the convolution integral

$$X(\omega) = \frac{1}{2\pi}\int_{-\infty}^{\infty} A(\eta)M(\omega - \eta)d\eta \tag{2.2.3}$$

where $A(\omega)$ and $M(\omega)$ represent the FTs of $a(t)$ and $m(t)$ respectively. In fact, $X(\omega)$ can be thought of as a smoothed version of $M(\omega)$ with $A(\omega)$ as the smoothing function.

Let $A(\omega)$ represent the FT of a lowpass window $a(t)$, and let B_a denote its BW. Moreover, assume that $A(\omega)$ is also a lowpass function. The Gaussian window $w(t) = e^{-\zeta t^2}$ is a good example. Let $M(\omega)$ denote the FT of $m(t)$, B_m its BW, and $\hat{B}_m$ its frequency support; i.e., assume that $M(\omega)$ is zero outside the interval $[\omega_1, \omega_2]$. Then, $\hat{B}_m = \omega_2 - \omega_1$. Note that $B_m \leq \hat{B}_m$. The frequency support is equal to the 100-percent BW of the signal.

We shall use the following heuristic reasoning to approximate the BW of the signal $x(t)$. Two cases are to be distinguished.

Case 1 The function $M(\omega)$ is a smooth lowpass function, and B_a and B_m are comparable. Given Eq. (2.2.3), the frequency support of $x(t)$ is approximated by the interval $[\omega_1 - B_a, \omega_2 + B_a]$. In this case, $X(\omega)$ is expected to be a lowpass signal, and its support is a good indication of the BW of $x(t)$. Hence, $B_x \simeq 2B_a + \hat{B}_m$. In this case, amplitude modulation results in an increase of BW.

Case 2. The function $M(\omega)$ is oscillatory or highpass, and $B_m \gg B_a$, i.e., the support of $M(\omega)$ is much larger than the support of $A(\omega)$. The support of $X(\omega)$ can still be approximated by $\hat{B}_m + 2B_a$, as can be seen from Eq. (2.2.3). In this case, however, the support of $X(\omega)$ is not a good indication of the BW of $x(t)$, and could be much larger. This is true because $A(\omega)$ is a lowpass function and $M(\omega)$ is a highpass function, and hence, $X(\omega)$ given by their convolution in Eq. (2.2.3) can be zero or negligibly small over any portion of its support. (Indeed, it can be identically zero in some ideal cases). In this case, amplitude modulation results in a decrease of BW.[1] Section 2.3.2 gives an example where amplitude modulation resulted in a decrease of BW, and of the TBP.[2]

In all cases, $B_x \leq B_m + B_a$. The equality holds approximately if $a(t)$ and $m(t)$ have comparable BWs. Since we are interested in designing filters with the narrowest possible filter, (see Chapter 4), the upper bound of B_x corresponds to the "worst case". Use the notation

$$B_x \tilde{<} B_a + B_m \tag{2.2.4}$$

to stress the fact that we are interested in the upper bound of B_x.

2.2.2 Frequency modulated signals

Consider the frequency modulated (FM) signal $x(t) = e^{j\phi(t)}$. Assume that the phase $\phi(t)$ is such that its derivative, $\Omega(t) = \dfrac{d\phi(t)}{dt}$, is a lowpass signal bandlimited to B_Ω. In the context of communication systems [S3], $\Omega(t)$ is known as the instantaneous frequency. It satisfies

---

[1] A more rigorous analysis can be done using the method of stationary phase. See [N1], section 3.4, and [P2].

[2] A simpler example is the following. Assume $M(\omega) = \cos \pi\omega^2$ consisting of a fat main lobe of unity width, and of ever narrower side lobes. It also has an infinite frequency support. Let $A(\omega) = e^{-\omega^2}$. Convolving these two functions together, the side lobes of $M(\omega)$ far from the origin will be averaged to zero. Only the main lobe and few surrounding side lobes will contribute to $X(\omega)$ significantly. The BW of $x(t)$ is finite and is of the order of unity.

$$0 < \omega_{min} \leq \Omega(t) = \omega_0 + \kappa\theta'_1(t) \leq \omega_{max} \tag{2.2.5}$$

where ω_0 is the carrier frequency, κ is a positive constant, and the information carrying signal $\theta'_1(t)$ is a modulating signal having a zero dc component. The instantaneous frequency can be equivalently written as

$$\Omega(t) = \omega_{min} + \kappa\theta'(t) \tag{2.2.6}$$

where $\theta'(t) = \theta'_1(t) + \frac{\omega_0 - \omega_{min}}{\kappa}$ is a properly biased version of $\theta'_1(t)$ such that $\theta'(t) > 0$.

The BW of an FM signal can be generally approximated using Carson's rule [S3] by

$$B_x \simeq 2(B_\Omega + \Delta\omega) \tag{2.2.7}$$

where $\Delta\omega = \frac{\omega_{max} - \omega_{min}}{2}$. Note that $2\Delta\omega$ represents the range of frequency swept by the instantaneous frequency over the duration of the signal. Define the modulation index

$$\beta = \frac{\Delta\omega}{B_\Omega} \tag{2.2.8}$$

representing the ratio of the frequency range swept by the instantaneous frequency to B_Ω, the BW of the information carrying signal. The parameters β and $\Delta\omega$ are directly proportional to the scaling factor κ, which can be set by the communication system designer. If κ is small enough so that $\beta < 1$, x(t) is said to be a narrow band FM (NBFM) signal. If κ is chosen such that $\beta > 1$, x(t) is said to be a wide band FM (WBFM) signal. In this case, the BW of the instantaneous frequency, B_Ω, is smaller than $\Delta\omega$.

2.2.2.1 *Instantaneous frequency*

The instantaneous frequency is formally defined in terms of a complex signal $x(t) = a(t)e^{j\phi(t)}$ as

$$\Omega_x(t) = \frac{d\phi(t)}{dt} \tag{2.2.9}$$

If this definition is applied directly to a real signal of the form $x(t) = \rho(t)\cos(\omega_0 t)e^{j\phi(t)}$ with $\phi(t) = 0$, a zero instantaneous frequency will always result, even if ω_0 is sufficiently large. The correct interpretation requires the use of the analytic version of the real signal.

The formal definition does not hold when a discrete-time signal is under consideration unless the differentiation is replaced by a difference operation. Moreover, the formal definition does not give a meaningful result when the signal is composed of many components. Consider, for example, the signal

$$\tilde{x}(t) = e^{j\phi_1(t)} + e^{j\phi_2(t)} \tag{2.2.10}$$

where both signal components $e^{j\phi_1(t)}$ and $e^{j\phi_2(t)}$ are FM signals for which the instantaneous frequency has a well-established meaning. This multicomponent signal can be expressed in the polar form $a(t)e^{j\phi(t)}$. Applying the formal definition in Eq. (2.2.9) to the signal in Eq. (2.2.10) yields values that are not meaningful.

Several methods of finding the instantaneous frequency have been reported in the literature. Standard FM demodulation techniques (based on hard limiters, discriminators, or phase lock loops) can be used to compute the instantaneous frequency of a monocomponent signal having a constant envelope [S3]. Alternative techniques are also available, such as the adaptive instantaneous frequency estimator proposed by Griffith [G3]. This method works for multicomponent signals too.

Several physical interpretations of the instantaneous frequency have been proposed. Those interpretations can be used to easily modify the definition of the instantaneous frequency, or the procedures to compute it, in order to accommodate discrete-time and multicomponent signals.

First interpretation : Papoulis [P2] gave the following physical interpretation for the instantaneous frequency. Consider the real signal $x(t) = a(t)\cos(\phi(t))$, where $\phi(t)$ is monotone increasing. To every time t associate an interval t_1 such that $\phi(t + t_1) = \phi(t) + 2\pi$. If in the interval $[t, t + t_1]$, the signal a(t) and the slope of the phase term $\Omega_x(t) = \dfrac{d\phi(t)}{dt}$ have negligible variations, then

$$a(t+\tau) \simeq a(t)\ , \quad \Omega_x(t+\tau) \simeq \Omega_x(t)\ , \quad \phi(t+\tau) \simeq \phi(t) + \Omega_x(t)\tau \qquad 0 \le \tau \le t_1 \tag{2.2.11}$$

In this case, the signal $x(t + \tau)$ is approximately a sine wave in the variable τ, with $\Omega_x(t)$ as its frequency :

$$x(t+\tau) \simeq a(t)\cos(\Omega_x(t)\tau + \phi(t)) \qquad 0 \le \tau \le t_1 \tag{2.2.12}$$

The conditions in Eq. (2.2.11) state that over the duration t_1 , the instantaneous frequency $\Omega_x(t)$ is approximately constant. It is reasonable to assume that there exists a duration $T \ge t_1$ over which the instantaneous frequency $\Omega(t + \tau)$ is linear in τ,

$$\Omega_x(t+\tau) \simeq \Omega_x(t) + \frac{d\Omega_x(t)}{dt}\tau\ , \qquad \tau < T. \tag{2.2.13}$$

Consider the multicomponent signal $\tilde{x}(t)$ defined in Eq. (2.2.10). Its real part is given by $x(t) = Re\,\tilde{x}(t) = \cos\phi_1(t) + \cos\phi_2(t)$. Define the times t_1 and t_2 such that $\phi_1(t + t_1) = \phi(t) + 2\pi$, and $\phi_2(t + t_2) = \phi_2(t) + 2\pi$. Then

$$x(t+\tau) \simeq \cos(\Omega_1(t)\tau + \phi_1(t)) + \cos(\Omega_2(t)\tau + \phi_2(t)) \tag{2.2.14}$$

for $\tau < \min(t_1, t_2)$. Hence, for a two-component signal, a pair of instantaneous frequencies $(\Omega_1(t), \Omega_2(t))$ can be assigned such that the above equation holds.

Second interpretation : Kodera et al. [K1] gave another physical interpretation of the instantaneous frequency based on the windowed signal

$$\tilde{x}_t(\tau) = w_{2T}(t-\tau)\tilde{x}(\tau) \tag{2.2.15}$$

obtained by windowing the analytic signal $\tilde{x}(\tau)$ by a window centered at t and of duration $2T$. The FT $\tilde{X}_t(\omega)$ of the windowed signal $\tilde{x}_t(\tau)$ is known as the Short Time Fourier Transform (STFT) of $\tilde{x}(t)$, and is given by

$$S_x(t,\omega) = \tilde{X}_t(\omega) = \int_{-\infty}^{\infty} \tilde{x}_t(\tau)e^{-j\omega\tau}d\tau \tag{2.2.16}$$

Its magnitude squared is known as the spectrogram.

The instantaneous frequency of the signal $x(t)$, at time t, is approximated by the center frequency of the windowed signal $\tilde{x}_t(\tau)$. Define the frequency $\overline{\Omega}(t)$ that minimizes the integral

$$\frac{1}{2\pi}\int_0^{\infty} (\omega - \overline{\Omega}(t))^2 |\tilde{X}_t(\omega)|^2 d\omega \tag{2.2.17}$$

If the window $w(\tau)$ is real, then $\tilde{x}_t(\tau) = a_0(\tau)e^{j\phi(\tau)}$, where $a_0(\tau) = w_{2T}(t-\tau)a(\tau)$ is the windowed amplitude. The solution of the minimization problem is given by

$$\overline{\Omega}(t) = \frac{\frac{1}{2\pi}\int_0^{\infty} \omega |\tilde{X}_t(\omega)|^2 d\omega}{\frac{1}{2\pi}\int_0^{\infty} |\tilde{X}_t(\omega)|^2 d\omega} \tag{2.2.18}$$

The quantity $\overline{\Omega}(t)$ denotes the normalized average frequency (NAF) of the spectrogram. At each time, the NAF gives the frequency around which most of the energy of the windowed signal is concentrated. It can be shown [K1], [C3] that $\overline{\Omega}(t)$ equals

$$\overline{\Omega}(t) = \frac{\int_0^{\infty} |w_{2T}(t-\tau)a(\tau)|^2 \Omega(\tau) dt}{\int_0^{\infty} |w_{2T}(t-\tau)a(\tau)|^2 dt} \tag{2.2.19}$$

and is a weighted average of the actual instantaneous frequency with the amplitude of the windowed signal as a weighting function [C3].

To recover the exact instantaneous frequency, the window duration should be made short enough so that $a(\tau)$ and $\Omega(\tau)$ have negligible variations in the interval $(t-T, t+T)$. Hence, as $T \to 0$, the NAF tends to the instantaneous frequency; i.e.,

$$\overline{\Omega}(t) \to \Omega(t) \quad as \quad T \to 0 \tag{2.2.20}$$

Multicomponent signals

Consider a multicomponent signal $x(t)$ composed of two components $x_1(t)$ and $x_2(t)$. Form the windowed signal $x_t(\tau) = x_{1t}(\tau) + x_{2t}(\tau)$. If the FTs of the signals $x_{1t}(\tau)$ and $x_{2t}(\tau)$ have disjoint frequency supports, then the instantaneous frequency of each signal component can be defined separately. Specifically, assume that $X_{1t}(\omega)$ is non-zero for $\omega \in [\omega_1, \omega_2]$, while $X_{2t}(\omega)$ is zero in that interval. In this case, the NAF of $x_1(t)$ defined as

$$\overline{\Omega}_1(t) = \frac{\frac{1}{2\pi}\int_{\omega_1}^{\omega_2} \omega |X_{1t}(\omega)|^2 d\omega}{\frac{1}{2\pi}\int_{\omega_1}^{\omega_2} |X_{1t}(\omega)|^2 d\omega} \tag{2.2.21}$$

is an approximation to the instantaneous frequency of $x_1(t)$.

2.3 *Slowly time-varying signals*

Time varying signals are defined as signals whose Mixed Time-Frequency Representations (MTFRs) exhibit a "time-varying pattern" in the time-frequency plane [C1], [K1]. Claasen et al. [C4] defined a stationary deterministic signal as a signal expressible as an infinite but countable sum of sinusoids. The signal is stationary in the sense that different windowed sections of the signal have similar spectral properties if the window is *long* enough. A sinusoidally frequency modulated signal [S3] would be stationary in this sense [S3], although it is intuitively a time-varying signal. In this thesis, we are interested in signals which are time-varying in the sense that different windowed sections of the signal have considerably different spectral properties provided that the window is *short* enough. Therefore, the definition in [C4] shall not be considered further.

Bouachache and Flandrin [B1] argued that signals with large TBP can be written in the form $x(t) = a(t)e^{j\phi(t)}$ where $a(t)$ is a slowly varying envelope and $\phi(t)$ is a fast varying phase.

Kodera et al. [K1] considered time-varying signals that can be described as quasi-monochromatic; i.e., signals whose amplitude and instantaneous frequency are slowly changing with time, and whose energy is concentrated along a curve in the time-frequency plane. This curve can be approximated using the instantaneous frequency or the group delay of the signal. Kodera et al. also noted that if the TBP of the signal is large, then the instantaneous frequency and group delay of the signal are practically the same. However, if the TBP is small (approximately equal to its lower bound), then the notions of instantaneous frequency and group delay are irrelevant.

Since the instantaneous frequency is assumed to be slowly varying, we shall denote these signals as slowly time-varying (STV) signals. The instantaneous frequency is slowly varying in the sense that it is a lowpass signal bandlimited to B_Ω, where B_Ω is much less than the BW of the signal.

The above discussion suggests that time-varying signals cannot have a small TBP, and that the TBP of a signal is important in determining its time-varying nature. Following, we consider two classical examples of time-varying signals, the linear chirp signal and the sinusoidally frequency modulated signal. We show that these signals are sophisticated; i.e., they have a large TBP. We also show that windowed sections of these signals have a reduced BW and TBP; in fact, the windowed sections can be made almost elementary with the proper choice of window.

2.3.1 Linear Chirp Signals

To illustrate the concept of a time-varying signal, we consider the well-known linear chirp signals. These signals are used in radar systems, and shall prove to be useful in Chapters 3 and 4. Consider the linear chirp signal

$$q_1(t) = e^{-st^2}, \qquad s = \gamma - j\mu, \qquad \gamma = \frac{1}{2\sigma^2} \geq 0 \tag{2.3.1}$$

where σ is a measure of the duration of the signal. In fact, since the amplitude of the signal is a Gaussian function, it can be easily shown, using tables of the complementary error functions, that 95 percent of the signal energy is contained in the time interval $(-\sigma\sqrt{2}, \sigma\sqrt{2})$. To find the FT $Q_1(\omega)$ of $q_1(t)$, we make use of the well-known integral [P2]

$$\int_{-\infty}^{\infty} e^{-s(t+c)^2} dt = \sqrt{\frac{\pi}{s}}, \qquad Re\left(\sqrt{\frac{\pi}{s}}\right) > 0 \tag{2.3.2}$$

where c is an arbitrary complex constant. Hence,

$$Q_1(\omega) = \int_{-\infty}^{\infty} e^{-st^2} e^{-j\omega t} dt$$

$$= \sqrt{\frac{\pi}{s}}\, e^{-\omega^2/4s} \tag{2.3.3}$$

The magnitude and argument of $Q_1(\omega)$ are given by

$$|Q_1(\omega)| = \frac{\sqrt{\pi}}{(\gamma^2 + \mu^2)^{1/4}} \exp\left[-\frac{\gamma}{4(\gamma^2 + \mu^2)} \omega^2 \right] \tag{2.3.4}$$

$$\arg[Q_1(\omega)] = -\frac{1}{2} \tan^{-1}\left(\frac{\mu}{\gamma} \right) + \frac{\mu\omega^2}{4(\gamma^2 + \mu^2)} \tag{2.3.5}$$

Now consider the signal

$$q_2(t) = q_1(t - t_0) e^{j\nu t}$$

$$= \exp\left[-\gamma(t - t_0)^2 + j\mu(t - t_0)^2 + j\nu t \right] \tag{2.3.6}$$

The signal $q_2(t)$ is obtained from $q_1(t)$ by first introducing a time shift followed by a frequency shift. Hence,

$$Q_2(\omega) = Q_1(\omega - \nu) e^{-j(\omega - \nu)t_0} \tag{2.3.7}$$

and the squared magnitude of $Q_2(\omega)$ can be written in the form

$$|Q_2(\omega)|^2 = \frac{\pi}{(\gamma^2 + \mu^2)^{1/2}} \exp\left[-\frac{(\omega - \nu)^2}{2\Sigma^2} \right], \qquad \Sigma = \sqrt{\frac{\gamma^2 + \mu^2}{\gamma}} \tag{2.3.8}$$

Clearly, $|Q_2(\omega)|^2$ has a Gaussian shape centered at the frequency ν and whose width is proportional to Σ.

Time-bandwidth product

Consider the signal $q_1(t)$. Using the integrals

$$\int_{-\infty}^{\infty} e^{-\alpha x^2} dx = \sqrt{\frac{\pi}{\alpha}}$$
$$\int_{-\infty}^{\infty} x^2 e^{-\alpha x^2} dx = \frac{1}{2\alpha}\sqrt{\frac{\pi}{\alpha}} \tag{2.3.9}$$

we can show that

$$E_q = \int_{-\infty}^{\infty} |q_1(t)|^2 dt = \frac{1}{2\pi}\int_{-\infty}^{\infty} |Q_1(\omega)|^2 d\omega = \sqrt{\frac{\pi}{2\gamma}}, \tag{2.3.10}$$

$$T_q^2 = \frac{1}{E_q}\int_{-\infty}^{\infty} t^2 |q_1(t)|^2 dt = \frac{1}{4\gamma} = \frac{\sigma^2}{2}, \tag{2.3.11}$$

The RMS BW B_q is given by

$$B_q^2 = \frac{1}{2\pi E_q}\int_{-\infty}^{\infty} \omega^2 |Q_1(\omega)|^2 d\omega = \Sigma^2 \tag{2.3.12}$$

Therefore, the RMS TBP is given by

$$\Pi_q = \frac{\Sigma\sigma}{\sqrt{2}} \tag{2.3.13}$$

Note that if $\mu = 0$, then $\Sigma^2 = \gamma = \frac{1}{2\sigma^2}$. In this case, the TBP is given by $\Pi_q = \frac{1}{2}$, and the corresponding signal is elementary.

If the signal $q_1(t)$ is shifted in time and frequency to obtain the signal $q_2(t)$, the value of the TBP will change. For example, consider the signal $q_2(t)$. If $v > B_q$, the new BW is $B_{q_2} = 2B_q$, and the TBP will be doubled. Moreover, if $t_0 \neq 0$, then Eq. (2.1.8) will have to be used to compute T_q instead of Eq. (2.3.11). In all cases, however, the product $\frac{\Sigma\sigma}{\sqrt{2}}$ can still be compared to $\frac{1}{2}$ to yield a measure of the sophistication of the signal $q_2(t)$ (see Section 2.1.4).

Analytic signal

Using tables of the complementary error function, it could be easily shown that the 95-percent BW of the linear chirp signal $q_2(t)$ is approximately

$$95-\text{percent } BW \simeq 4\Sigma \tag{2.3.14}$$

Hence, 95-percent of the energy of the signal $q_2(t)$ is contained in the frequency band $(\nu - 2\Sigma, \nu + 2\Sigma)$. Clearly, if $\nu - 2\Sigma > 0$, the signal $q_2(t)$ has negligibly small spectral components at negative frequencies, and hence is a good approximation to the analytic version of the real signal

$$q_{2r}(t) = e^{-\gamma(t-t_0)^2}\cos\left[\mu(t-t_0)^2 + \nu t\right] \tag{2.3.15}$$

The instantaneous frequency of $q_2(t)$ is given by

$$\Omega_2(t) = 2\mu(t-t_0) + \nu \tag{2.3.16}$$

Example 2.1

Specifically, consider the linear chirp signal $q_2(t)$ with the following parameters

$$\begin{aligned} &\sigma = 30 \text{ sec}, && \gamma = \frac{1}{1800} \simeq 5.56 \times 10^{-4} \\ &t_0 = 50 \text{ sec}, && \nu = \frac{\pi}{2} \text{ rad/sec} \\ &\mu = 0.0035\pi \simeq 0.011 \text{ rad/sec}^2 \end{aligned} \tag{2.3.17}$$

In this case, $\Sigma \simeq 0.466$ rad/sec, and $\nu - 2\Sigma = 0.637 \text{ rad/sec} > 0$. Therefore, $q_2(t)$ can be accurately described as an analytic signal, since at most 2.5 percent of its energy is located over the negative frequency axis. Therefore, the instantaneous frequency of $q_2(t)$ can be approximated by

$$\Omega_2(t) = \frac{\pi}{2} + 0.007\pi(t-t_0) \tag{2.3.18}$$

The real component of $q_2(t)$ is shown in Fig. 1. The FT squared magnitude $|Q_2(\omega)|^2$ is shown in Fig. 2.

Effect of windowing

For linear chirp signals which are truly time-varying signals,

$$\frac{\mu}{\gamma} = 2\mu\sigma^2 \gg 1 \tag{2.3.19}$$

This implies that the instantaneous frequency of the signal changes appreciably during the duration of the signal. Note that in example 2.1, we have $\frac{\mu}{\gamma} \simeq 20$. If Eq. (2.3.19) holds, Eq. (2.3.8) implies that

$$\Sigma \simeq \frac{\mu}{\sqrt{\gamma}} = \sqrt{2}\,\mu\sigma\,, \qquad \frac{\Sigma\sigma}{\sqrt{2}} \simeq \mu\sigma^2 \gg \frac{1}{2} \tag{2.3.20}$$

For the parameters given in Eq. (2.3.17), $\frac{\Sigma\sigma}{\sqrt{2}} \simeq 10 \gg \frac{1}{2}$ and the signal $q_1(t)$ is sophisticated.

To illustrate the time-varying nature of the signal $q_2(\tau)$, consider the case where $t_0 = 0$. Form the windowed signal centered at time t, $x_t(\tau) = q_2(\tau)w(t-\tau)$, where $w(\tau)$ is a Gaussian window defined as $w(\tau) = e^{-\zeta\tau^2}$, $\zeta = \frac{1}{2\sigma_w^2}$. Note that

$$x_t(\tau) = e^{-\gamma\tau^2 + j\mu\tau^2 + j\nu\tau - \zeta(t-\tau)^2} \tag{2.3.21}$$

is a linear chirp signal. The spectrogram of $q_2(t)$ can be computed as the squared magnitude of the FT of the windowed signal $x_t(\tau)$. It is given by the Gaussian function

$$S_{q_2}(t, \omega) = |X_t(\omega)|^2 = \frac{\pi |A|^2}{((\gamma+\zeta)^2 + \mu^2)^{1/2}} \exp\left[-\frac{(\omega - \nu')^2}{2\Sigma'^2} \right] \tag{2.3.22}$$

where

$$\nu' = \nu + 2\mu\hat{t} \ , \qquad \Sigma'^2 = \gamma + \zeta + \frac{\mu^2}{\gamma + \zeta}$$

$$\hat{t} = \frac{\zeta}{\gamma + \zeta} t \ , \qquad |A|^2 = \exp\left[-2(\gamma + \zeta)\hat{t}^2 - 2\zeta t^2\right]. \tag{2.3.23}$$

For the signal $x_t(\tau)$, to have a reduced BW, the window has to be much shorter than the signal; i.e., $\sigma_w^2 \ll \sigma^2$, and hence, $\zeta \gg \gamma$. The optimal value of the window length of the spectrogram minimizing Σ' is characterized by Eq. (3.4.8) which can be written as $\zeta = |\mu|$ (see also section 3.5.1.2.). In this case, we have

$$\Sigma' \simeq \sqrt{2\zeta} = \frac{1}{\sigma_w}$$
$$\Sigma \simeq \frac{\sigma}{\sqrt{2}\,\sigma_w^{\,2}} \tag{2.3.24}$$

The BW and TBP of the windowed signal are reduced by the following ratios

$$\frac{\Sigma'}{\Sigma} = \sqrt{2}\,\frac{\sigma_w}{\sigma}$$
$$\frac{\Pi'_q}{\Pi_q} = \sqrt{2}\left(\frac{\sigma_w}{\sigma}\right)^2 \tag{2.3.25}$$

where primed quantities correspond to the windowed signals. The reduction in BW is proportional to the ratio $\frac{\sigma_w}{\sigma}$. The reduction in the TBP is proportional to the square of that ratio. For the linear chirp signal of example 2.1, $\sigma = 30$ secs, and the optimal window length is given by $\sigma_w = 6.7$ secs. The BW is reduced by a factor of 0.32, while the TBP is reduced by a factor of 0.071. In fact, the TBP of the windowed signal Π'_q is given by $\frac{\Sigma'\sigma_w}{\sqrt{2}} = \frac{1}{\sqrt{2}} = 0.707 \simeq \frac{1}{2}$. The windowed signal is nearly elementary.

2.3.2 Sinusoidally frequency modulated signal

Consider the sinusoidally frequency modulated signal $q_3(t)$

$$q_3(t) = \exp\,[j\phi(t)] = \exp\,[j\omega_0 t + j2\pi\rho\cos\omega_m t] \tag{2.3.26}$$

If $q_3(t)$ was an analytic signal, its instantaneous frequency would be expressed as

$$\Omega_3(t) = \frac{d\phi}{dt} = \omega_0 - \Delta\omega\sin\omega_m t \tag{2.3.27}$$

where ω_m is the frequency of the frequency modulating function $\theta'_1(t) = \sin\omega_m t$, and $\Delta\omega = 2\pi\rho\omega_m$ represents the frequency range swept by the instantaneous frequency of $q_3(t)$. Using Carson's rule, the BW of this FM signal can be approximated by

$$B_3 \simeq 2(\Delta\omega + \omega_m) = 2(2\pi\rho + 1)\omega_m \tag{2.3.28}$$

Example 2.2 Let

$$\omega_0 = \frac{\pi}{2}\ , \qquad \rho = 6\ , \qquad \beta = 0.005(2\pi) \tag{2.3.29}$$

Hence, $B_3 = 2.431$ rad/sec, and $\omega_0 - \frac{B_3}{2} = 0.3552$ rad/sec > 0 , which implies that the signal $q_3(t)$ is approximately an analytic signal, since $\omega_0 - \frac{B_3}{2} > 0$ implies that the spectrum of $q_3(t)$ nearly vanishes for negative frequencies. The real part of the signal is shown in Fig. 3, over the time interval $-100 < t < 120$. The discrete-time signal

$$q_4(nT) = (0.54 + 0.46\cos(\frac{2\pi n}{1025}))q_3(nT) \tag{2.3.30}$$

with T=1, and $-512 < n < 512$, is a properly sampled and windowed version of $q_3(t)$. The discrete-time signal $q_4(nT)$ is used to approximate the FT magnitude of $q_3(t)$ shown in Fig. 4 which illustrates the fact that $q_3(t)$ is approximately an analytic signal.

To illustrate the time-varying nature of $q_3(t)$, consider the windowed signal $x_t(\tau) = q_3(\tau)w(t-\tau)$, where the window $w(\tau) = e^{-\zeta\tau^2}$ is the same Gaussian window defined above with $\zeta = \frac{1}{2\sigma_w^2}$. The phase of $x_t(\tau)$ is still given by $\phi(\tau)$. The modulating function $\Omega_3(t)$ is periodic with period $\frac{2\pi}{\omega_m} = 200$ secs. If the duration of the window is chosen short enough such that $\sigma_w \ll \frac{2\pi}{\omega_m}$, then the phase of the windowed signal can be approximated by the second order Taylor series expansion about t

$$\phi(t+\tau) = \phi_0 + j\nu\tau + j\mu\tau^2 \tag{2.3.31}$$

where

$$\begin{aligned} \phi_0 = \phi(t) &= \omega_0 + 2\pi\rho\cos\omega_m t \\ \nu &= \frac{d\phi(t)}{dt} = \omega_0 - \Delta\omega\sin\omega_m t \\ \mu &= \frac{d^2\phi(t)}{2dt^2} = -\omega_m\Delta\omega\cos\omega_m t \end{aligned} \tag{2.3.32}$$

Note that $\nu = \Omega_3(t)$. Substituting the phase by its Taylor series expansion, the windowed signal can be approximated by

$$x_t(\tau) \simeq e^{-\zeta\tau^2}\exp\left[j\phi_0 + j\nu\tau + j\mu\tau^2\right] \tag{2.3.33}$$

where the transformation $\tau - t \rightarrow t$ has been used. This is a linear chirp signal signal very similar to the signal $q_2(\tau)$ defined in the previous section except for the constant phase term $e^{j\phi_0}$. Provided that the Taylor series expansion in Eq. (2.3.31) is a reasonable approximation to the phase of the signal, the windowed sinusoidally frequency modulated signal is a linear chirp signal. With a judicial choice of the window length, the windowed signal will be an elementary signal.

Note that the FT of $x_t(\tau)$ with respect to τ is centered at $\omega = \nu$ which is equal to the instantaneous frequency of $q_3(t)$. For $\sigma_w = 10$, the BW of $x_t(\tau)$ varies between 2.09 rad/sec when $t_1 = 0.$, and 0.4 when $t_1 = 50$.

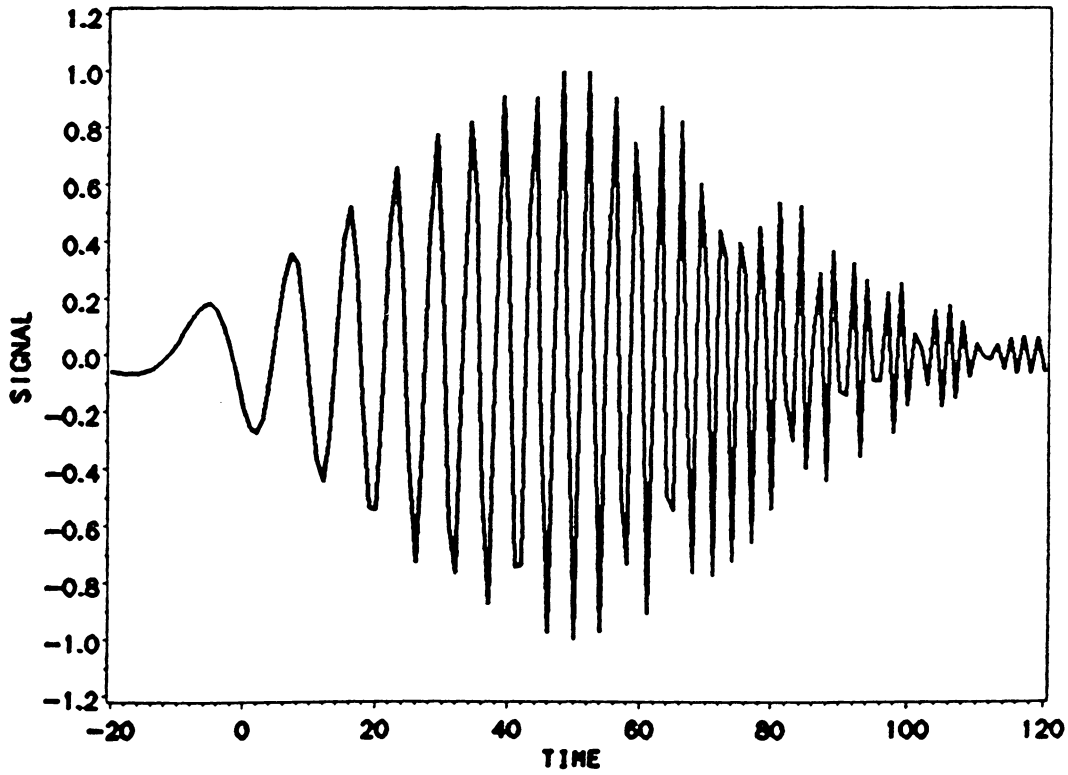

Figure 1. Real part of the linear chirp signal $q_2(t)$.

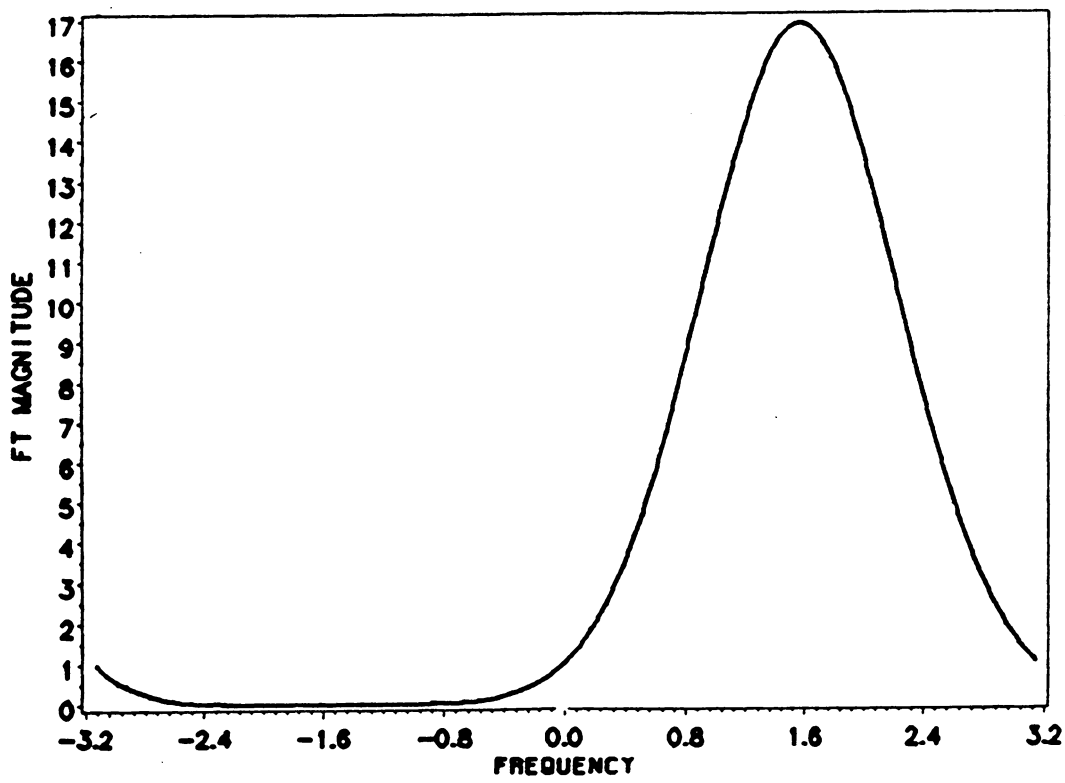

Figure 2. Magnitude of the FT of the linear chirp signal signal $q_2(t)$.

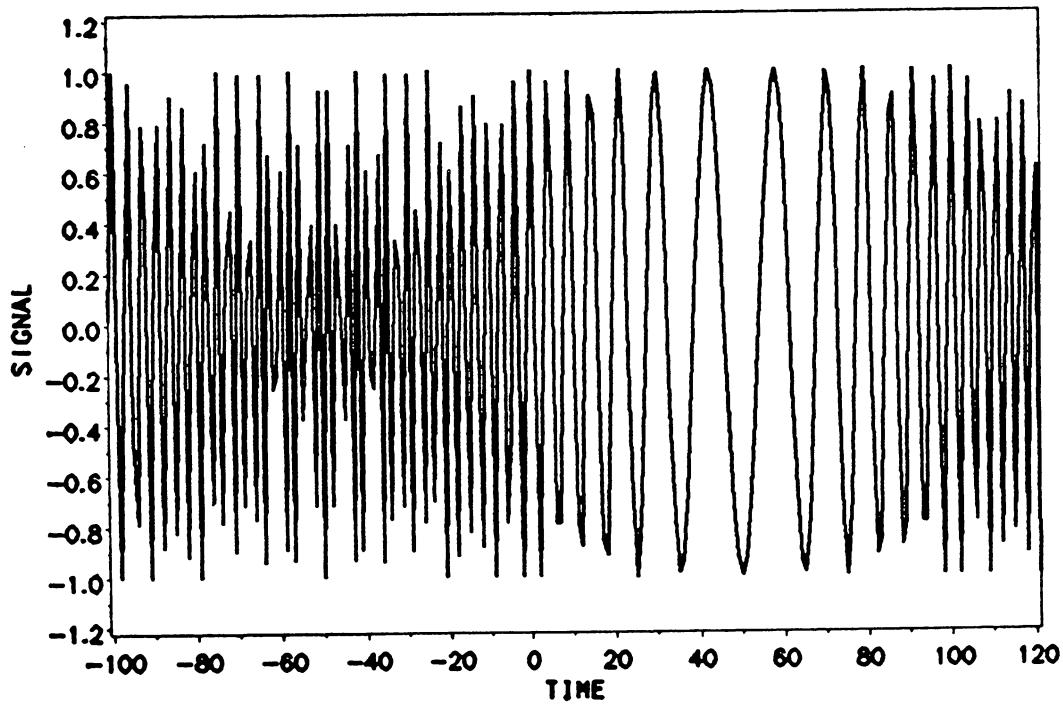

Figure 3. Real part of the SFM signal $q_3(t)$.

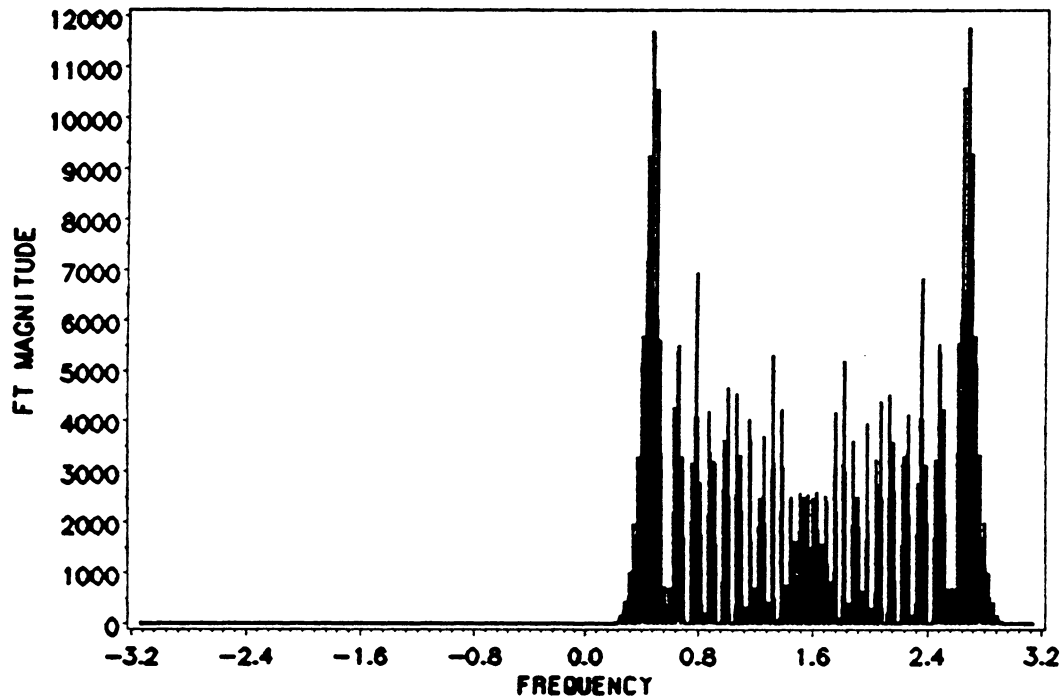

Figure 4. Magnitude of the FT of the SFM signal $q_3(t)$.

3.0 Analysis of STV signals using mixed time-frequency representations

3.1 Introduction

The Fourier Transform (FT) has proven to be a very useful tool in many signal processing applications. In the case of a time-varying signal, however, the usefulness of the FT is rather limited. A STV deterministic signal can have a conceptually simple structure, but its FT can exhibit a complicated undiscernible pattern, thus providing little insight into the spectral structure of the time-varying signal, or the values of its defining parameters. The SFM signal studied in Section 2.7.2 is a clear example of this fact.

A natural question is whether one can incorporate or impose a time-varying character on the FT in such a way that the simple structure of a STV signal can be easily recognized. There are several generalizations of the FT to the STV signal case. These include the Short Time Fourier Transform (STFT) and its magnitude squared (STFTM) also known as the spectrogram, the Wigner Distribution (WD), the Pseudo-Wigner Distribution (PWD) and the Optimally Smoothed Wigner Distribution (OSWD).

Each of the MTFRs mentioned above has merits of its own. In this chapter we conduct a comparative study aimed at answering the following question: which MTFR is more successful at characterizing the ROS of a quasi-monochromatic signal and identifying the ROS of the different components of a STV signal? Answering this question shall be based on the careful consideration of several relevant issues. These include : the positivity of the MTFR, the MTFR manageability to pattern recognition, the available time-frequency resolution, the ability to separate closely spaced signal components, the computational complexity, and storage requirements.

One specially relevant issue is the ability of the MTFR to correctly estimate the instantaneous frequency of a signal component. Given the MTFR $M(t, \omega)$ of the signal $x(t)$, the instantaneous frequency is approximated by the normalized average frequency (NAF) of $M(t, \omega)$ defined as

$$\overline{\Omega}(t) = \frac{\overline{\omega}(t)}{E_{\omega}(t)} = \frac{\frac{1}{2\pi}\int_{-\infty}^{\infty} \omega M(t, \omega) d\omega}{\frac{1}{2\pi}\int_{-\infty}^{\infty} M(t, \omega) d\omega} \tag{3.1.1}$$

where $\overline{\omega}(t)$ and $E_{\omega}(t)$ denote the first and zero-order moment of the MTFR in the frequency direction. The NAF can be thought of as a solution of the optimization problem

$$\min_{\overline{\Omega}(t)} \quad B_x(t) = \frac{1}{2\pi}\int_{-\infty}^{\infty} (\omega - \overline{\Omega}(t))^2 M(t, \omega) d\omega \tag{3.1.2}$$

When $M(t, \omega)$ is real and positive, the minimization problem is equivalent to finding the frequency $\overline{\Omega}(t)$ around which most of the signal energy is concentrated. Note that the above definition of the NAF is slightly different from the one given in Chapter 2 (see Eq. (2.2.18)), specifically in the lower limit of integration. The definition given in Eq. (3.1.1) is the one usually used in the literature of MTFRs [C1], and shall be adopted in this chapter. This definition yields a zero NAF if the signal is real. If the NAF is to correspond to the physical instantaneous

frequency, the MTFR of the analytic version of the signal has to be used [B2], in which case the definitions in Eq. (3.1.1) and Eq. (2.2.18) become the same.

In the following, we review the definitions of several MTFRs and some of their properties. We also derive two new properties of the OSWD pertaining to its NAF and its BW. We study the MTFRs of the linear chirp signal and of the SFM signal. Finally, we compare the performance of the MTFRs in identifying and characterizing the ROS of a STV signal.

3.2 Wigner Distribution

The Wigner distribution (WD) has recently gained importance as a signal analysis tool after a series of papers by Claasen and Mecklenbraucker [C1], [C2], [C3], who showed that it possesses many interesting and useful characteristics. Following, we define the WD and summarize its properties.

3.2.1 Definition

Consider two signals $x(t)$ and $y(t)$. The Cross-Wigner distribution function is defined as

$$W_{xy}(t, \omega) = \int_{-\infty}^{\infty} x(t + \frac{\tau}{2}) y^*(t - \frac{\tau}{2}) e^{-j\omega\tau} d\tau \tag{3.2.1}$$

An alternative definition exists in the frequency domain

$$W_{xy}(t, \omega) = \int_{-\infty}^{\infty} X(\omega + \frac{\eta}{2}) Y^*(\omega - \frac{\eta}{2}) e^{-j\eta t} d\eta \tag{3.2.2}$$

The Auto-Wigner Distribution function, or simply the Wigner Distribution (WD) is defined for $y(t) = x(t)$

$$W_x(t, \omega) = \int_{-\infty}^{\infty} x(t + \frac{\tau}{2}) x^*(t - \frac{\tau}{2}) e^{-j\omega\tau} d\tau \tag{3.2.3}$$

It can be easily shown that the WD of a real or a complex signal is always real. Unlike the FT, the WD is not a linear transformation, but is quadratic in nature, and hence, may lead to undesirable cross terms. For example, the WD of the signal $z(t) = x(t) + y(t)$ is given by

$$W_z(t, \omega) = W_x(t, \omega) + W_y(t, \omega) + 2Re\, W_{xy}(t, \omega) \tag{3.2.4}$$

The cross term $W_{xy}(t, \omega)$ does not have any physical meaning, and will tend to obscure the general picture of the WD. Furthermore, the cross-terms are oscillatory and can assume negative values, thus preventing the WD from being interpreted as a true time-varying energy density function.

3.2.2 Properties of the WD

The WD possesses many useful and desirable properties [C1]. They are listed below:

1. The WD preserves shifts in time : If $y(t) = x(t - t_0)$ then

$$W_y(t, \omega) = W_x(t - t_0, \omega) \tag{3.2.5}$$

2. The WD preserves shifts in frequency : If $Y(\omega) = X(\omega - \omega_0)$ then

$$W_y(t, \omega) = W_x(t, \omega - \omega_0) \tag{3.2.6}$$

3. The zero-order average of the WD in the frequency direction yields the instantaneous power of the signal

$$\frac{1}{2\pi}\int_{-\infty}^{\infty} W_x(t, \omega)d\omega = |x(t)|^2 \tag{3.2.7}$$

4. The zero-order average of the WD in the time direction yields the energy spectral density of the signal

$$\int_{-\infty}^{\infty} W_x(t, \omega)dt = |X(\omega)|^2 \tag{3.2.8}$$

5. The WD is real,

$$W_x(t, \omega) = W_x^*(t, \omega) \tag{3.2.9}$$

6. The NAF of the WD is equal to the derivative of the phase of the signal.

Consider the signal $x(t) = a(t)e^{j\phi(t)}$, where $a(t)$ and $\phi(t)$ are both real. Note that $x(t)$ is not necessarily analytic. The derivative of the phase $\Omega_x(t) = \frac{d\phi(t)}{dt}$ is given by

$$\Omega_x(t) = \frac{\frac{1}{2\pi}\int_{-\infty}^{\infty} \omega W_x(t, \omega)d\omega}{\frac{1}{2\pi}\int_{-\infty}^{\infty} W_x(t, \omega)d\omega} \tag{3.2.10}$$

If $x(t)$ is an analytic signal, $\Omega_x(t)$ can be correctly interpreted as the instantaneous frequency of the signal. Note however that if the signal $x(t) = a(t)$ is real, $\Omega_x(t)$ is identically zero.

7. The group delay $T_x(\omega)$ of the signal is the normalized first-moment of the WD in the frequency direction

$$T_x(\omega) = \frac{\int_{-\infty}^{\infty} tW_x(t, \omega)dt}{\int_{-\infty}^{\infty} W_x(t, \omega)dt} \tag{3.2.11}$$

8. The WD has the same time support as the signal

$$\text{If } x(t) = 0 \text{ for } |t| > T \text{ then } W_x(t, \omega) = 0 \text{ for } |t| > T. \tag{3.2.12}$$

9. The WD has the same frequency support as the signal

$$\text{If } X(\omega) = 0 \text{ for } |\omega| > \Omega \text{ then } W_x(t, \omega) = 0 \text{ for } |\omega| > \Omega. \tag{3.2.13}$$

10. Effect of linear filtering : If $y(t) = \int_{-\infty}^{\infty} x(\tau)v(t-\tau)d\tau$, then

$$W_y(t, \omega) = \int_{-\infty}^{\infty} W_x(\tau, \omega)W_v(t-\tau, \omega)d\tau \tag{3.2.14}$$

11. Effect of modulation : If $y(t) = x(t)m(t)$, then

$$W_y(t, \omega) = \frac{1}{2\pi}\int_{-\infty}^{\infty} W_x(t, \eta)W_m(t, \omega-\eta)d\eta \tag{3.2.15}$$

Of special interest to us is property (6) which shows that the instantaneous frequency of a signal can be calculated exactly from the WD through an averaging operation. The instantaneous frequency $\Omega_x(t)$ can still be thought of as a solution to the optimization problem

$$B_x^o(t) = \min_{\Omega_x} \frac{1}{2\pi}\int_{-\infty}^{\infty} (\omega - \Omega_x)^2 W_x(t, \omega)d\omega \tag{3.2.16}$$

Since $W_x(t, \omega)$ can be negative in general, the minimum value of the integral might be negative and hence can not be used as an estimate of the RMS bandwidth of the signal.

3.3 Pseudo-Wigner distribution

To overcome the computational problems of the WD, and to reduce the effects of cross-terms, an evolutionary version of the WD, kmown as the Pseudo-Wigner Distribution (PWD), is advocated [C1].

3.3.1 Definition

The PWD is defined as

$$P_x(t, \omega) = \int_{-\infty}^{\infty} v(\frac{\tau}{2})x(t+\frac{\tau}{2})v^*(-\frac{\tau}{2})x^*(t-\frac{\tau}{2})e^{-j\omega\tau}d\tau \qquad (3.3.1)$$

where $v(\tau)$ is usually taken to be a real, positive, symmetric and lowpass window, such as the Hamming window. To recover the signal $x(t)$ from a valid PWD, we use

$$v(\frac{\tau}{2})x(t+\frac{\tau}{2})v^*(-\frac{\tau}{2})x^*(t-\frac{\tau}{2}) = \frac{1}{2\pi}\int_{-\infty}^{\infty} P_x(t, \omega)e^{j\omega\tau}d\omega \qquad (3.3.2)$$

By setting $\tau = 0$, the signal $x(t)$ is reccovered to within a constant phase term. It can be shown that the PWD can be obtained from the WD through a smoothing operation in the frequency direction, where the smoothing kernel is the WD of the analysis window $v(\tau)$.

$$P_x(t,\omega) = \frac{1}{2\pi}\int_{-\infty}^{\infty} W_x(t,\eta)W_v(0,\omega-\eta)d\eta \tag{3.3.3}$$

3.3.2 Properties

The cross-terms usually present in the WD are reduced but are still existing. Clearly, a shorter analysis window results in a smoother PWD. It has been shown [C3] that the PWD still posseses many of the properties of the WD listed in the previous section, namely, properties 2,3,5, and 6. In particular, the instantaneous frequency can still be found for a monocomponent signal via an averaging operation. Note first, that

$$E_\omega(t) = \frac{1}{2\pi}\int_{-\infty}^{\infty} P_x(t,\omega)d\omega = |v(0)x(t)|^2 \tag{3.3.4}$$

Consider the integral

$$\overline{\omega}(t) = \frac{1}{2\pi}\int_{-\infty}^{\infty} \omega P_x(t,\omega)dt \tag{3.3.5}$$

Substituting the expression for $P_x(t,\omega)$ in Eq. (3.3.3) into the above equation, and using Eq. (3.2.7) and Eq. (3.2.10) gives

$$\overline{\omega}(t) = \frac{1}{2\pi}\int_{-\infty}^{\infty} W_x(t,\eta)\left[\Omega_v(0) + \eta|v(0)|^2\right]d\eta \tag{3.3.6}$$

Clearly, $\Omega_v(0) = 0$ for any real window. Using Eq. (3.2.10) and Eq. (3.2.7) again, we get

$$\overline{\omega}(t) = \Omega_x(t)|v(0)x(t)|^2 \tag{3.3.7}$$

Hence, the NAF $\frac{\overline{\omega}(t)}{E_{\omega}(t)}$ of the PWD is equal to the normalized average frequency of the WD, and hence is equal to the instantaneous frequency of the signal if $x(t)$ is an analytic signal.

$$\Omega_x(t) = \frac{\frac{1}{2\pi}\int_{-\infty}^{\infty} \omega P_x(t, \omega) d\omega}{\frac{1}{2\pi}\int_{-\infty}^{\infty} P_x(t, \omega) d\omega} \tag{3.3.8}$$

3.4 Short-time Fourier transform

3.4.1 Definition

The Short-Time Fourier Transform (STFT) [P8] was defined in Section 2.6.2.1, as

$$S_x(t, \omega) = \int_{-\infty}^{\infty} x(\tau) v(t - \tau) e^{-j\omega\tau} d\tau \tag{3.4.1}$$

where $v(\tau)$ is a suitable real, symmetric, low pass window, usually referred to as the analysis window of the STFT. The inverse Fourier relation corresponding to Eq. (3.4.1) is given by

$$x(\tau)v(t - \tau) = \frac{1}{2\pi}\int_{-\infty}^{\infty} S_x(t, \omega) e^{j\omega\tau} d\omega \tag{3.4.2}$$

The signal x(t) can be recovered from Eq. (3.4.2) by setting $\tau = t$, and normalizing by $v(0)$, the value of the window at the origin $v(0)$. In the subsequent sections, we shall use a window normalized such that $v(0) = 1$.

3.4.2 Properties

The STFT is complex and its magnitude squared $|S_x(t, \omega)|^2$ is referred to as the spectrogram. In [C3], it was shown that the spectrogram can be derived from the WD via a smoothing operation in both the time and frequency directions

$$\begin{aligned} |S_x(t, \omega)|^2 &= \frac{1}{2\pi} \int_{-\infty}^{\infty} \int_{-\infty}^{\infty} W_x(\tau, \eta) W_v(t - \tau, \eta - \omega) d\tau d\eta \\ &= \frac{1}{2\pi} \int_{-\infty}^{\infty} \int_{-\infty}^{\infty} W_x(t - \tau, \omega + \eta) W_v(\tau, \eta) d\tau d\eta \end{aligned} \tag{3.4.3}$$

where $W_v(t, \omega)$ is the WD of the analyzing window $v(\tau)$. The spectrogram is real and positive, but out of all the properties of the WD listed in Section 3.2.2, it satisfies the shift properties only. In fact, for a real analyzing window, one can show [C3] that the time and frequency supports of the spectrogram are roughly increased by the time and frequency supports of the window. In particular, one can show that

$$\frac{1}{2\pi} \int_{-\infty}^{\infty} |S_x(t, \omega)|^2 d\omega = \int_{-\infty}^{\infty} |x(\tau)|^2 |v(t - \tau)|^2 d\tau \tag{3.4.4}$$

$$\int_{-\infty}^{\infty} |S_x(t, \omega)|^2 dt = \frac{1}{2\pi} \int_{-\infty}^{\infty} |X(\eta)|^2 |V(\omega - \eta)|^2 d\eta \tag{3.4.5}$$

Moreover, for a real window, second-order moments of the spectrogram yield averaged values of the desired quantities :

$$\overline{\Omega}_{xS}(t) = \frac{\int_{-\infty}^{\infty} \Omega_x(\tau) |x(\tau) v(t - \tau)|^2 d\tau}{\int_{-\infty}^{\infty} |x(\tau) v(t - \tau)|^2 d\tau} \tag{3.4.6}$$

$$T_{xs}(\omega) = \frac{\frac{1}{2\pi}\int_{-\infty}^{\infty} T_x(\eta)\,|X(\eta)V(\omega-\eta)|^2 d\eta}{\frac{1}{2\pi}\int_{-\infty}^{\infty} |X(\eta)V(\omega-\eta)|^2 d\eta} \tag{3.4.7}$$

Recovering the exact instantaneous frequency using Eq. (3.4.6) requires that the duration of the window $v(\tau)$ be as small as possible, while recovering the group delay from Eq. (3.4.7) requires that the support of $V(\omega)$, the FT of $v(\tau)$, be as small as possible. As can be seen from the Uncertainty principle, these two requirements are contradictory, and a tradeoff has to be reached. This tradeoff between frequency resolution (requiring a long duration window) and time resolution (requiring a short duration window) is a general characteristic of the STFT. Storey [S2] has shown that the optimal window length needed to obtain the sharpest (minimum BW) spectrogram is signal dependent, and is of the order of

$$\text{optimal } \sigma_w = \left| \frac{d^2\phi}{dt^2} \right|^{-1/2} \tag{3.4.8}$$

where $\phi(t)$ is the phase of the analytic version of the signal. Note that Storey's optimal window length is time-varying, and hence the window itself is time-varying. The notation $v(\tau;t)$ can be used to stress the time dependence.

3.5 *Optimally smoothed Wigner distribution*

In a recent paper, Andrieux et al. [A1] proposed an optimal smoothing scheme of the WD in both the time and frequency directions. The resulting MTFR, known as the OSWD, is optimal in the sense that $O_x(t,\omega)$, the OSWD of a unimodular signal $x(t) = e^{j\phi(t)}$, where the phase $\phi(t)$ is locally quadratic, is as sharp as possible; i.e., it has a minimum bandwidth at

each time instant. It was also noted that the OSWD is equal to a spectrogram computed with a complex signal-dependent window.

3.5.1 Definition

A time-frequency smoothed WD (SWD) of a signal x(t) is given by

$$\tilde{W}_x(t, \omega) = \frac{1}{2\pi} \int_{-\infty}^{\infty} \int_{-\infty}^{\infty} K(t - \tau, \omega - \eta) W_x(\tau, \eta) d\tau d\eta \tag{3.5.1}$$

$$\tilde{W}_x(t, \omega) = \frac{1}{2\pi} \int_{-\infty}^{\infty} \int_{-\infty}^{\infty} K(\tau, \eta) W_x(t - \tau, \omega - \eta) d\tau d\eta \tag{3.5.2}$$

The smoothing kernel $K(\tau, \eta)$ acts uniformly on the entire time-frequency plane; i.e., the same kernel is used to compute $\tilde{W}(t_1, \omega_1)$ and $\tilde{W}(t_2, \omega_2)$. The kernel $K(\tau, \eta)$ is said to be time- and frequency-independent. A more general smoothing is obtained when the smoothing kernel is time- and frequency-dependent

$$\tilde{W}_x(t, \omega) = \frac{1}{2\pi} \int_{-\infty}^{\infty} \int_{-\infty}^{\infty} K(\tau, \eta; t, \omega) W_x(t - \tau, \omega - \eta) d\tau d\eta \tag{3.5.3}$$

Andrieux et al. [A1] have required that the OSWD satisfies the two conditions

1. The distribution is positive everywhere.
2. The BW of the distribution is minimal at each time.

3.5.1.1 *Positivity of the OSWD*

Positivity of the OSWD is insured if the two-dimensional smoothing kernel $K(\tau, \eta)$ is chosen such that $K(\tau, -\eta) = W_v(\tau, \eta)$ where $W_v(\tau, \eta)$ is the WD of a window $v(\tau)$ to be determined. This could be readily seen by comparing equations (3.27) and (3.33a). In this case, the OSWD can be interpreted as a spectrogram obtained with the analysis window $v(\tau)$. The above result still holds if the window is chosen to be time-varying, which is the case considered in [A1]. The time-varying window is denoted by $v(\tau;t)$. The correponding kernel $K(\tau, \eta;t) = W_v(\tau, -\eta; t)$ is time-varying, but is frequency-independent (independent of ω in Eq. (3.5.3)). Hence, the OSWD can be expressed in the form of a smoothed WD:

$$O_x(t, \omega) = \frac{1}{2\pi} \int_{-\infty}^{\infty} W_v(\tau, \eta; t) W_x(t - \tau, \theta + \eta) d\tau d\eta \tag{3.5.4}$$

Equivalently, the OSWD can be expressed as a spectrogram:

$$\begin{aligned} O_x(t, \omega) &= \left| \int_{-\infty}^{\infty} x(\tau) v(t - \tau;t) e^{-j\omega\tau} d\tau \right|^2 \\ &= \left| \int_{-\infty}^{\infty} x(t - \tau) v(\tau;t) e^{j\omega\tau} d\tau \right|^2 \end{aligned} \tag{3.5.5}$$

where the analysis window $v(\tau;t)$ is still to be designed so as to minimize the BW of the OSWD. Once the optimal window $v(\tau;t)$ has been found, a STFT of the signal $x(t)$ can be computed using the analysis window $v(\tau;t)$:

$$C_x(t, \omega) = \int_{-\infty}^{\infty} x(\tau) v(t - \tau;t) e^{-j\omega\tau} d\tau \tag{3.5.6}$$

We shall refer to this STFT as the Optimal Short-Time Fourier Transform (OSTFT). Its magnitude squared is given by the OSWD of the signal, and hence, has a minimum BW. The OSTFT is optimal in this sense.

3.5.1.2 Window design

In this section, the window $v(\tau;t)$ is designed so as to satisfy the second condition required by Andrieux. The development presented here follows that in [A1], with a slight modification. Unlike Andrieux's approach, we constrain the length of the window by an upper bound, in order to insure that the Taylor series expansion of the signal phase is valid over the duration of the window.

Class of signals under consideration

Consider the constant amplitude STV signal

$$x(t) = e^{j\phi(t)} \tag{3.5.7}$$

Consider the second order Taylor series expansion of $\phi(t+\tau)$ in the vicinity of t

$$\phi(t+\tau) \simeq \phi(t) + \tau\frac{d\phi(t)}{dt} + \frac{\tau^2}{2}\frac{d^2\phi(t)}{dt^2} = \phi(t) + \tau\Omega + \tau^2\mu \ , \qquad \tau \le \tau_{max} \tag{3.5.8}$$

where $\Omega = \dfrac{d\phi(t)}{dt}$ is the instantaneous frequency of the signal, and $\mu = \dfrac{1}{2}\dfrac{d^2\phi(t)}{dt^2}$ is half the derivative of the instantaneous frequency. The parameters Ω and μ depend on time t. To simplify the notation, we shall not show this dependence explicitly.

The parameter τ_{max} is chosen such that the expansion in Eq. (3.5.8) is valid for $\tau \le \tau_{max}$; i.e.,

$$\frac{\tau^n}{n!}\frac{d^n\phi}{dt^n} \simeq 0 \ , \qquad n \ge 3, \qquad \tau \le \tau_{max} \tag{3.5.9}$$

The signal is said to be a quadratic-phase signal if there exists a τ_{max} such that Eq. (3.5.9) holds and $\tau_{max} > T_{min}$ where T_{min} is the minimum window length necessary to achieve the desirable frequency resolution (see Eq. (2.1.12)). The desirable frequency resolution and the nature of approximation in Eq. (3.5.9) are rather subjective; they are generally at the discretion of the application engineer. For example, if in a given application, one is interested in resolving signal components that are 0.1 Hertz apart, then it is required that $T_{min} \geq 10$ secs.

OSWD window.

Consider a Gaussian window modulated with a quadratic phase term

$$v(\tau; t) = w(\tau;t)e^{j\beta\tau^2} = e^{-\zeta\tau^2 + j\beta\tau^2}, \qquad w(\tau;t) = e^{-\zeta\tau^2}, \qquad \zeta = \frac{1}{2\sigma_w^2} \tag{3.5.10}$$

where σ_w and β are both functions of time t. To simplify the notation, we have not indicated this dependence explicitly. The parameter σ_w is a measure of the length of the window. The added term $e^{j\beta\tau^2}$ is introduced to cancel the time-varying character of the signal. The parameters σ_w and β will be chosen such that the OSWD has a minimum BW. To achieve this goal, Andrieux et al. calculated the BW of the OSWD of the given signal, and then minimized it over the allowable values of σ_w and β.

The integrand in Eq. (3.5.5) is given by

$$x_t(\tau) = x(t-\tau)v(\tau;t) = \exp\left(j\phi(t) - j\Omega\tau + j\mu\tau^2 - \zeta\tau^2 + j\beta\tau^2\right) \tag{3.5.11}$$

Except for the constant phase term $e^{j\phi(t)}$, $x_t(\tau)$ is a linear chirp signal similar to $q_2(\tau)$ (see Eq. (2.3.6-7)) whose FT magnitude is given in Eq. (2.2.8). The OSWD of the signal $x(t)$ is given by the FT magnitude squared of $x_t(\tau)$, evaluated at $-\omega$ (see Eq. (3.5.5)); i.e.,

$$O_x(t, \omega) = \frac{\pi}{\sqrt{\zeta^2 + (\beta+\mu)^2}} \exp\left(-\frac{(-\omega+\Omega)^2}{2\Sigma^2}\right)$$
$$\Sigma^2 = \zeta + \frac{(\mu+\beta)^2}{\zeta} \tag{3.5.12}$$

Σ is a measure of the BW of the OSWD of the signal. It is to be minimized over the set of all permissible values of ζ and β.

STFT case

The spectrogram can be obtained from the OSWD by setting $\beta = 0$. In this case, the analysis window becomes $v(\tau;t) = e^{-\zeta\tau^2}$. Minimizing Σ^2 in Eq. (3.5.12) with respect to ζ , with no constraint on ζ, implies the necessary condition:

$$\frac{\partial\Sigma^2}{\partial\zeta} = 1 - \frac{(\mu+\beta)^2}{\zeta^2} = 0 \ , \qquad \text{or} \qquad |\mu+\beta| = \zeta \tag{3.5.13}$$

where $\beta = 0$ in the case of the spectrogram. The optimum value of ζ that minimizes Σ^2 is given by $\zeta = |\mu|$. Hence,

$$\beta = 0, \quad \zeta = |\mu| \ , \quad \sigma_w = \left| \frac{d^2\phi}{dt^2} \right|^{-1/2} , \quad \Sigma = \left| \frac{d^2\phi}{dt^2} \right|^{1/2} \tag{3.5.14}$$

The value of σ in Eq. (3.5.14) is the same as Storey's optimal window size given in Eq. (3.4.8).

OSWD case

Let the values of β and σ_w be unconstrained. Then, in addition to Eq. (3.5.13), the following equation should be satisfied

$$\frac{\partial\Sigma^2}{\partial\beta} = \frac{2(\mu+\beta)}{\zeta} = 0 \tag{3.5.15}$$

To satisfy Eq. (3.5.15), set $\beta = -\mu$. In this case, $\Sigma^2 = \zeta$ (see Eq. (3.5.12)). Since ζ is positive, Σ^2 is minimized by setting $\zeta = 0$. Hence, the optimum values are given by

$$\beta = -\mu = -\frac{d^2\phi}{2dt^2} \ , \quad \zeta = 0, \quad , \sigma_w = \infty \ , \quad \Sigma = 0 \tag{3.5.16}$$

The zero BW ($\Sigma = 0$) shows the advantage of incorporating the quadratic phase term in the definition of the window. An infinitely long window, however, is quite undesirable, because the Taylor series expansion in Eq. (3.5.8) is valid only for $\tau \leq \tau_{max} < \infty$.

To circumvent the problem of an inifinite window length without imposing any constraint on σ, Andrieux & al. [A1] included one additional (cubic) term in the Taylor series expansion of the phase:

$$\phi(t+\tau) \simeq \phi(t) + \Omega\tau + \mu\tau^2 + \frac{d^3\phi}{3!\,dt^3}\tau^3 , \quad \text{for} \quad \tau \leq \hat{\tau}_{\max} \tag{3.5.17}$$

Choosing $\beta = -\mu$, Andrieux et al. expressed the OSWD of the resulting cubic phase in terms of Airy functions, and obtained the following optimal values

$$\beta = -\mu = -\frac{d^2\phi}{2dt^2} , \quad \sigma_w = \left| \frac{d^3\phi}{dt^3} \right|^{-1/3} , \quad \Sigma = O\left(\left| \frac{d^3\phi}{dt^3} \right|^{1/3} \right) \tag{3.5.18}$$

under the condition

$$\left| \frac{d\phi}{dt} \right| \gg \left| \frac{d^3\phi}{dt^3} \right|^{1/3} \gg \left| \frac{d^4\phi}{dt^4} \right|^{1/4} \tag{3.5.19}$$

The optimum Σ is of the order of $\left| \frac{d^3\phi}{dt^3} \right|^{1/3}$

Note that in general $\frac{d^3\phi}{dt^3}$ can be small enough so that the optimal value of σ_w is larger than $\hat{\tau}_{max}$. In this case, the optimal solution is not valid since the window will cover a time support where the phase of the signal cannot be accurately approximated by the cubic Taylor series expansion. Moreover, computing the optimal window length requires that $\frac{d^3\phi}{dt^3}$ be estimated, in addition to $\frac{d^2\phi}{dt^2}$.

To eliminate this problem, we depart from Andrieux's approach by restricting σ_w to be less than the parameter τ_{max}. We consider the case of a quadratic phase signal only; i.e., we assume that the higher order expansion is not available, and we set $\frac{d^i\phi}{dt^i} = 0.,\ i > 2$. We

seek to minimize Σ^2 subject to the constraint $\sigma_w \leq \tau_{max}$. Clearly, the constraint is active; i.e., $\sigma_w = \tau_{max}$. The optimum values are given by

$$\beta = -\mu = -\frac{d^2\phi}{2dt^2}, \quad \zeta = \frac{1}{2\tau_{max}^2}, \quad \sigma_w = \tau_{max}, \quad \Sigma = \frac{1}{\sqrt{2}\,\sigma_w} \tag{3.5.20}$$

Unless otherwise specified, the values in Eq. (3.5.17) shall be used to compute the OSWD.

Finally, we consider the RMS TBP of the windowed signal $x_t(\tau)$ in Eq. (3.5.11). It is given by $\frac{\Sigma\sigma}{\sqrt{2}} = \frac{1}{2}$, showing that the windowed signal is elementary.

3.5.2 Properties

The OSWD is a spectrogram computed with a generalized complex window, and hence, it is expected to have properties similar to those of the spectrogram listed in Section 3.4.2. We note, however, that some of these properties have been derived assuming real windows, such as Eq. (3.4.6). This fact is not stated explicitly in many references including the well known review [C3]. In the following, we derive a more general formula for the NAF that is valid for complex windows. Specifically, we show that the NAF of the OSWD is equal to the instantaneous frequency under the condition that the phase of the signal is quadratic.

Moreover, the OSWD was defined and shown to be optimal in the absence of amplitude modulation. In the following, we study the OSWD of the amplitude modulated quadratic-phase signal $x(t) = a(t)e^{j\phi(t)}$. The OSWD is computed using the parameters in Eq. (3.5.20), which are obtained using $e^{j\phi(t)}$, the constant amplitude part of the signal. In this section, we also study the BW of the OSWD in the presence of amplitude modulation and we compare it to that of the OSWD.

3.5.2.1 *Normalized average frequency of the OSWD*

Now we consider the NAF of the OSWD, and show its relationship to the instantaneous frequency of the signal. We assume that $x(t)$ is an analytic signal. Consider the average frequency $\overline{\omega}(t) = \frac{1}{2\pi}\int_{-\infty}^{\infty} \omega O_x(t, \omega)d\omega$. Substituting Eq. (3.5.4) in the above equation and rearranging terms yields

$$\overline{\omega}(t) = \int_{-\infty}^{\infty} \frac{1}{2\pi}\int_{-\infty}^{\infty} W_v(\tau, \eta)\left[\frac{1}{2\pi}\int_{-\infty}^{\infty} (\omega + \eta - \eta)W_x(t-\tau, \omega+\eta)d\omega\right]d\eta d\tau \qquad (3.5.21)$$

Using Eq. (3.2.10) and Eq. (3.2.7), the above equation becomes

$$\overline{\omega}(t) = \int_{-\infty}^{\infty} |x(t-\tau)|^2\left[\Omega_x(t-\tau)\frac{1}{2\pi}\int_{-\infty}^{\infty} W_v(\tau, \eta;t)d\eta - \frac{1}{2\pi}\int_{-\infty}^{\infty} \eta W_v(\tau, \eta;t)d\eta\right]d\tau \qquad (3.5.22)$$

Applying Eq. (3.2.10) and Eq. (3.2.7) again yields

$$\overline{\omega}(t) = \int_{-\infty}^{\infty} |x(t-\tau)v(\tau)|^2[\Omega_x(t-\tau) - \Omega_v(\tau)]d\tau \qquad (3.5.23)$$

where $\Omega_x(t)$ and $\Omega_v(\tau)$ are the NAFs of the analytic signal $x(t)$ and the signal $v(\tau;t)$ respectively.

The NAF of the spectrogram

The window $v(\tau;t)$ of the STFT is real; hence, its NAF $\Omega_v(t)$, as given by Eq. (3.2.10), is simply zero. As a result, the second term in Eq. (3.5.22) drops, and the NAF of the spectrogram becomes an averaged version of the exact instantaneous frequency. This result is the same as that in Eq. (3.4.6).

The NAF of the OSWD

The Taylor series expansion of the instantaneous frequency is given by

$$\Omega_x(t+\tau) = \Omega_x(t) + 2\mu\tau$$

The window of the OSWD specified in Eq. (3.5.10) has an instantaneous frequency $\Omega_v(\tau) = 2\beta\tau$ where $\beta = -\mu$ (see Eq. (3.5.17)). Hence,

$$\Omega_x(t-\tau) = \Omega_x(t) - 2\mu\tau\,, \text{ and} \qquad \Omega_v(\tau) = -2\mu\tau \tag{3.5.24}$$

Therefore, $\Omega_x(t-\tau) - \Omega_v(\tau) = \Omega_x(t) - 2\mu\tau + 2\mu\tau = \Omega_x(t)$. Eq. (3.5.23) becomes

$$\overline{\omega}(t) = \Omega_x(t)\int_{-\infty}^{\infty} |x(t-\tau)v(\tau;t)|^2 d\tau \tag{3.5.25}$$

Normalizing by the energy $E(t) = \int_{-\infty}^{\infty} |x(t-\tau)v(\tau;t)|^2 d\tau$, we obtain the NAF of the OSWD:

$$\overline{\Omega}_x(t) = \Omega_x(t) \tag{3.5.26}$$

Therefore, the NAF of the OSWD of the quadratic phase signal $x(t) = a(t)e^{j\phi(t)}$ is equal to the exact instantaneous frequency. Note that this result is also valid for amplitude modulated signals.

3.5.2.2 *Bandwidth of the OSWD*

Let the signal $x(t) = a(t)e^{j\phi(t)}$ have a locally quadratic phase as in Eq. (3.5.8) and Eq. (3.5.9), and consider the window defined in Eq. (3.5.10). Use Eq. (3.5.5) to compute the OSWD :

$$O_x(t,\omega) = \left| e^{j\phi(t)}\int_{-\infty}^{\infty} [e^{-\zeta\tau^2} a(t-\tau)] e^{-j(\Omega_x(t)-\omega)\tau} d\tau \right|^2 \tag{3.5.27}$$

Let $t - \tau = u$, then

$$O_x(t,\omega) = \left| e^{-j(\Omega_x(t)-\omega)t} \int_{-\infty}^{\infty} [a(u)e^{-\zeta(t-u)^2}] e^{-j(\omega-\Omega_x(t))u} du \right|^2 \tag{3.5.28}$$

Let $a_t(u)$ represent the signal envelope windowed by $e^{-\zeta u^2}$, the envelope of the window $v(u;t)$ centered at time t, with u as the running variable; i.e., let $a_t(u) = a(u)e^{-\zeta(t-u)^2}$. Eq. (3.5.28) reduces to

$$O_x(t,\omega) = |A_t(\omega - \Omega_x(t))|^2 \tag{3.5.29}$$

where $A_t(\omega)$ is the FT of the windowed signal envelope $a_t(u)$ shifted in frequency by the amount $\Omega_x(t)$. Since frequency shifts do not affect the BW of a signal (except by a factor of 2), the BW of the OSWD can be correctly interpreted as the BW of the windowed signal envelope, under the assumption of a locally quadratic phase. Since both the amplitude of the signal and the amplitude of the window are smooth, we assume that their BWs add up (see Section 2.3.1). Hence, the BW of the OSWD satisfies

$$B_{OSWD} \lesssim 2(B_a + B_w) \tag{3.5.30}$$

3.5.3 Instantaneous bandwidth

In the previous section, the BW of the OSWD was shown to be approximately equal to the BW of a windowed version of the signal envelope. In this section, we compare this BW to a rough estimate of the BW of the spectrogram obtained using Carson's rule. For quadratic-phase signals, the BW of the OSWD can be reasonably interpreted as an instantaneous BW, while the BW of the spectrogram cannot.

3.5.3.1 *Bandwidth of the spectrogram*

Consider $x_{t_0}(t)$, the windowed version of the FM signal $e^{j\phi(t)}$ (see Section 2.3.1)

$$x_{t_0}(t) = w_{2T}(t_0 - t)e^{j\phi(t)} \tag{3.5.31}$$

whose FT with respect to t gives the STFT of $e^{j\phi(t)}$ at time t_0. Assuming a rectangular window of length $2T$, the range swept by the instantaneous frequency of $x_{t_0}(t)$ depends on t_0, the location of the window, and on $2T$, the window length. Define the two numbers $\omega_{\min}(t_0)$ and $\omega_{\max}(t_0)$ such that the instantaneous frequency $\Omega(t)$ satisfies $\omega_{\min}(t_0) \leq \Omega(t) \leq \omega_{\max}(t_0)$, for all $t \in [t_0 - T, t_0 + T]$. The frequency range swept by the instantaneous frequency of the windowed signal is approximately given by

$$\Delta\omega(t_0) \simeq \frac{\omega_{\max}(t_0) - \omega_{\min}(t_0)}{2} \tag{3.5.32}$$

By Carson's rule, the BW of an FM signal is approximately given by $2[B_\Omega + \Delta_\omega(t_0)]$, where B_Ω is the BW of the instantaneous frequency. As was discussed in Section 2.2.1.1, we argue that windowing will increase the BW of the FM signal by B_w , the BW of the window; i.e.,

$$B_{x_{t_0}}(t_0) \lesssim 2(B_\Omega + \Delta\omega(t_0) + B_w) \tag{3.5.33}$$

The above discussion can be easily extended to the case of the amplitude modulated signal $x(t) = a(t)e^{j\phi(t)}$. The BW of the windowed signal $x_{t_0}(t) = w_{2T}(t_0 - t)x(t)$ is now given by

$$B_{x_{t_0}}(t_0) \lesssim 2[(B_a + B_\Omega) + \Delta\omega(t_0) + B_w] \tag{3.5.34}$$

This BW is clearly time-dependent, and represents the BW of the spectrogram.

3.5.3.2 *Discussion*

In general, the BW of the spectrogram is strongly dependent on the shape and especially the length of the analysis window. For a signal with a locally quadratic phase, the frequency range swept by the instantaneous frequency is given by

$$\Delta_{\omega}(t_0) \simeq \frac{d\Omega(t)}{dt}.T \tag{3.5.35}$$

Hence, the BW of the spectrogram is given by

$$B_{x_{t_0}}(t_0) \simeq 2[B_w + B_a + B_{\Omega} + T\frac{d\Omega(t_0)}{dt_0}] \tag{3.5.36}$$

The last term in the above equation can be dominant, in which case the BW of the spectrogram is directly proportional to the length of the analysis window. Therefore, the BW of the spectrogram of a quadratic phase signal cannot be interpreted as a true charactersitic of the signal. In comparison, the BW of the OSWD shown in Eq. (3.5.30) is independent of T, smaller than the BW of the spectrogram, and approximately time-invariant. Actually, the BW of the OSWD is time-varying (see Fig. 29). This time variation stems from two facts. First, the windowed amplitude might itself possess a time-varying BW. Second, the neglected terms of the Taylor series expansion will contribute to the value of the BW of the OSWD, in a time-varying way.

Therefore, the BW of the OSWD of a signal with locally quadratic phase can be reasonably interpreted as an instantaneous BW of the signal.

3.6 Examples

In the following, we consider the different MTFRs of the linear chirp signal $q_2(t)$, and of the SFM signal $q_3(t)$, defined and analyzed in Section 2.7. Since the two signals have BWs sufficiently below π rad/sec (see Fig. 2 and Fig. 4), they can be sampled every one second without aliasing [OS]. Similarly, since the windowed signals have a reduced BW in general, the resulting STFT and OSWD will be free of aliasing too. Moreover, the WD and PWD of the signals are also free of aliasing, since the analytic versions of the signals are used, and hence, there is no need to sample the signals at twice the Nyquist rate [C2].

In the following analysis and simulations, a real window shall be used to compute the PWD and the STFT. The window used is given by

$$w(\tau) = e^{-\zeta\tau^2}, \qquad \zeta = \frac{1}{2\sigma_w^2} \tag{3.6.1}$$

To compute the OSWD, we use the window $v(\tau;t) = w(\tau)e^{j\beta\tau^2}$, where β and σ_w are functions of time. These windows are used because analytical expressions can be obtained for the different MTFRs of the linear chirp signal when the window is Gaussian. In the experiments the window is sampled every one second, and is truncated for $|t| > 2\sigma_w$.

3.6.1 Linear chirp signals

The Linear Chirp Signal (linear chirp signal) has been a favorite example of STV signals and is usually considered when evaluating the performance of MTFRs [B1], [B2], [B5], [C1], [G2], [H2], [K1], [K2], [P2], [S2]. In [C1], the WD and the PWD of the linear chirp signal were calculated; in [K1], its STFT was calculated and analyzed. Bouachache and Flandrin [B1] compared the WD and the spectrogram of the linear chirp signal. To make the analysis

simpler, they normalized the time and frequency axes. They noted that the isoamplitude curves of the resulting WD and spectrogram are ellipses, and they found the equations and lengths of the ellipses as the eigenvalues and eigenvectors of some matrix related to the parameters of the linear chirp signal. By comparing the lengths of the minor axes of the WD and the spectrogram, they reached the conclusion that the WD is more sharp. They failed to notice, however, that the lengths of the axes are dependent on the normalization. A similar dependence has been noted in [K1].

The different MTFRs of the signal $q_2(t)$ are studied below. A synthesis of the results discussed in the above mentioned papers is presented. The MTFRs are written in such a way as to make it easy to compare the BWs of different MTFRs. In addition, we show that the BWs of the PWD and the OSWD are the same for the same window.

3.6.1.1 Wigner distribution

Consider the simple chirp signal $q_1(t) = e^{-\gamma t^2 + j\mu t^2}$. Use the definition of the WD to get

$$W_1(t,\omega) = e^{-2\gamma t^2}\int_{-\infty}^{\infty} \exp\Big(-\frac{\gamma}{2}\tau^2 - j(\omega - 2\mu t)\tau\Big)d\tau$$

$$= \sqrt{\frac{2\pi}{\gamma}}\, e^{-2\gamma t^2} \exp\left(-\frac{(\omega - 2\mu t)^2}{2\Sigma^2}\right) \qquad (3.6.2)$$

$$\Sigma = \sqrt{\gamma}$$

Eq. (2.3.4) has been invoked. Using the fact that the Dirac Delta function $\delta(t)$ can be approximated by $\delta(t) = \lim_{c\to 0}\sqrt{\frac{1}{c\pi}}\, e^{-t^2/c}$, one can show that if $c = 2\gamma \to 0$, then

$$W_1(t,\omega) = 2\pi\delta(\omega - 2\mu t) \qquad (3.6.3)$$

In this case, the BW of the WD is exactly zero, which shows the high resolution of the WD in the case of a linear chirp signal. Similarly, the WD of $q_2(t)$ defined in Eq. (2.3.9) is given by

$$W_2(t,\omega)=\sqrt{\frac{2\pi}{\gamma}}\ \exp\left(-2\gamma(t-t_0)^2-\frac{(\omega-2\mu(t-t_0)-\nu)^2}{2\gamma}\right) \tag{3.6.4}$$

The WD of $q_2(t)$) is computed numerically, and is shown in Fig. 5.

3.6.1.2 Pseudo-Wigner distribution

The PWD of $q_1(t)$ where the window $v(\tau)=e^{-\zeta\tau^2}$ is used, can be written as

$$\begin{aligned}P_1(t,\omega)&=e^{-2(\gamma+\zeta)t^2}\int_{-\infty}^{\infty}\exp\left(-\frac{(\gamma+\zeta)}{2}\tau^2-j(\omega-2\mu t)\tau\right)d\tau\\&=\sqrt{\frac{2\pi}{\gamma+\zeta}}\ \exp\left(-2\gamma t^2-\frac{(\omega-2\mu t)^2}{2\Sigma^2}\right)\end{aligned} \tag{3.6.5}$$

$$\Sigma=\sqrt{\gamma+\zeta} \tag{3.6.6}$$

Eq. (2.3.4) has been invoked. The PWD of $q_2(t)$ can be easily obtained from that of $q_1(t)$ by suitable time and frequency shifts as was done in Eq. (2.3.6-7). Note that as $\gamma\to 0$, $P_1(t,\omega)$ will have a nonzero BW proportional to $\Sigma=\sqrt{\zeta}\neq 0$. Figures 6 ,7, 8 and 9 show the PWD of the signal $q_2(t)$ with $\zeta=\frac{1}{2\sigma_w^2}$, where $\sigma_w=30$, 20, 10 and 7 secs respectively.

3.6.1.3 Short-time Fourier transform

The spectrogram of the signal $q_2(t)$ was given in Eq. (2.3.22) and (2.3.23) and is reproduced here

$$|S_2(t,\omega)|^2=\frac{\pi|A|^2}{((\gamma+\zeta)^2+\mu^2)^{1/2}}\exp\left[-\frac{(\omega-\nu')^2}{2\Sigma^2}\right] \tag{3.6.7}$$

where

$$\nu' = \nu + 2\mu t_1 , \qquad \Sigma = \left(\frac{(\gamma+\zeta)^2 + \mu^2}{(\gamma+\zeta)} \right)^{1/2}$$
$$t_1 = \frac{\zeta t}{\zeta + \gamma} , \qquad |A|^2 = \exp\left[-2(\gamma+\zeta)t_1^2 - 2\zeta t^2 \right]. \tag{3.6.8}$$

Its RMS BW is given by 2Σ. Note that if μ is much larger than $\gamma + \zeta$, the BW of the spectrogram can be substantially larger than the BW of the PWD.

Figures 10, 11 and 12 show the spectrogram of the signal $q_2(t)$, with $\sigma_w =$ 12, 6.7 and 5 secs respectively. The value $\sigma_w = 6.7$ secs corresponds to Storey's optimal window length given in Eq. (3.4.8). Note that the BW of the STFT is considerably larger than that of the PWD.

3.6.1.4 *Optimally smoothed Wigner distribution*

Consider the signal $q_1(t)$ and the window $v(t) = e^{-\zeta t^2 + j\beta t^2}$ with $\beta = -\mu$. The OSWD of this signal is given by

$$O_1(t,\omega) = e^{-2\gamma\left(\frac{\zeta}{\gamma+\zeta}\right)t^2} \left| \int_{-\infty}^{\infty} \exp\left[-(\gamma+\zeta)(\tau-\tau_0)^2 + j(\mu+\beta)(\tau-\tau_0)^2 + j\nu t \right.\right.$$
$$\left.\left. - j(\omega - 2\beta t)\tau + 2(\mu+\beta)\tau_0\tau \right] d\tau \right|^2 \tag{3.6.9}$$

where $\tau_0 = \dfrac{\zeta t}{\gamma+\zeta}$. Since $\beta = -\mu$ the above integral assumes a particularly simple form, and the OSWD becomes (see Eq. (2.3.8)),

$$O_1(t,\omega) = \frac{\pi}{\sqrt{\gamma^2+\zeta^2}} e^{-2\gamma\left(\frac{\zeta}{\gamma+\zeta}\right)t^2} \exp\left(-\frac{(\omega - \nu - 2\mu t)^2}{2\Sigma^2} \right) \tag{3.6.10}$$

where
$$\Sigma = \sqrt{\gamma+\zeta} \tag{3.6.11}$$

Note that this bandwidth is the same as that of the PWD (see Eq. (3.6.6)). Therefore, the PWD and the OSWD have the same frequency sharpness in the case of signals with locally

quadratic phases. The BW of the OSWD is simply equal to the BW of the envelope $e^{-\gamma t^2}$ of the signal $q_1(t)$, incremented by the BW of the envelope of the window $v(\tau)$. The OSWD of the signal $q_2(t)$ can be obtained from that of $q_1(t)$ by appropriately shifting it in time and frequency. The OSWD of the signal $q_2(t)$ is shown in Fig. 13, 14 and 15, with $\sigma_w = 20$, 12 and 6.7 secs respectively. Comparing Fig. 7, 8 and 9 with Fig. 13, 14 and 15 respectively shows that PWD and OSWD have equal BW. If the window is short, the OSWD has a time support similar to that of the PWD. This time support is known to be equal to that of the signal. If the window is long, however, the OSWD will have a duration longer than that of the signal (see Fig. 13). In fact, the time support of the OSWD is equal to that of the envelope $e^{-2\frac{\gamma\zeta}{\gamma+\zeta}t^2}$ (see Eq. (3.6.10)). If $\gamma \ll \zeta$, then $\frac{\gamma\zeta}{\gamma+\zeta} \simeq \gamma$, and the envelope becomes $e^{-2\gamma t^2}$, which is the envelope of the WD shown in Eq. (3.6.2). In this case, the time support of the OSWD is roughly that of the WD, and hence of the signal $x(t)$.

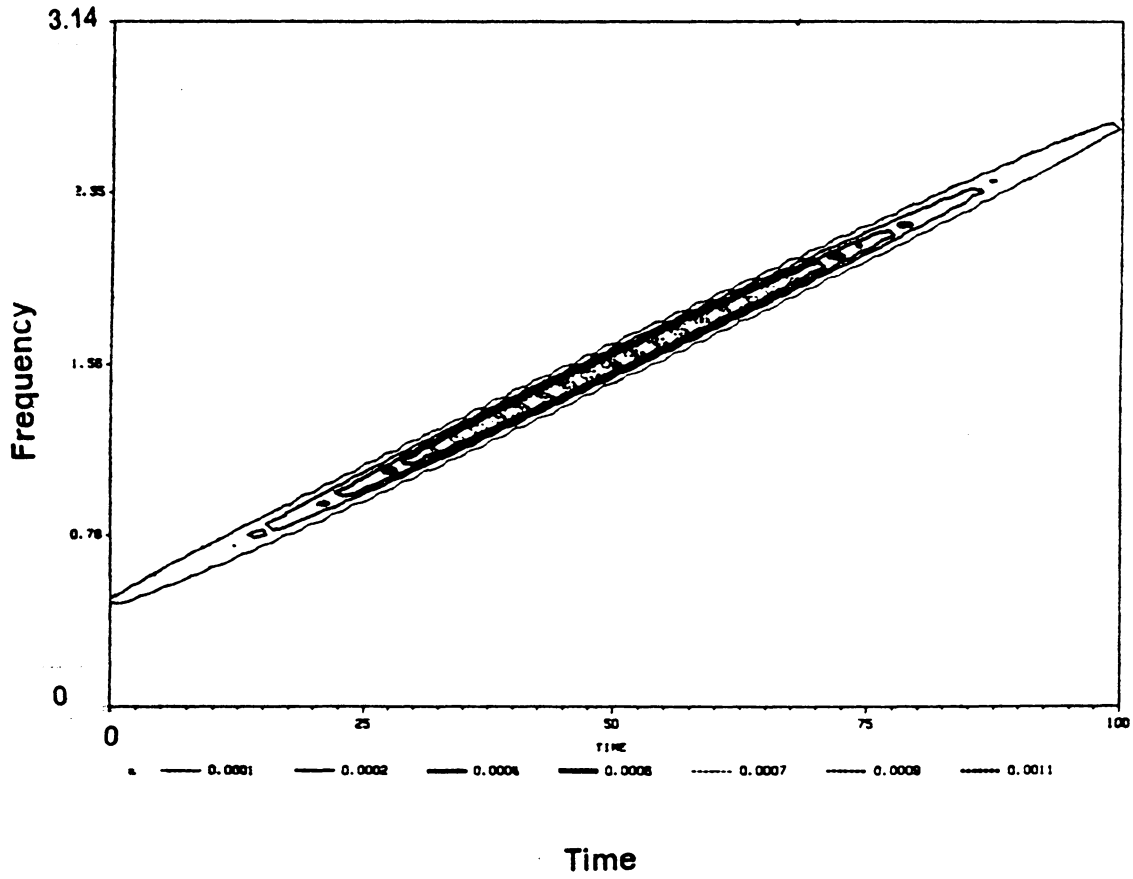

Figure 5. WD of the LCS $q_2(t)$.

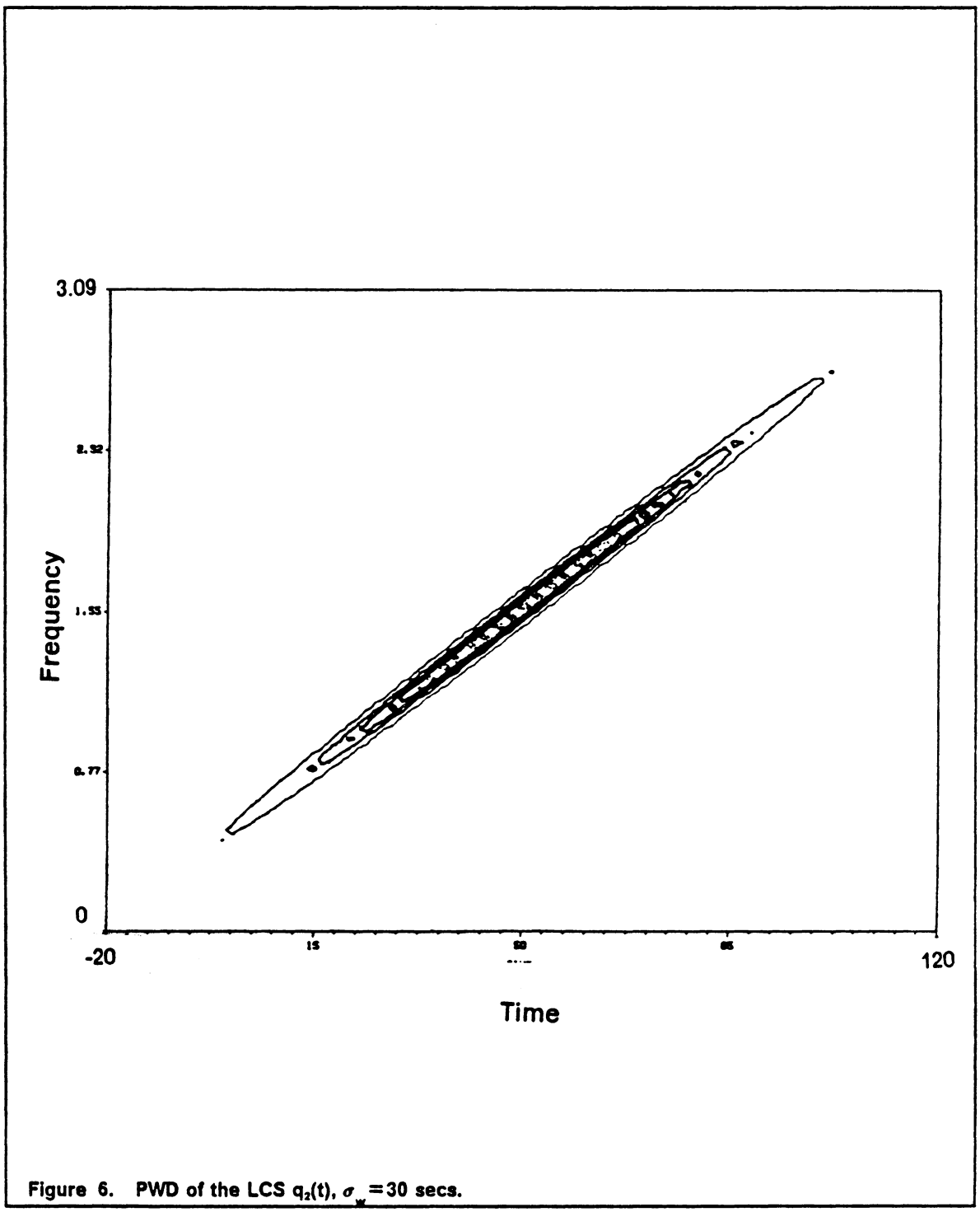

Figure 6. PWD of the LCS $q_2(t)$, $\sigma_w = 30$ secs.

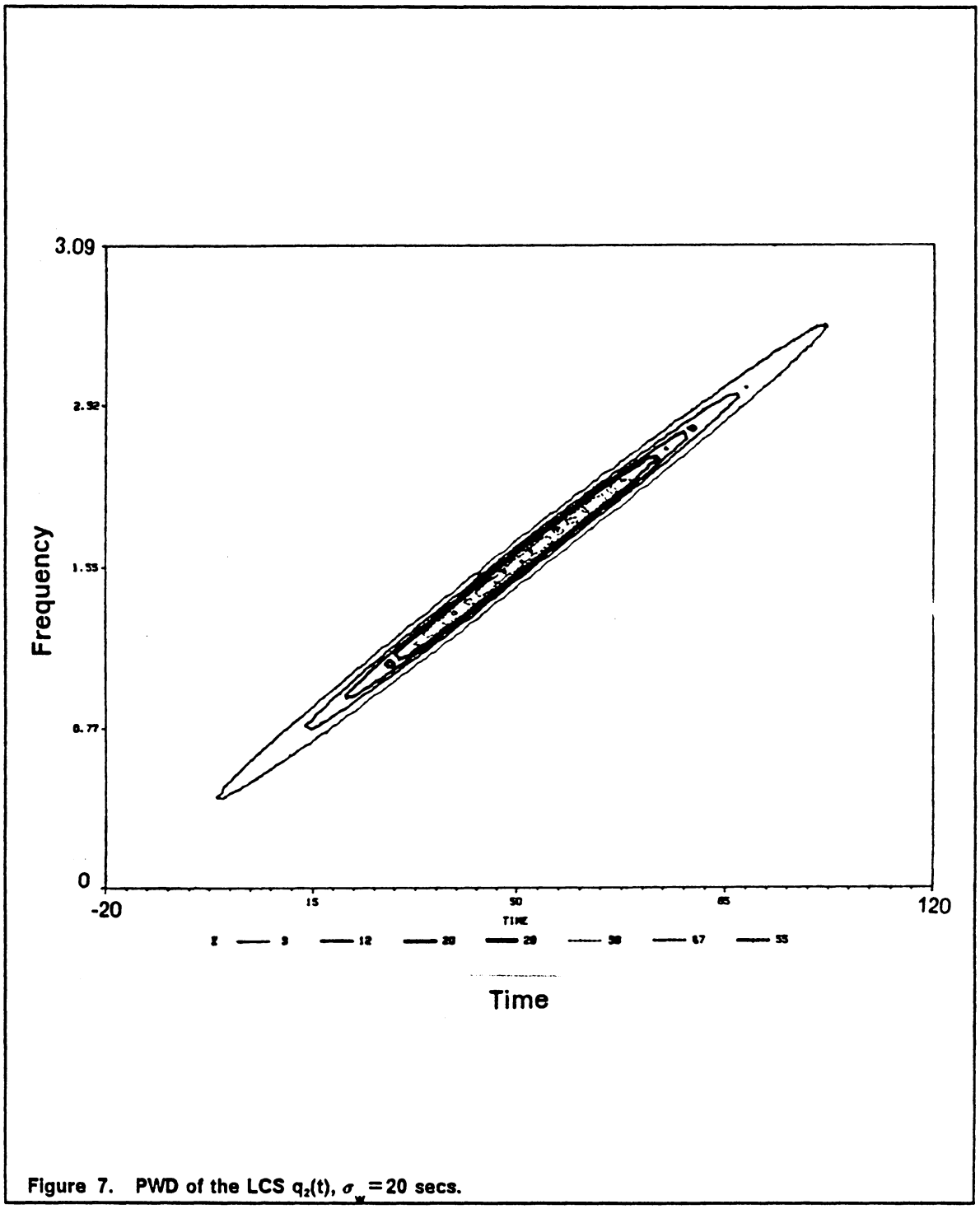

Figure 7. PWD of the LCS $q_2(t)$, $\sigma_w = 20$ secs.

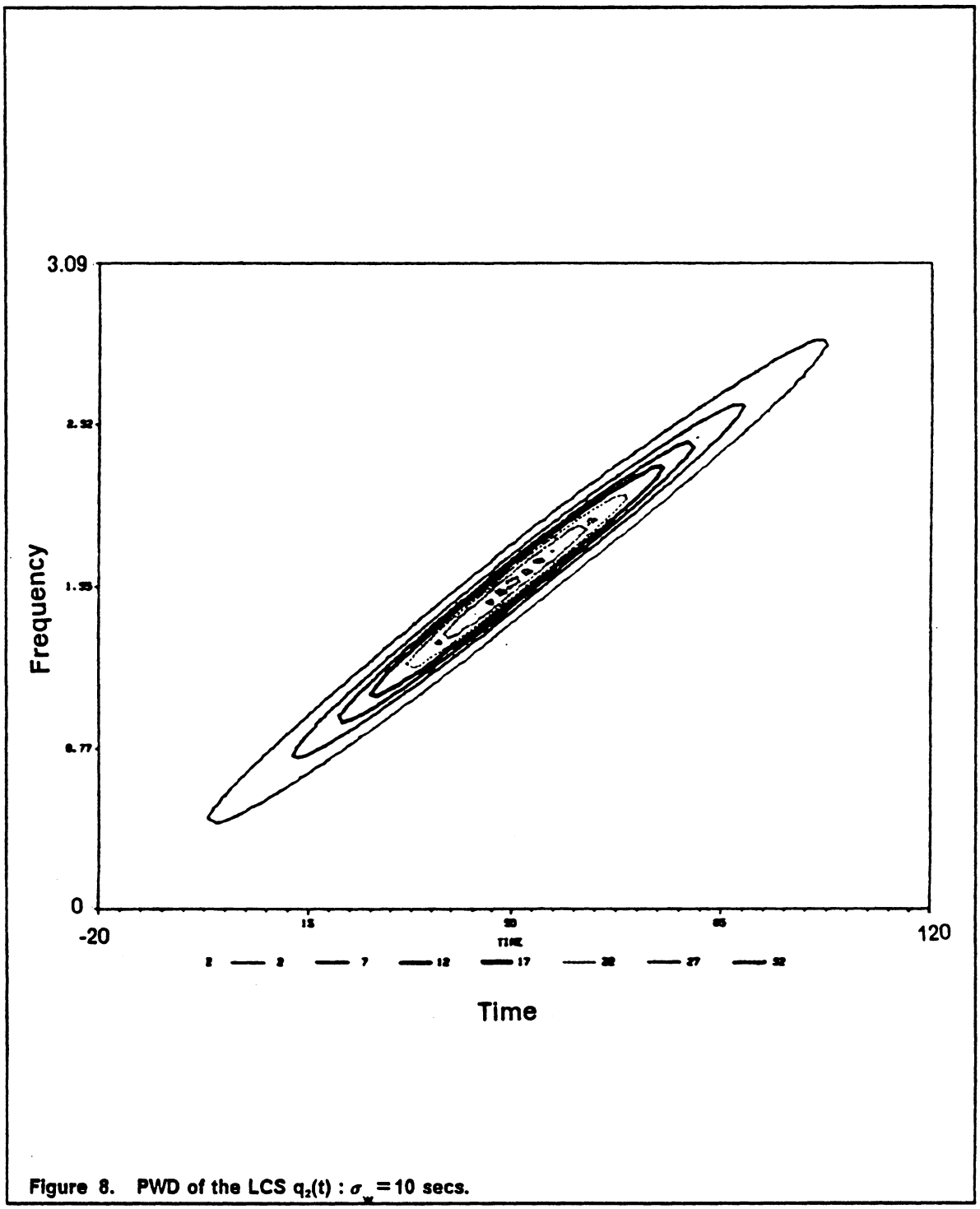

Figure 8. PWD of the LCS $q_2(t)$: $\sigma_w = 10$ secs.

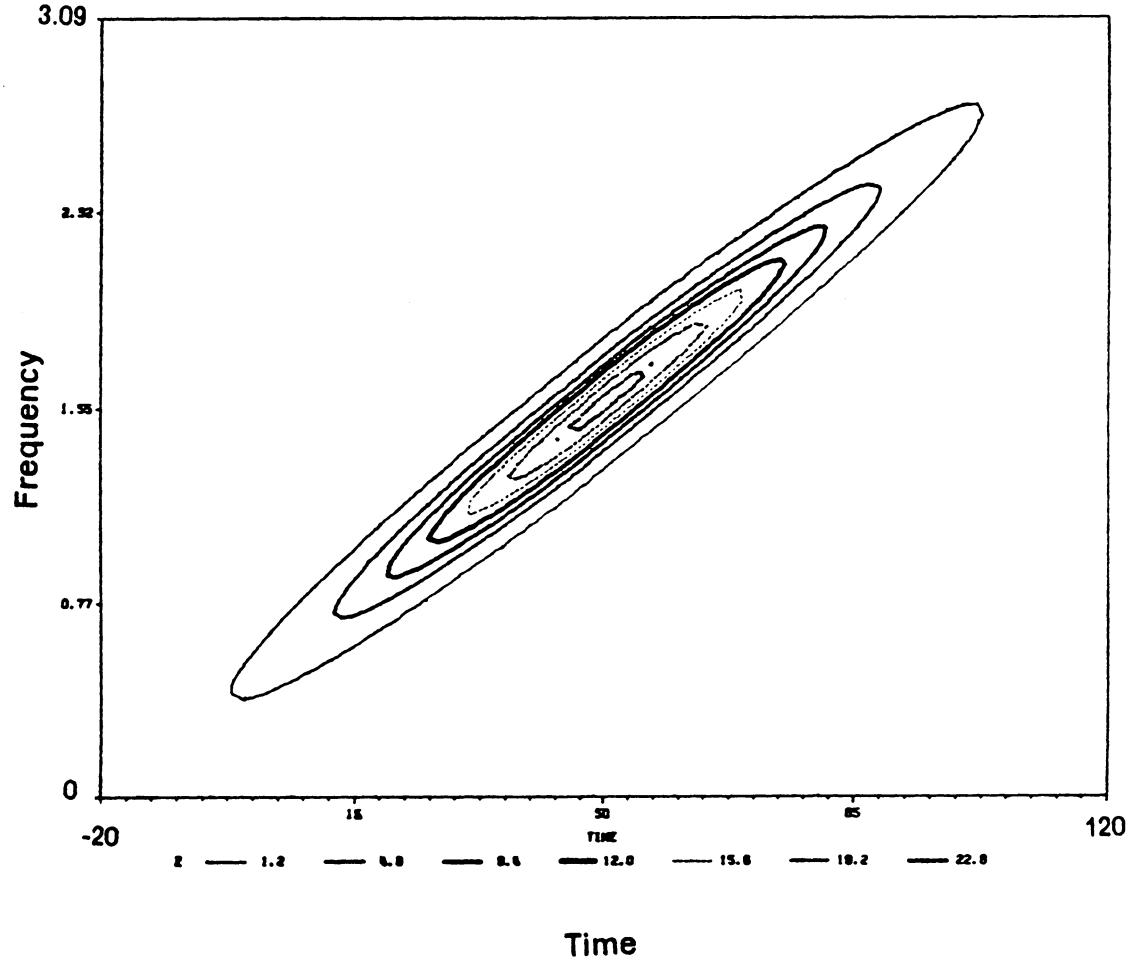

Figure 9. PWD of the LCS $q_2(t)$, $\sigma_w = 7$ secs.

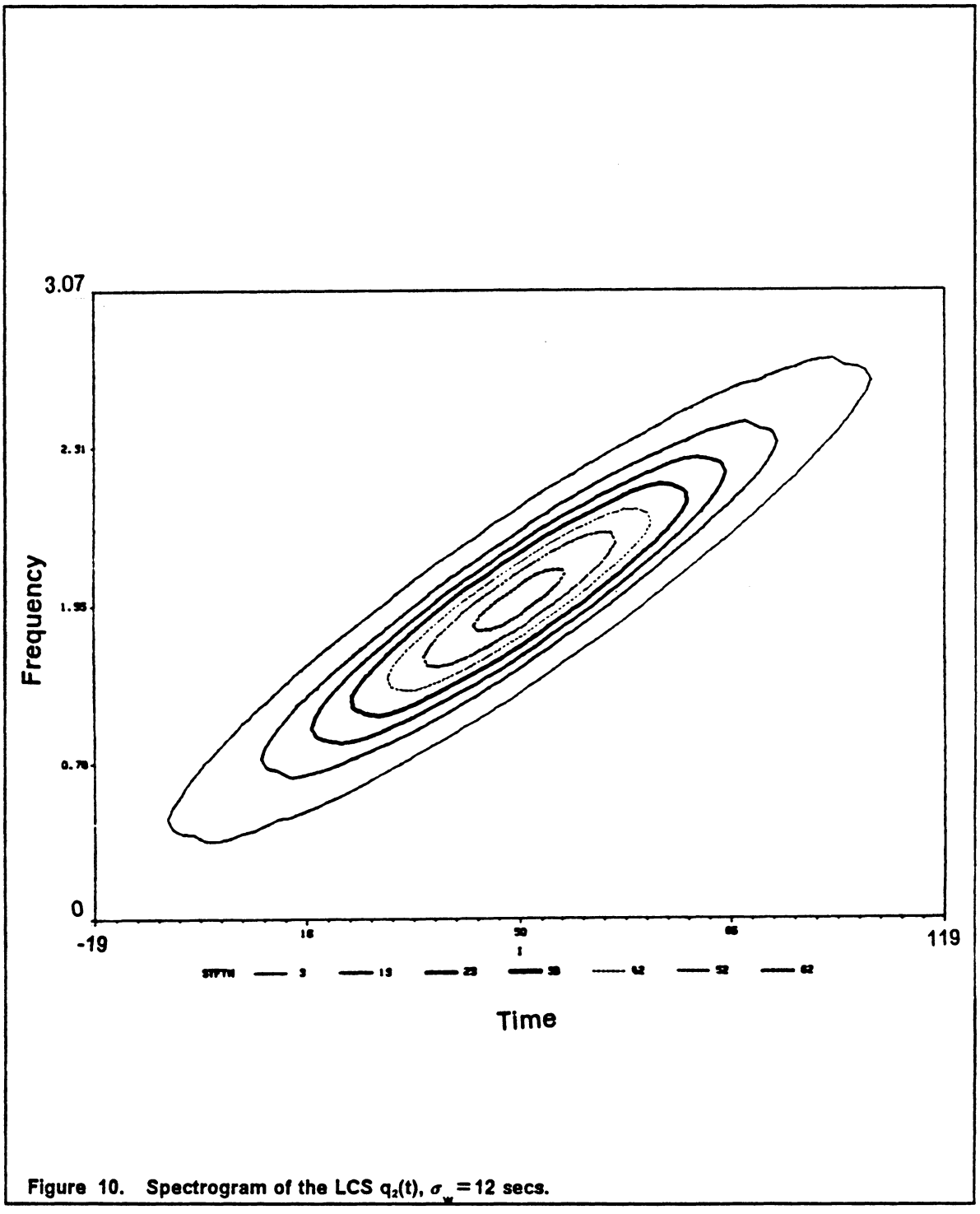

Figure 10. Spectrogram of the LCS $q_2(t)$, $\sigma_w = 12$ secs.

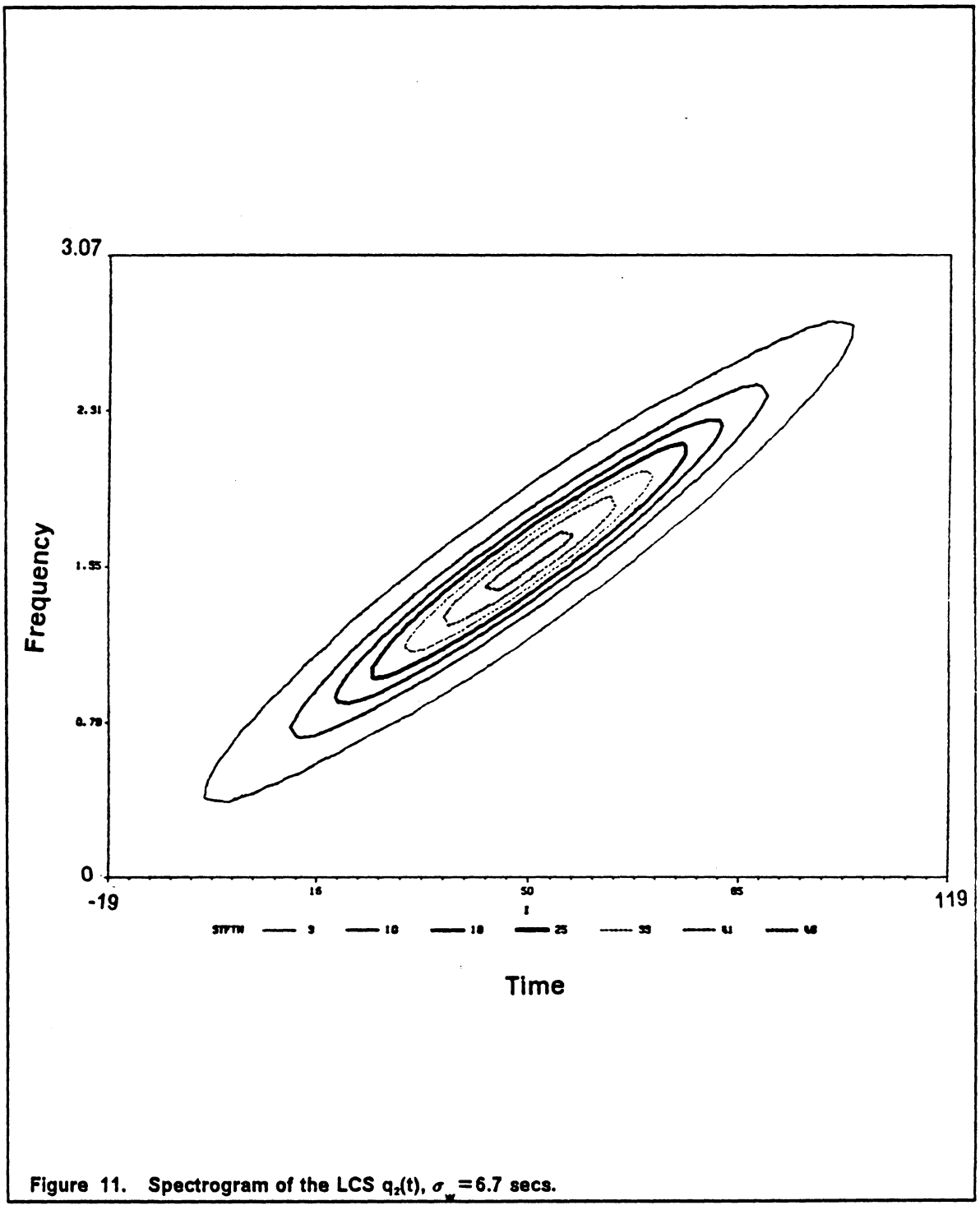

Figure 11. Spectrogram of the LCS $q_2(t)$, $\sigma_w = 6.7$ secs.

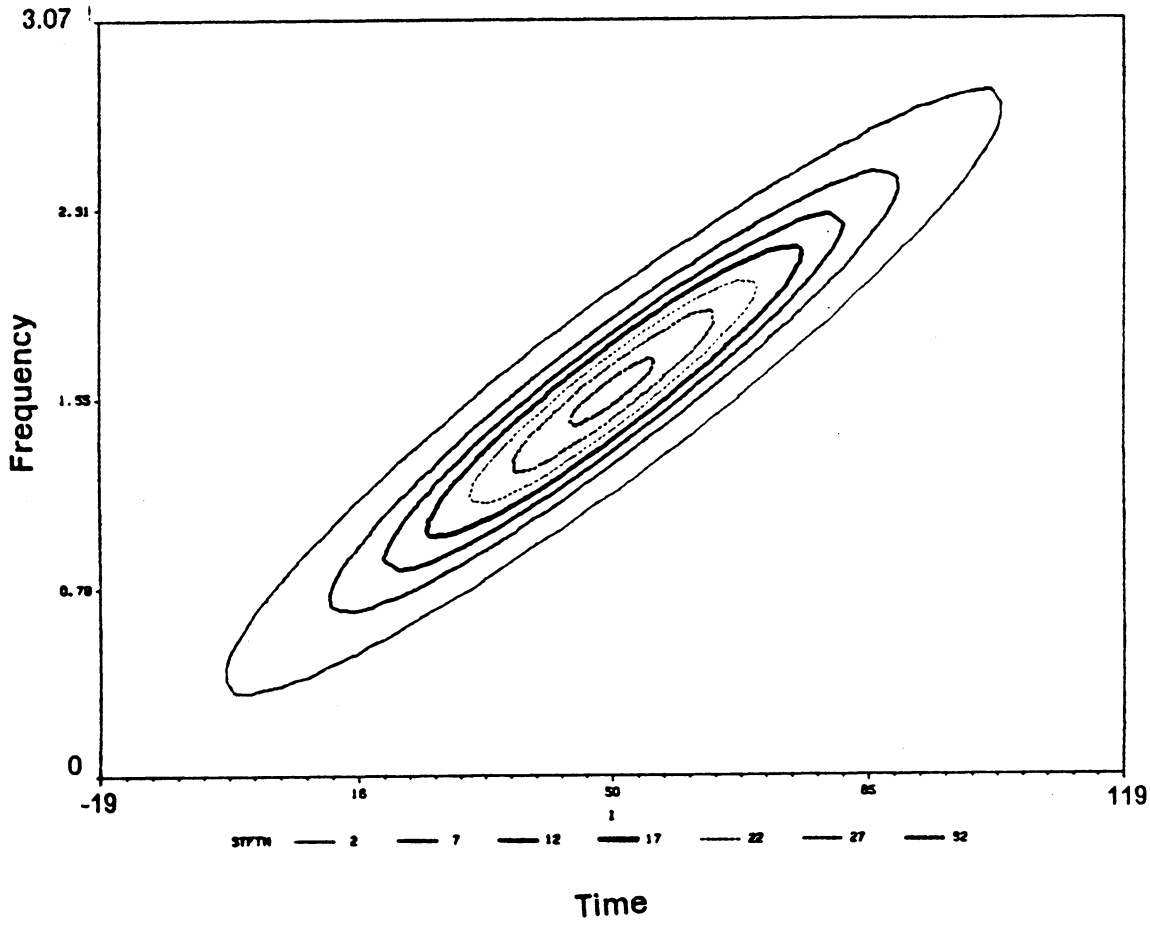

Figure 12. Spectrogram of the LCS $q_2(t)$, $\sigma_w = 5$ secs.

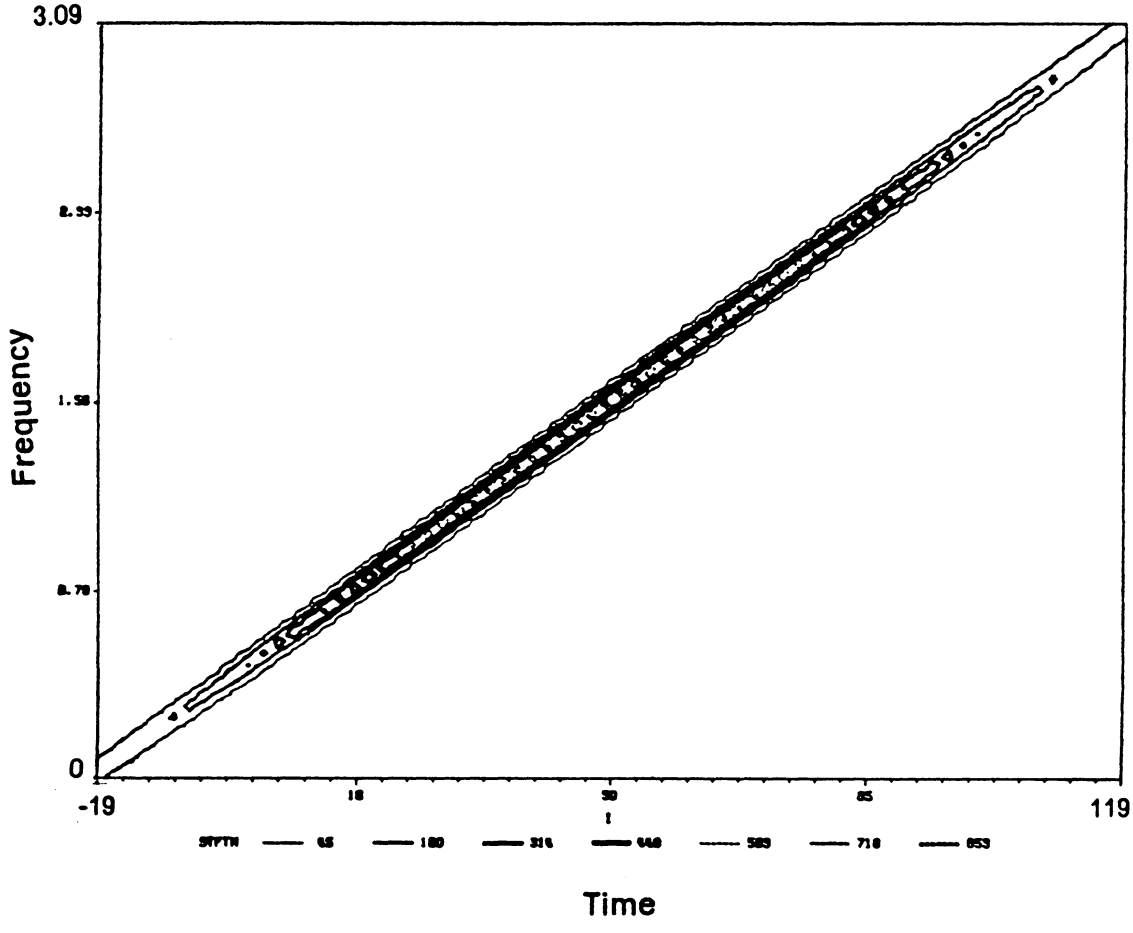

Figure 13. OSWD of the LCS $q_2(t)$, $\sigma_w = 20$ secs.

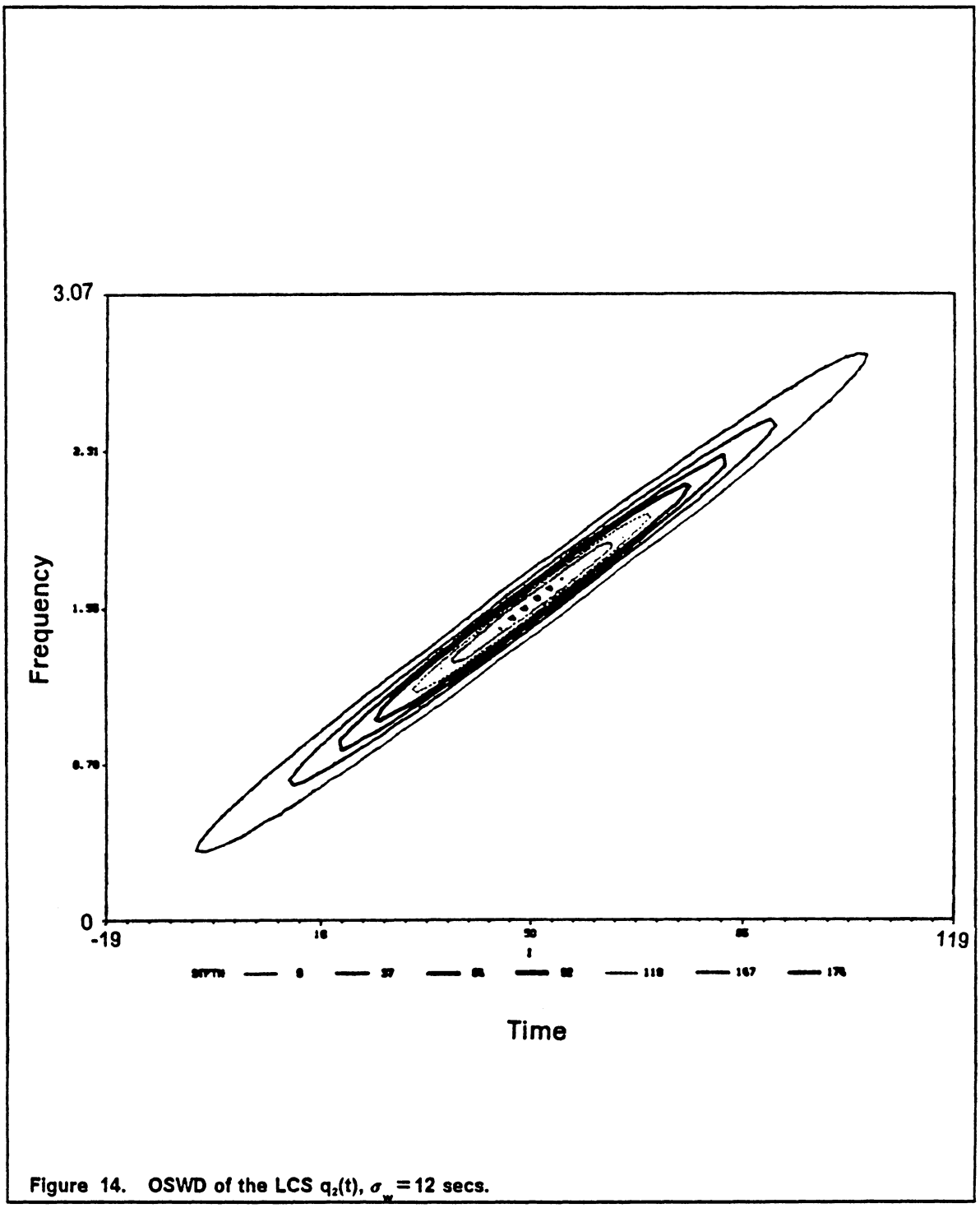

Figure 14. OSWD of the LCS $q_2(t)$, $\sigma_w = 12$ secs.

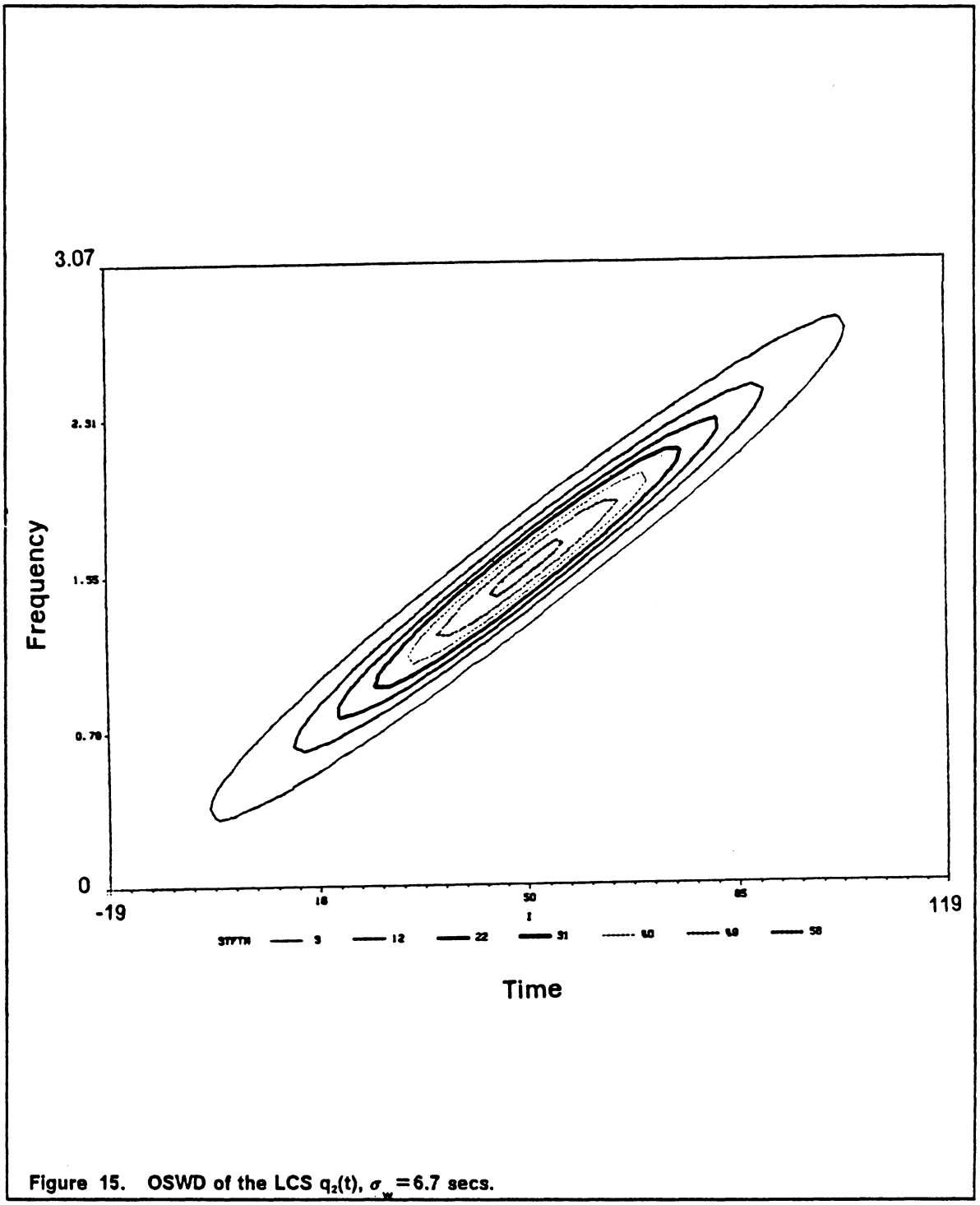

Figure 15. OSWD of the LCS $q_2(t)$, $\sigma_w = 6.7$ secs.

3.6.2 Sinusoidally frequency modulated signal

The linear chirp signal $q_2(t)$ is a rather special case where the instantaneous frequency is a linear function of time, and the signal is of short duration. A more general example is the SFM signal defined in Section 2.6.2. It shall be considered here to further illustrate the properties of the MTFRs and assess their performance. In this case, however, analytical expressions for the MTFRs are hard to obtain. Hence, we shall resort to numerical simulation.

3.6.2.1 Wigner distribution

The WD of the signal $q_3(t)$ is shown in Fig. 16. Notice the complexity of the pattern given by the WD to represent this rather simple signal. This complexity arises from the fact that the SFM signal generates "internal" cross-terms which can assume negative values. The problem of negative cross-terms does not arise in the case of the linear chirp signal.

3.6.2.2 Pseudo-Wigner distribution

The PWD of the signal $q_3(t)$ for different analysis windows length are shown in Fig. 17, 18, 19 and 20, with σ_w = 30, 20, 10 and 7 secs respectively. Close inspection has shown that the PWD has negative values for σ_w = 30, 20, and 10 secs. The PWD is positive, however, when σ_w = 7 secs.

3.6.2.3 Short-time Fourier transform

The spectrogram of $q_3(t)$ for different analysis windows is shown in Fig. 21, 22, 23 and 24, with σ_w = 20, 10, 7 and 5 sec respectively. The spectrogram in Fig. 21 (σ_w = 20 secs) is

unsatisfactory for two reasons. First, it has large BW around t=0, and second, it gives the impression that the signal consists of two high-energy pulses at $t = -50$ and $t = 50$. Hence, wrong conclusions about the structure of the signal might be reached. The spectrogram in Fig. 23 is computed with $\sigma_w = 7$ secs. It gives a very clear pattern and a reasonably small BW, which is narrower than the BW given in Fig. 21. Reducing σ_w further, however, results in a less sharp representation.

3.6.2.4 Optimally smoothed Wigner distribution

The OSWD of $q_3(t)$ for different analysis windows are shown in Fig. 25, 26, and 27, with $\sigma_w = 20$, 10, and 7 secs respectively. The OSWD given in Fig. 25 ($\sigma_w = 20$) is sharp and has a narrow BW. The highest sharpness is obtained around $t = 0$ where the assumption of a locally quadratic phase (linear instantaneous frequency) holds. The largest BW occurs at $t = \pm 50$ where the assumption is not accurate, since the instantaneous frequency is asymptotic to a shifted parabola. Decreasing σ_w results in a more uniform OSWD at the expense of less sharpness. When the window is short, the PWD and the OSWD of the SFM signal look remarkably similar.

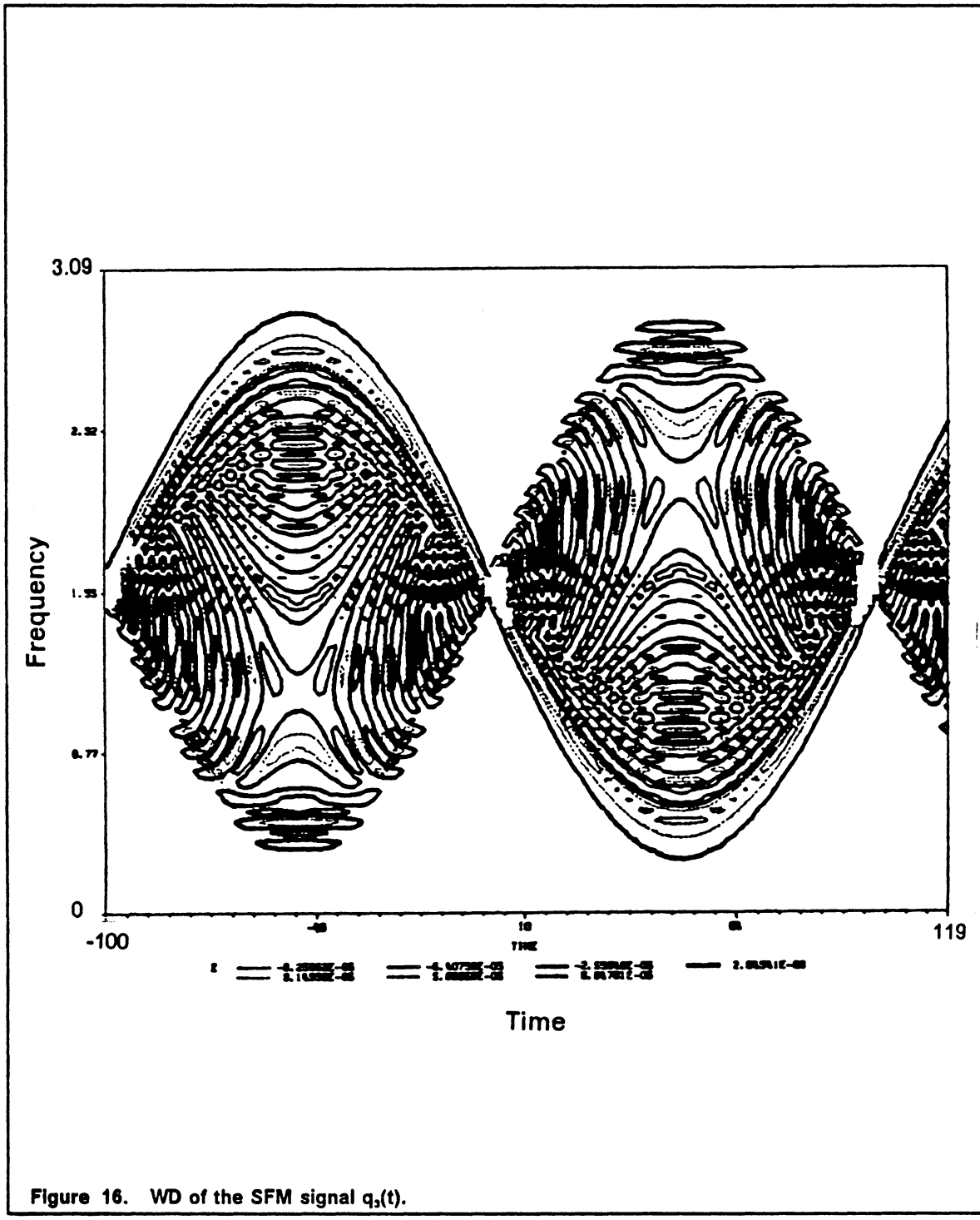

Figure 16. WD of the SFM signal $q_3(t)$.

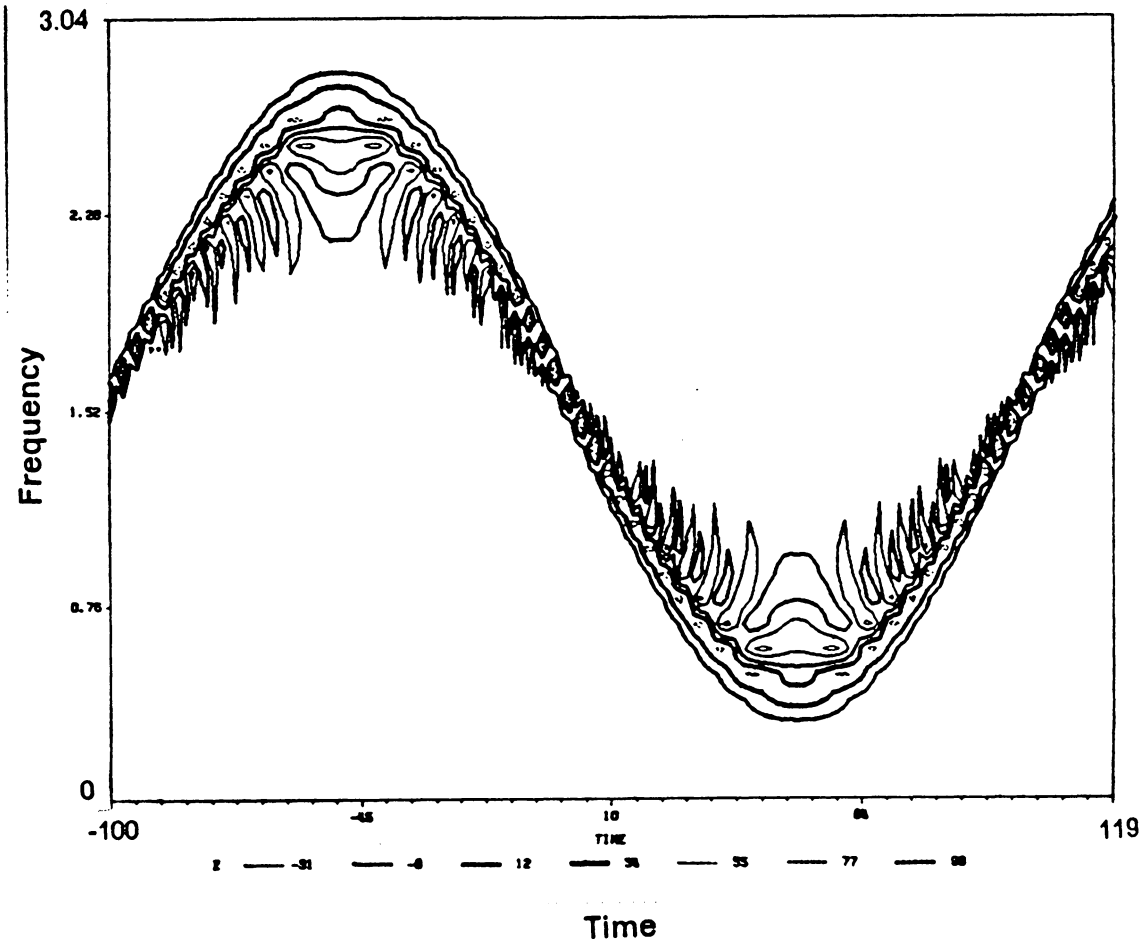

Figure 17. PWD of the SFM signal $q_3(t)$, $\sigma_w = 30$ secs.

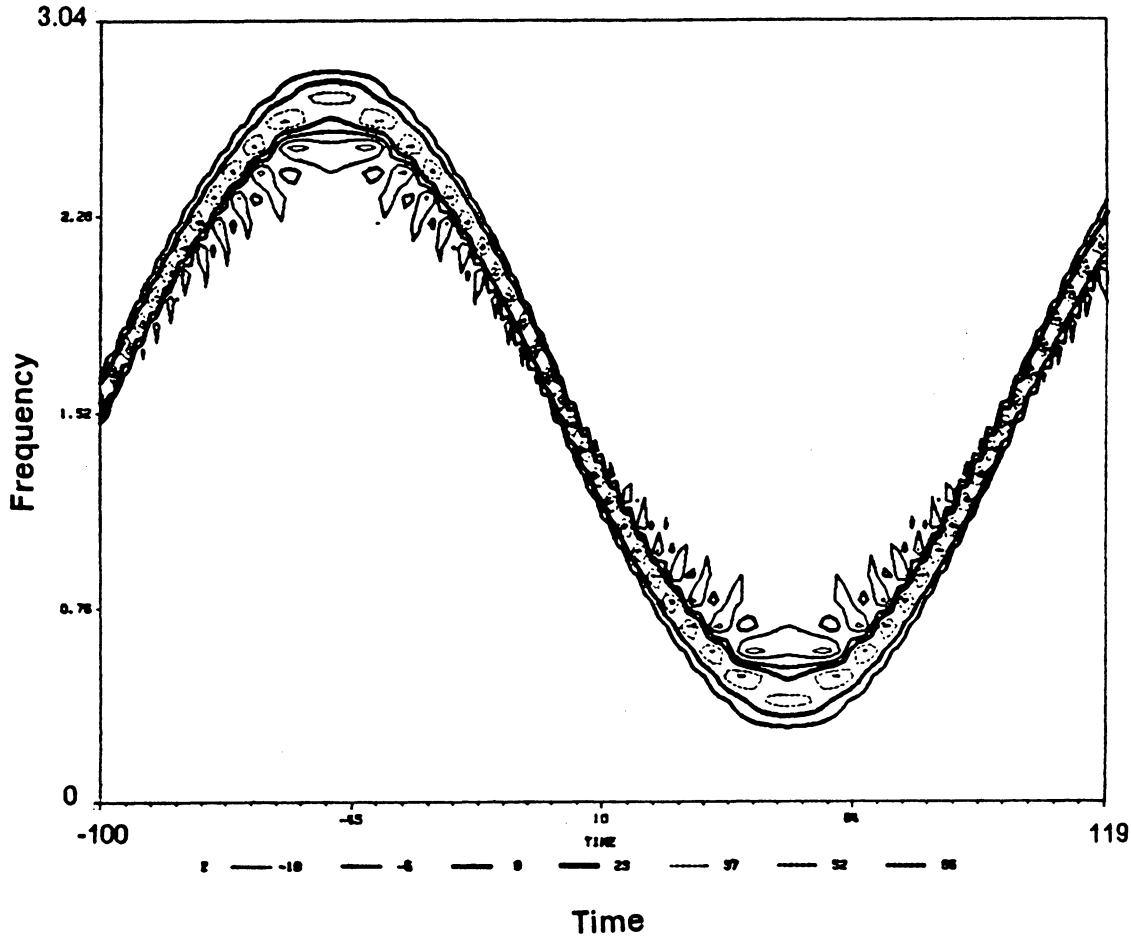

Figure 18. PWD of the SFM signal $q_3(t)$, $\sigma_w = 20$ secs.

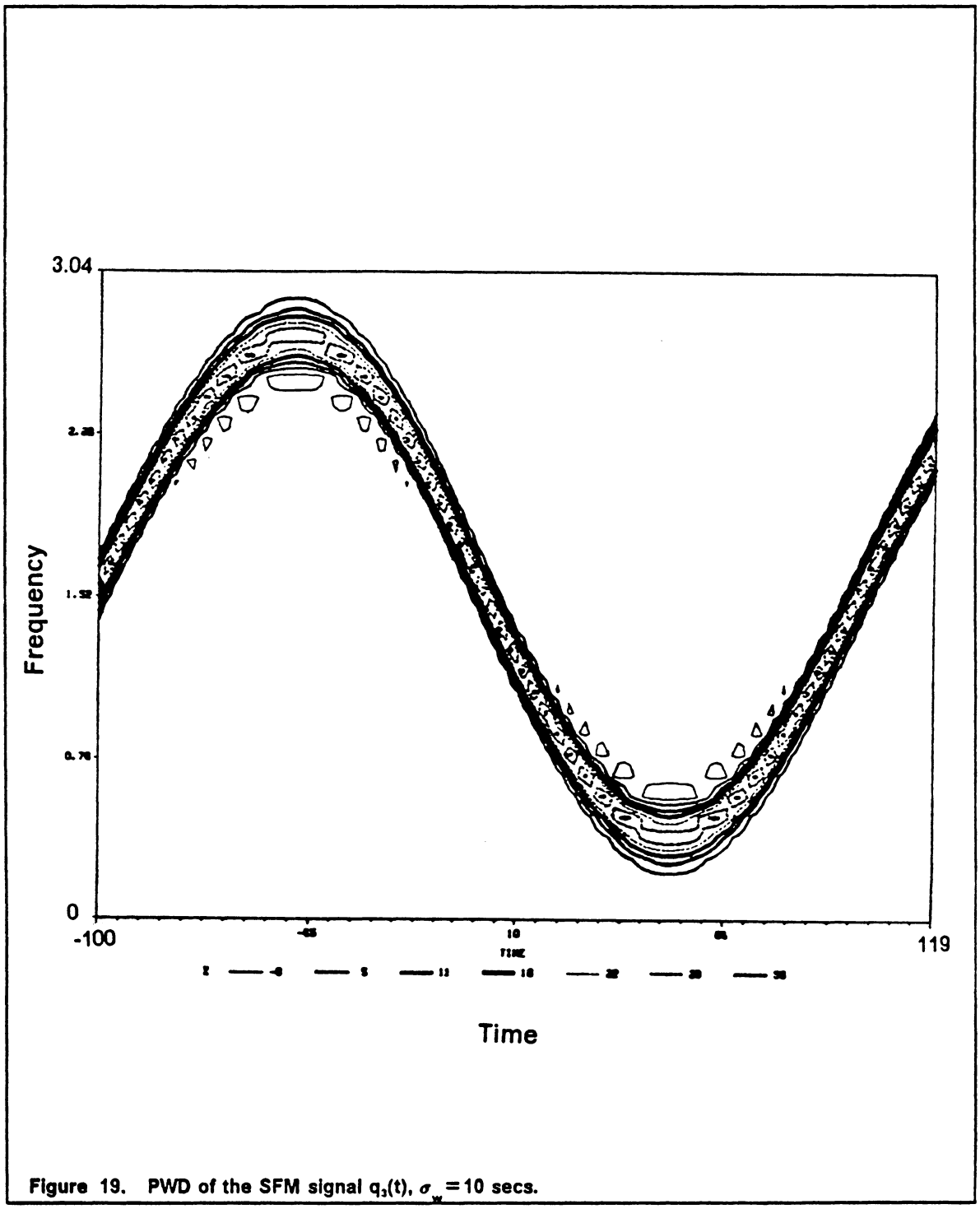

Figure 19. PWD of the SFM signal $q_3(t)$, $\sigma_w = 10$ secs.

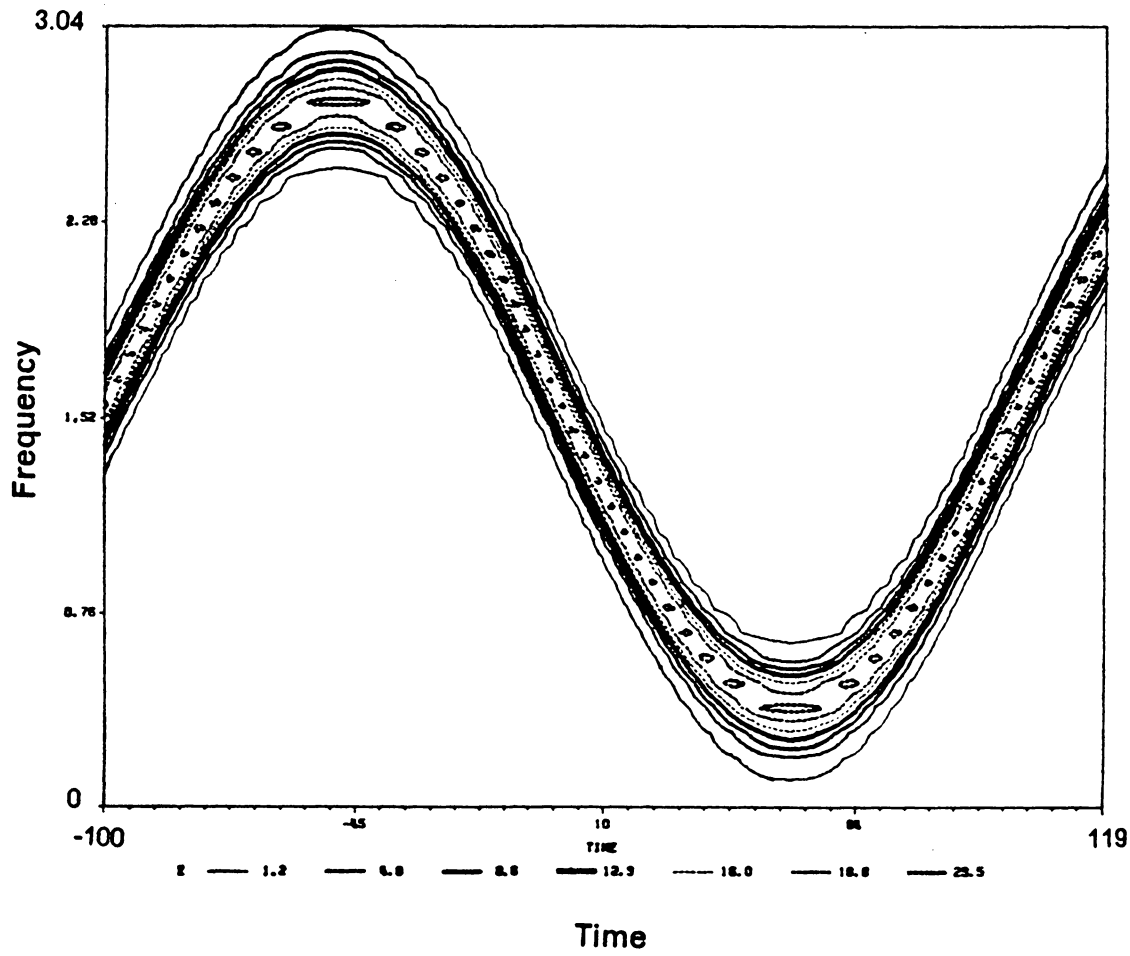

Figure 20. PWD of the SFM signal $q_3(t)$, $\sigma_w = 7$ secs.

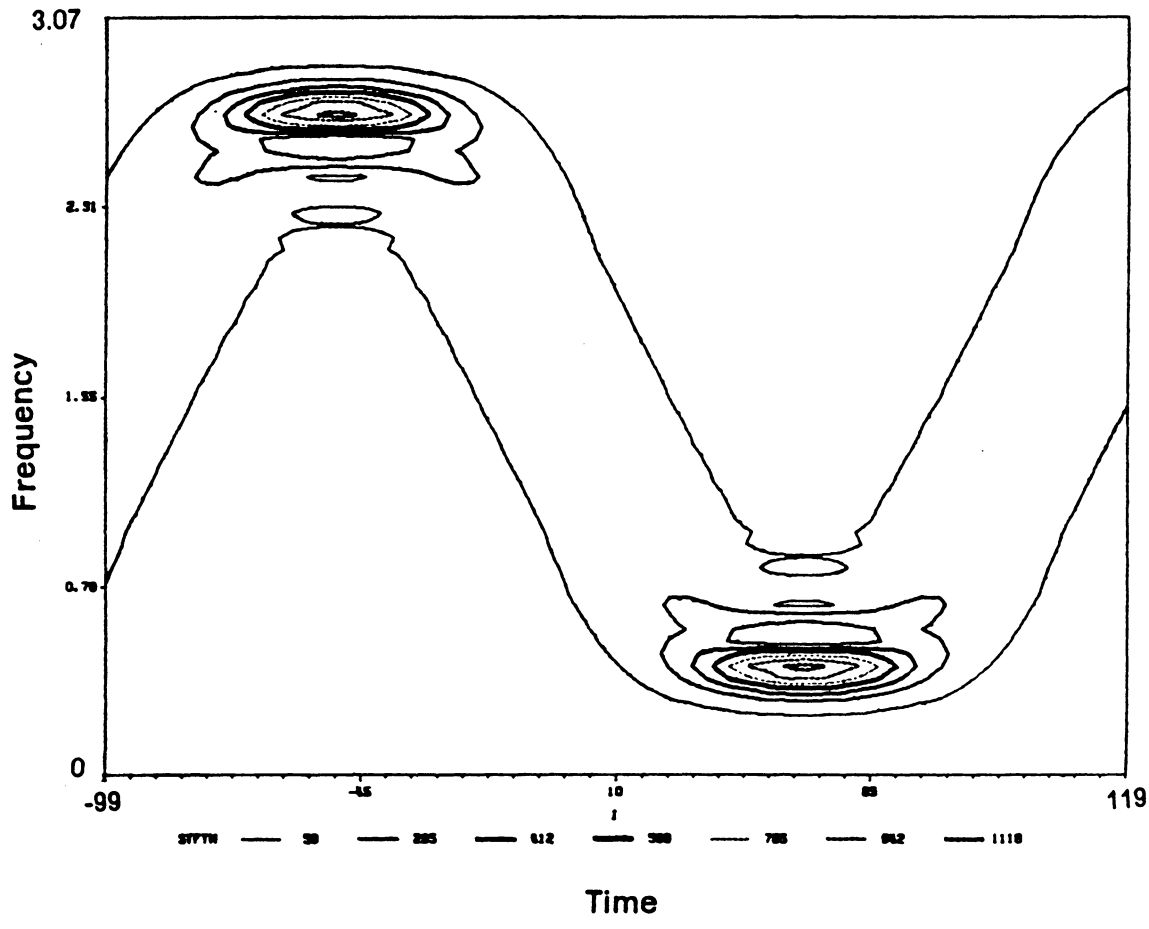

Figure 21. Spectrogram of the SFM signal $q_3(t)$, $\sigma_w = 20$ secs.

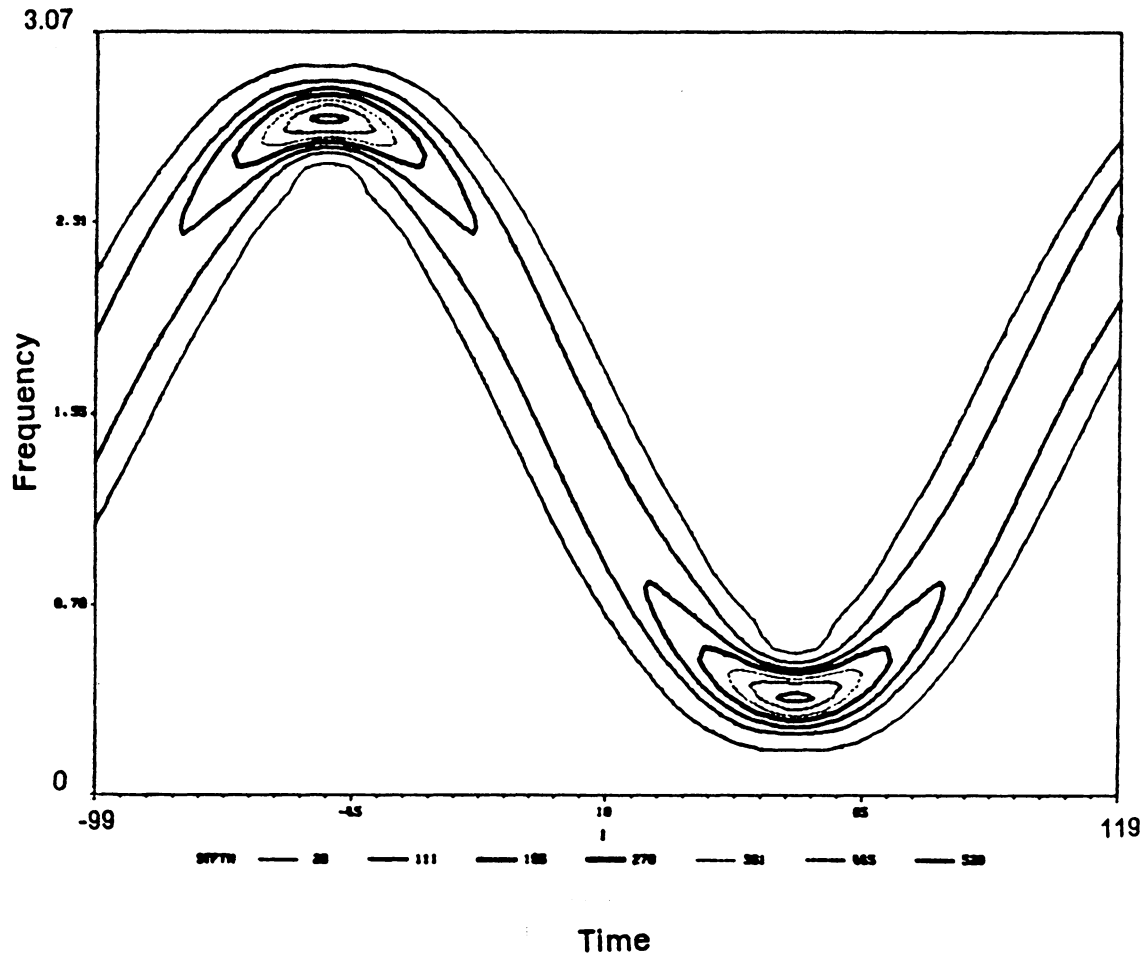

Figure 22. Spectrogram of the SFM signal $q_3(t)$, $\sigma_w = 10$ secs.

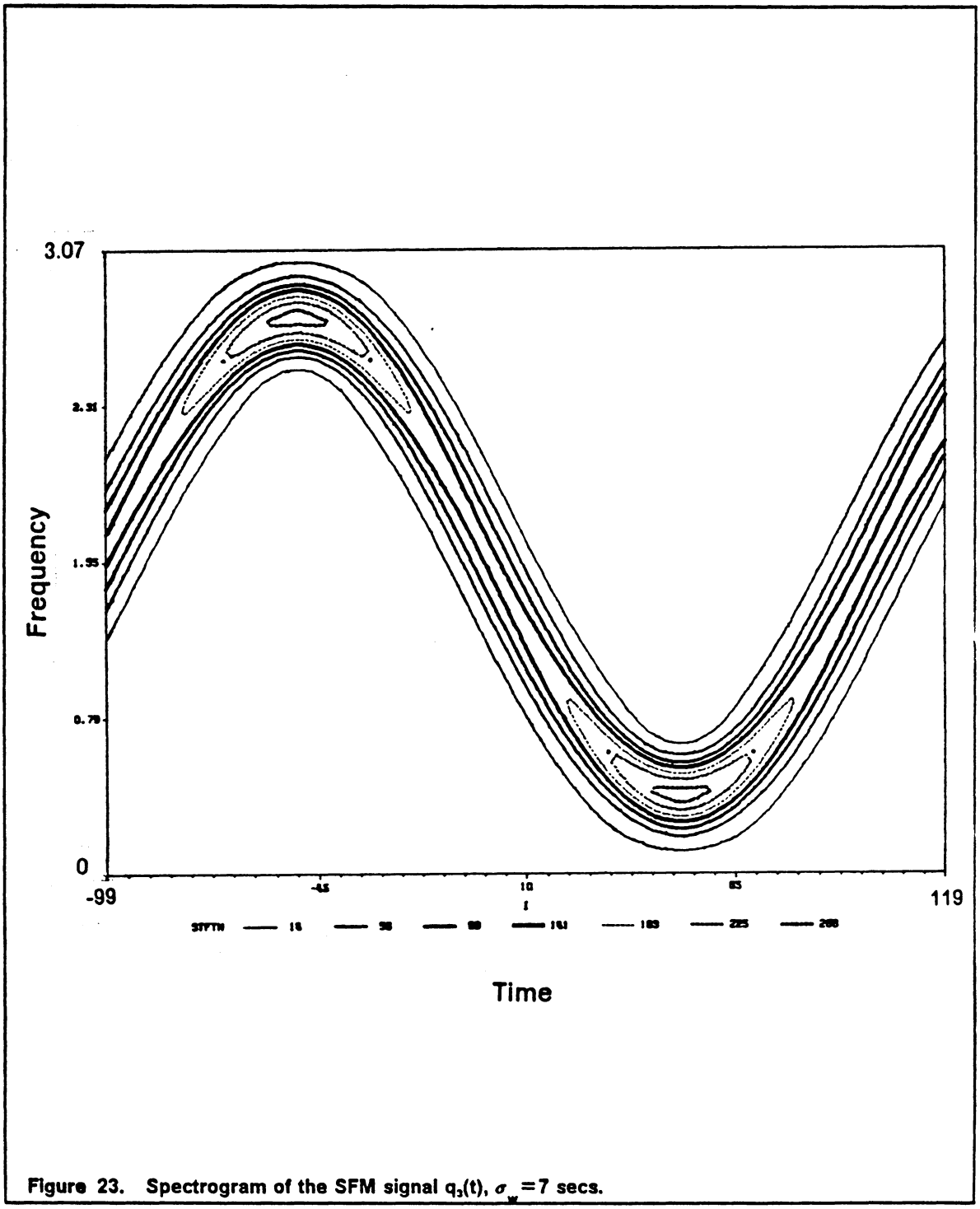

Figure 23. Spectrogram of the SFM signal $q_3(t)$, $\sigma_w = 7$ secs.

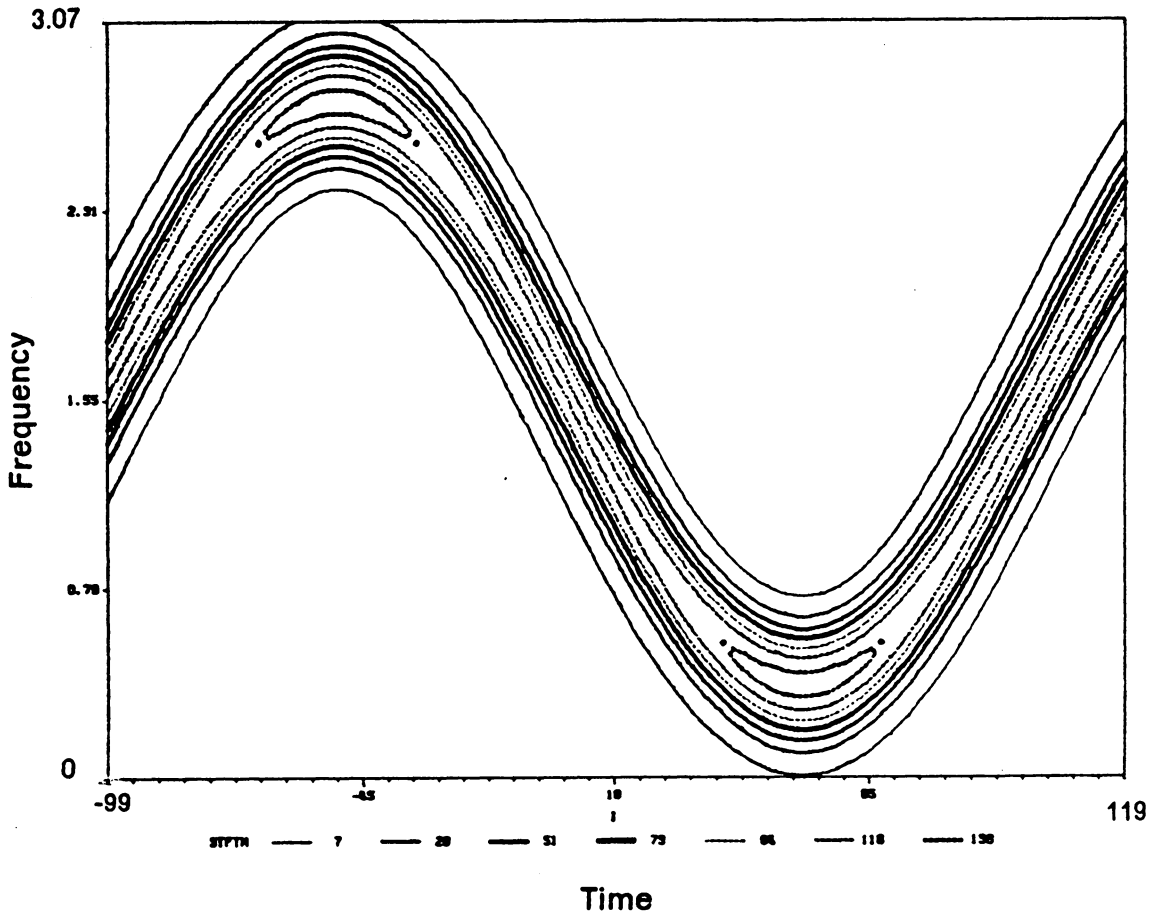

Figure 24. Spectrogram of the SFM signal $q_3(t)$, $\sigma_w = 5$ secs.

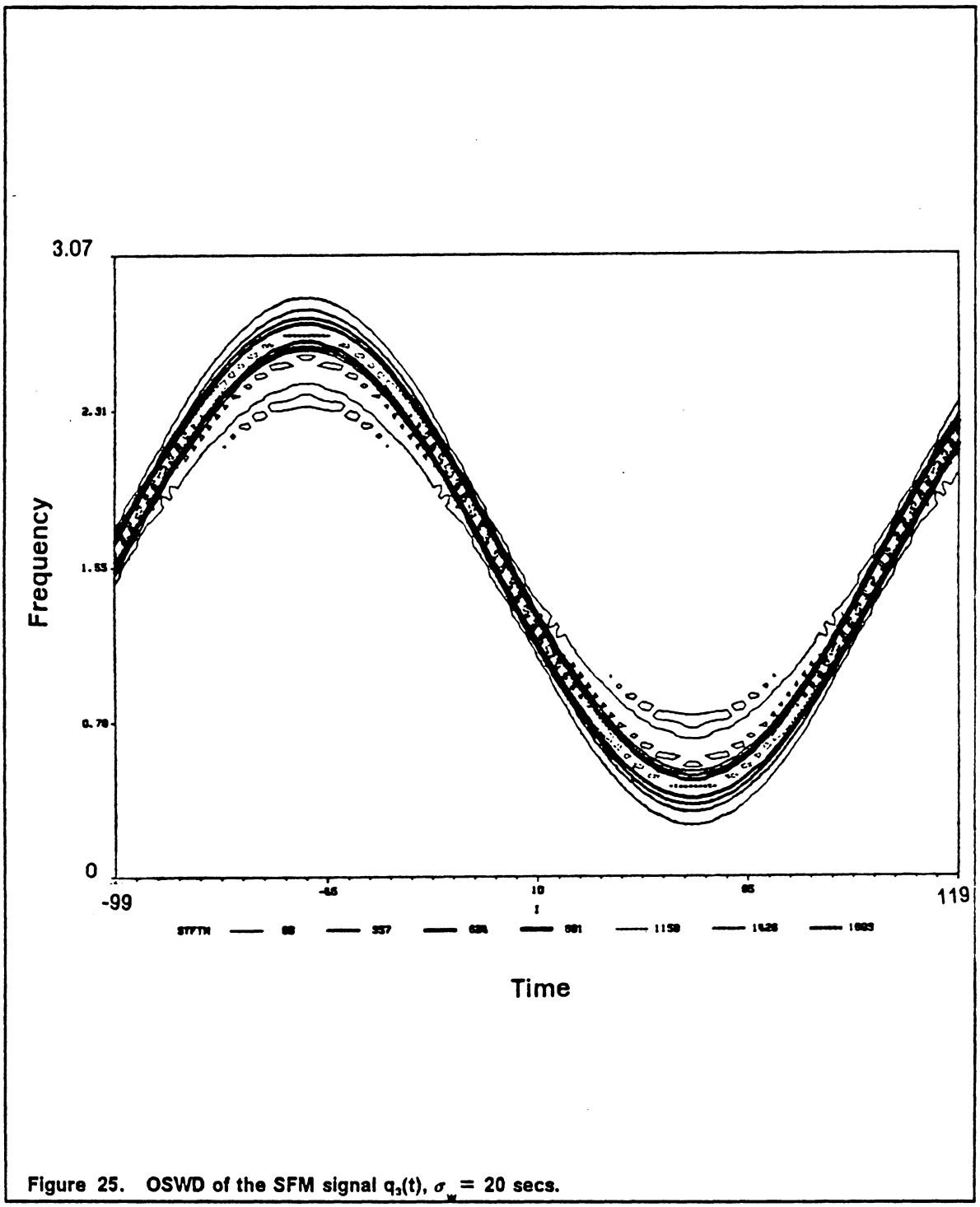

Figure 25. OSWD of the SFM signal $q_3(t)$, σ_w = 20 secs.

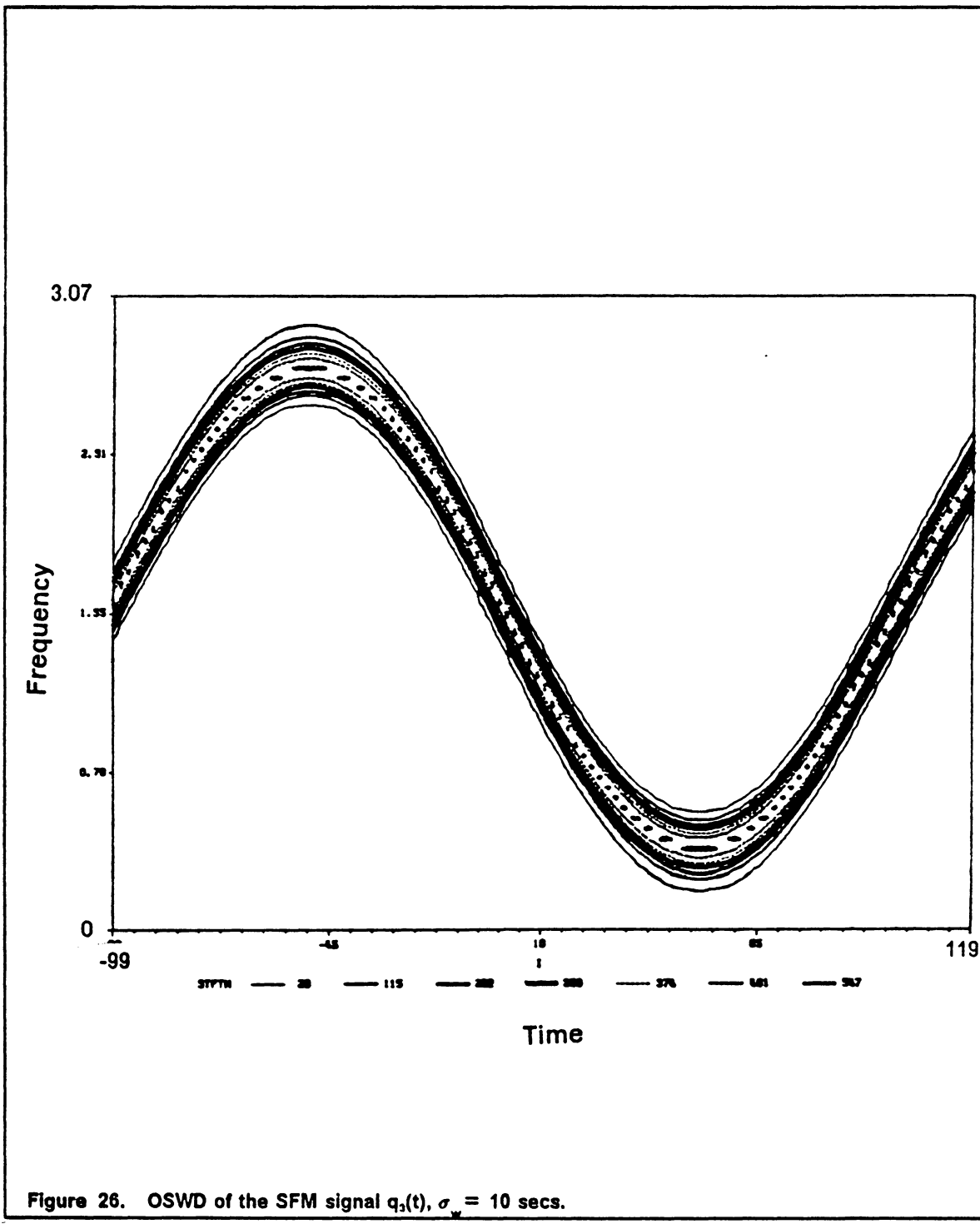

Figure 26. OSWD of the SFM signal $q_3(t)$, σ_w = 10 secs.

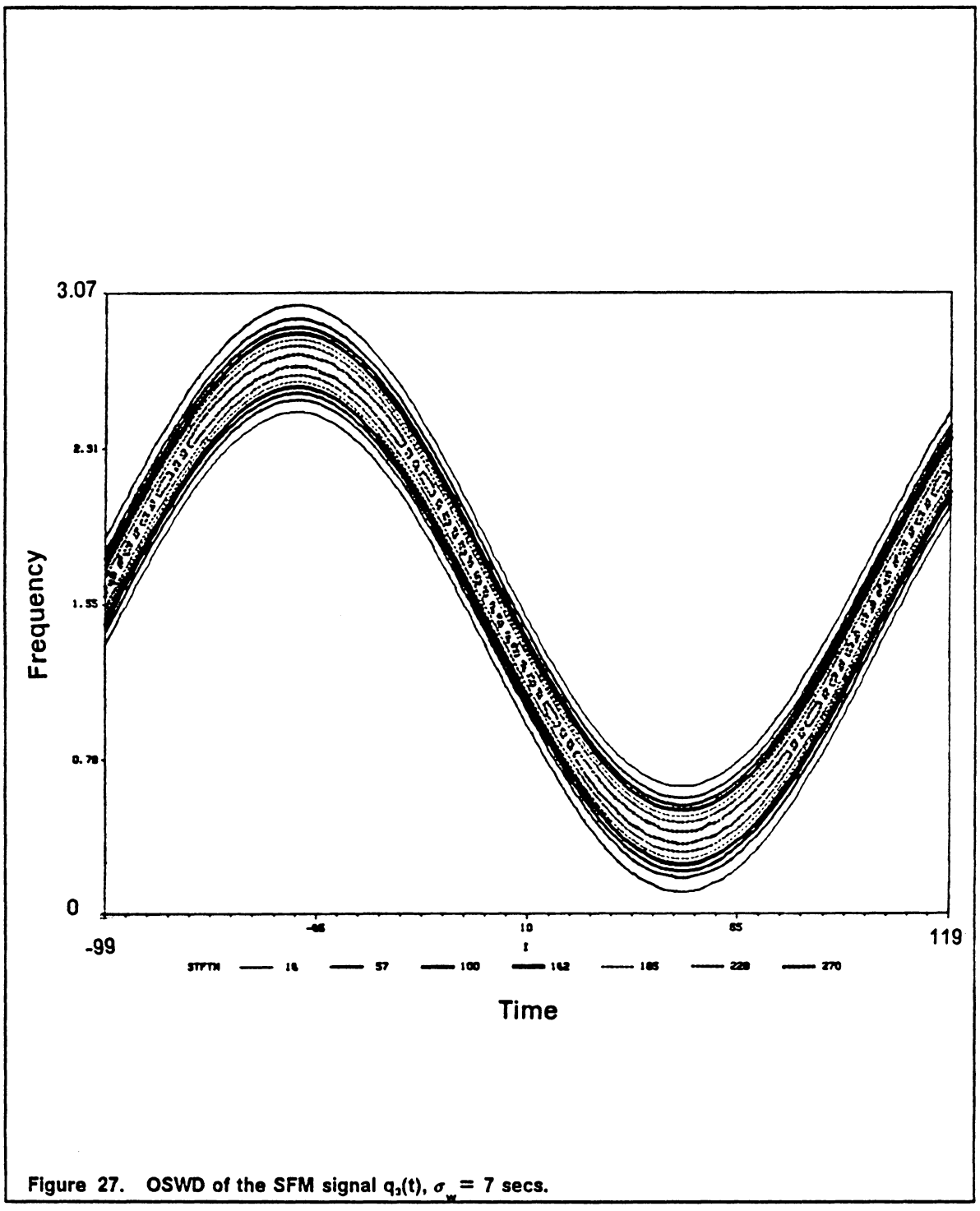

Figure 27. OSWD of the SFM signal $q_3(t)$, σ_w = 7 secs.

3.7 Comparison of different MTFRs

3.7.1 Characterization of the region of support

The NAF of the OSWD of the SFM signal $q_3(t)$, computed with $\sigma_w = 20$ secs, is shown in Fig. 28(a) where it is compared to the exact instantaneous frequency of the signal. Close agreement is noted. Fig. 30 shows the NAF of the spectrogram of $q_3(t)$, computed with $\sigma_w = 20$ secs. The figure shows close agreement when the instantaneous frequency is locally linear ($t = 0$), but shows some bias when the instantaneous frequency is locally quadratic ($t \simeq \pm 50$).

Fig. 29 shows the 90-percent BWs of the OSWD and the spectrogram, both computed with $\sigma_w = 20$ secs. Clearly, the BW of the spectrogram is higher than that of the OSWD. Note that at $t \simeq \pm 50$ the two BWs are equal. This is true because, at $t \simeq \pm 50$, the Taylor series expansion of the phase contains a linear and a cubic term in τ, but not a quadratic term. At $t \simeq 0$, however, where the phase has a quadratic term, the BW of the OSWD is substantially smaller than that of the spectrogram.

Fig. 30(a) shows the NAF of the OSWD of the amplitude-modulated SFM signal

$$q_5(t) = \left(1.5 + 1.3\cos(\frac{2\pi}{100}t)\right)q_3(t) \tag{3.7.1}$$

where $\sigma_w = 20$ secs. Fig. 30(b) shows the corresponding region of support, based on the 90-percent BW.

Fig. 31(a) shows the NAF of the spectrogram of $q_5(t)$ and Fig. 31(b) shows the corresponding 90-percent BW ROS.

For the unimodular signal $q_3(t)$, the NAFs of the spectrogram and OSWD are similar and close to the exact instantaneous frequency. This is not true for the amplitude modulated SFM signal $q_5(t)$. The NAF of the spectrogram is considerably different from the exact instantaneous frequency while the NAF of the OSWD is sufficiently close. The above result is further illustrated in Fig. 32, which shows the NAF of the spectrogram and OSWD of the signal $q_5(t)$, both computed with $\sigma_w = 7$ secs.

Fig 33. shows the NAF and ROS of the spectrogram computed with the optimal length window given by $\sigma_w = |d^2\phi/dt^2|^{-1/2}$. In comparison, Fig. 32 shows that the OSWD computed with a window of constant length, $\sigma_w = 7$ secs, gives better results.

The NAF of the PWD and WD have not been shown because it is well known that they will yield the exact values [C1]. The BW of the PWD is not meaningful unless the PWD is positive, which is not usually the case.

3.7.2 Easy recognition of patterns exhibited by MTFRs

It is desirable for a MTFR to have a simple structure. In particular, the number and ROS of the signal components should be reasonably easy to identify. In the case of the WD and the PWD, cross-terms tend to make this identification difficult. Internal cross-terms can exist even for a monocomponent signal such as a SFM signal (see Fig. 16 and fig. 17). The problem of cross-terms becomes more pronounced when more than one signal component is present. As an example, consider the signal $x(t) = 1 + q_3(t)$, where a DC level has been added to the SFM signal $q_3(t)$. The corresponding PWD is shown in Fig. 34 ($\sigma_w = 7$ secs). Figures 35 and 36 show the PWD of the signal $x(t)$ made of the sum of two SFM signals :

$$x(t) = \exp(j\frac{\pi}{2}t + j2\pi\rho\cos 2\pi\beta t) + \exp(j\frac{\pi}{2}t + 2\pi\rho\cos(2\pi\beta t + \frac{3\pi}{4})) \qquad (3.7.2)$$

for σ_w = 7 and 3 secs respectively. Fig. 36 shows that even excessive smoothing (using a very short window) does not eliminate the negatively-valued cross-terms.

Note that if the signal is made up of $n+1$ components, then there are $1+2+\cdots+n=\frac{n(n+1)}{2}$ cross-terms. For a five-component signal, there are ten external cross-terms. These do not include the internal cross-terms.

Fig. 37 shows the spectrogram of the signal with σ_w = 10 secs. The pattern is more easily recognizable as the summation of two SFM signals.

3.7.3 Separation of closely spaced signal components

In this section, we consider a problem closely related to the problem of recognizing the number and patterns of different signal components; namely, we consider the ability of an MTFR to resolve or separate two closely spaced signal components. Since the WD suffers heavily from the existence of cross-terms, it is not included here. The signal

$$x(t) = q_2(t) + q_2(t - S) \tag{3.7.3}$$

consisting of the sum of two identical linear chirp signals separated by S secs is studied. The spectrogram of $x(t)$ is shown in Fig. 38, with $\sigma_w = 14$ and $S = 30$ secs. The spectrogram shows a pattern consisting of several horizontal lines, hence suggesting that the signal is a sum of several sinusoidal pulses centered at different times. This phenomenon has been detected in [G3]. The PWD of the same signal is computed with the same window and is shown in Fig. 39. Ignoring the cross-terms, the human eye can distinguish the two linear chirp signal components of the signal. If the components are more closely spaced, i.e. $S = 20$, the pattern shown in Fig. 40. is obtained. The two components become barely separable. Fig. 41, 42 and 43 show the PWD of x(t) for $S = 20, 10$ and 5 secs respectively, all computed with $\sigma_w = 30$. Clearly, increasing the window length of the PWD improves our ability to separate linear chirp signal components using the PWD. Note, however, that if more general components such as

SFM signals are used, or if more components are present, increasing σ_w will increase the effect of cross-terms and hence make the separation more difficult.

Finally, Fig. 44 and 45 show the OSWD of x(t) computed with a window length $\sigma_w = 15$, for $S = 15$ and 10 respectively. Clearly, one can separate closely spaced linear chirp signal components more easily using the OSWD.

3.7.4 Positivity

For a MTFR to be interpreted as an energy density function, the MTFR has to be real and positive. In this case only, the MTFR can be used to compute a time-varying BW of the signal. The RMS BW of a signal has no physical meaning. The WD and PWD are not always positive, and hence cannot be used to compute a time-varying BW.

3.7.5 Computational complexity and storage requirements

The WD is among the most computationally expensive MTFRs, and hence is at a disadvantage unless the signals of interest have a short duration. The PWD uses a signal independent window to limit the size of computations and storage needed at the expense of reduced resolution. The STFT and the spectrogram are computationally efficient but might give unsatisfactory results unless a signal dependent optimal window is used. Storey's optimal window length requires the derivative of the instantaneous frequency of the signal, which is not known and has to be determined. One way to estimate this quantity is to find the instantaneous frequency of the signal and then estimate its derivative. Clearly, an iterative procedure has to be adopted [K1]. First, one analyzes the signal using an arbitrary size window in order to get a first estimate of the signal instantaneous frequency and its derivative. Using these estimates, a new window, having a length closer to the optimum length, is

subsequently designed and then used to recompute the spectrogram. In general, several iterations will be necessary, but relatively few might actually be sufficient. We note, however, that the presence of amplitude modulation in the analyzed signal will severely bias the NAF of the spectrogram even if the optimal window length is used (see Eq. (3.4.7) and Fig. 31, 32 and 33). Therefore, Amplitude modulation might cause this iterative scheme to diverge.

The computation of the OSWD for locally quadratic phase signals has essentially the same computational complexity as the optimal window size spectrogram. The windows used in both cases require the same information, namely, the instantaneous frequency and its derivative. Since the NAF of the OSWD is the exact instantaneous frequency of the signal even if amplitude modulation is present (see Fig. 30), convergence to the exact instantaneous frequency is expected to be faster and more reliable in the case of the OSWD. Convergence of the iterative determination of the instantaneous frequency using the spectrogram and the OSWD remains to be investigated.

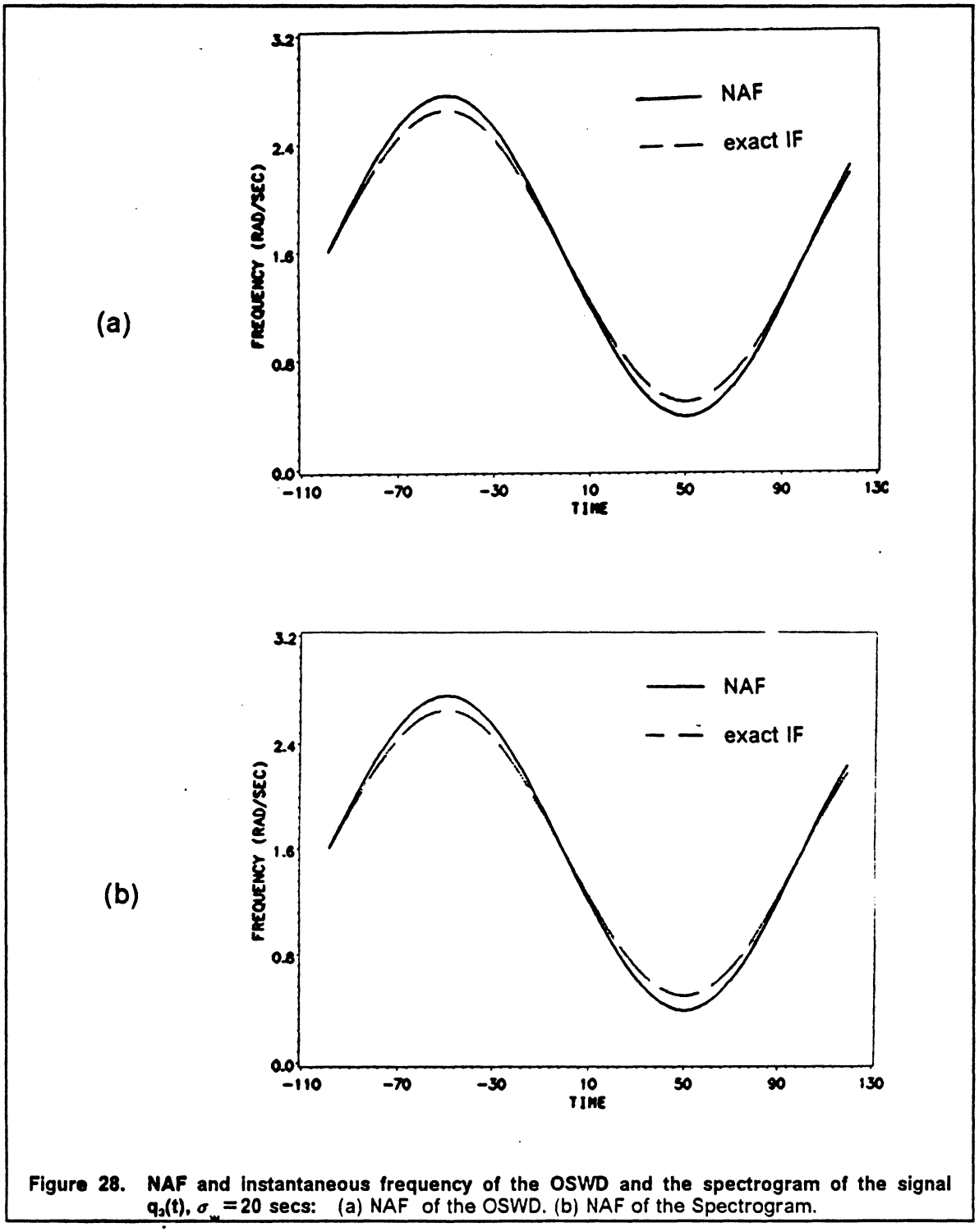

Figure 28. **NAF and instantaneous frequency of the OSWD and the spectrogram of the signal $q_3(t)$, $\sigma_w = 20$ secs:** (a) NAF of the OSWD. (b) NAF of the Spectrogram.

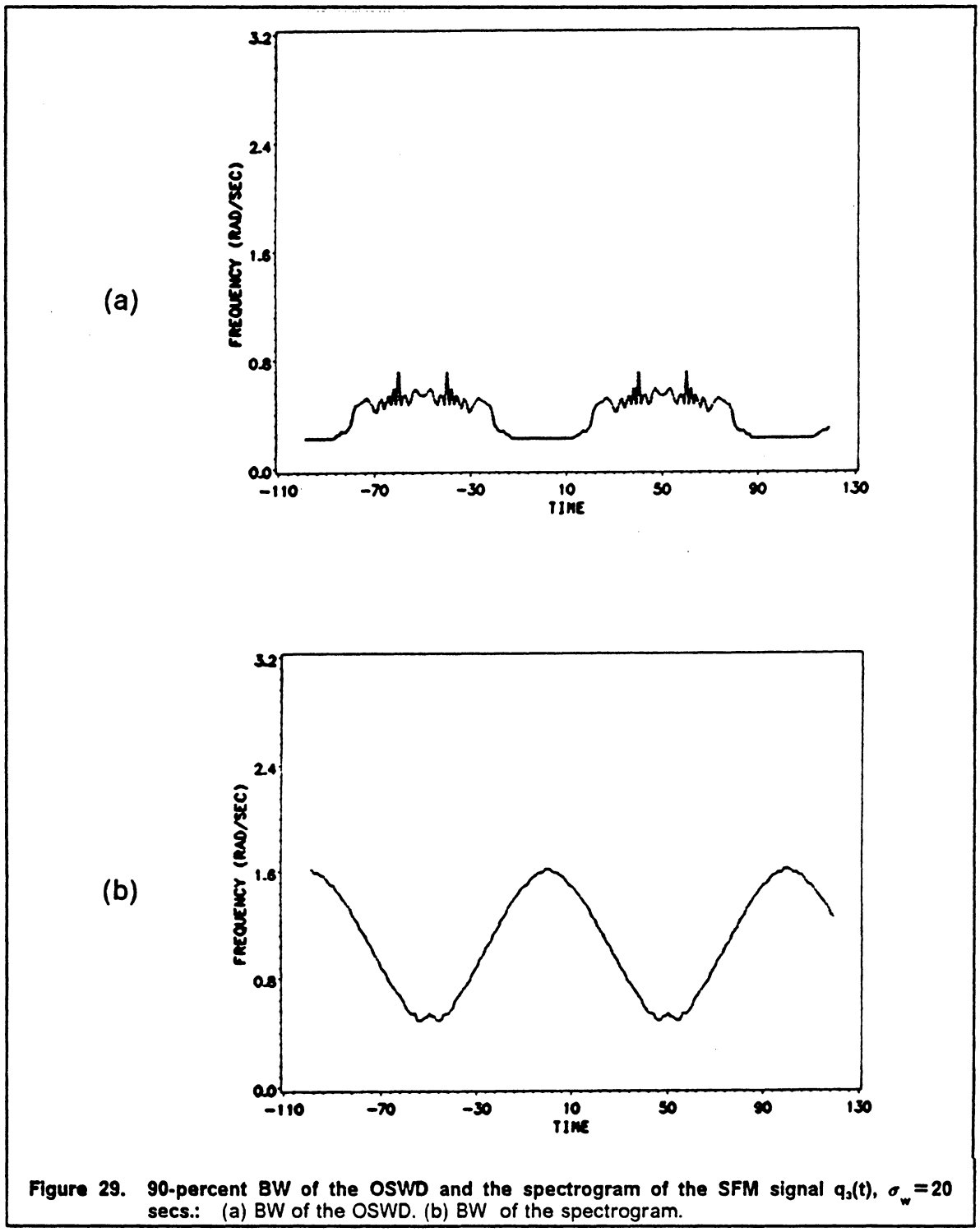

Figure 29. **90-percent BW of the OSWD and the spectrogram of the SFM signal $q_3(t)$, $\sigma_w = 20$ secs.:** (a) BW of the OSWD. (b) BW of the spectrogram.

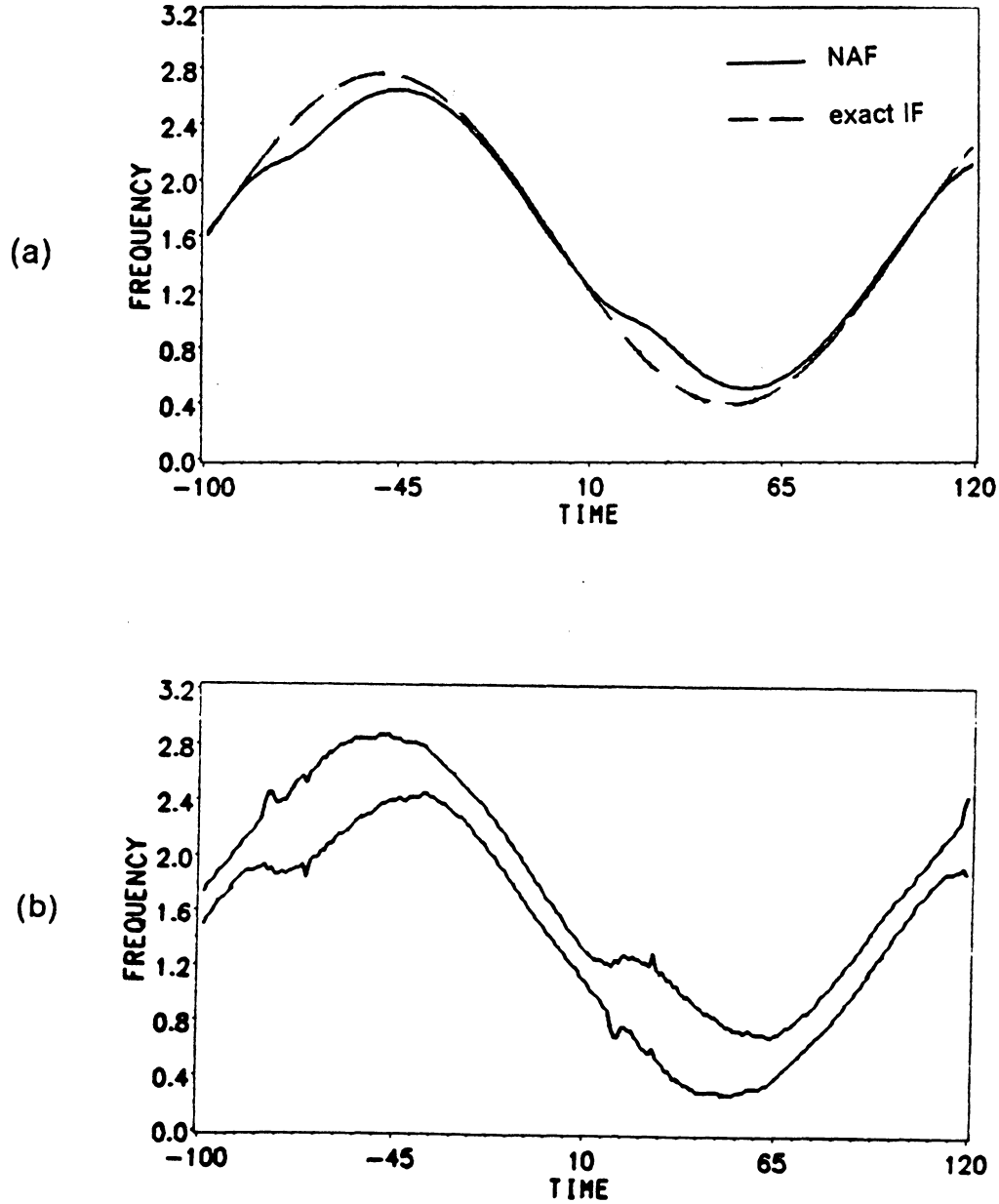

Figure 30. NAF and ROS of the OSWD of the amplitude modulated SFM signal $q_5(t)$, $\sigma_w = 20$ secs: (a) NAF of the OSWD. (b) ROS of the OSWD based on the 90-prercent BW.

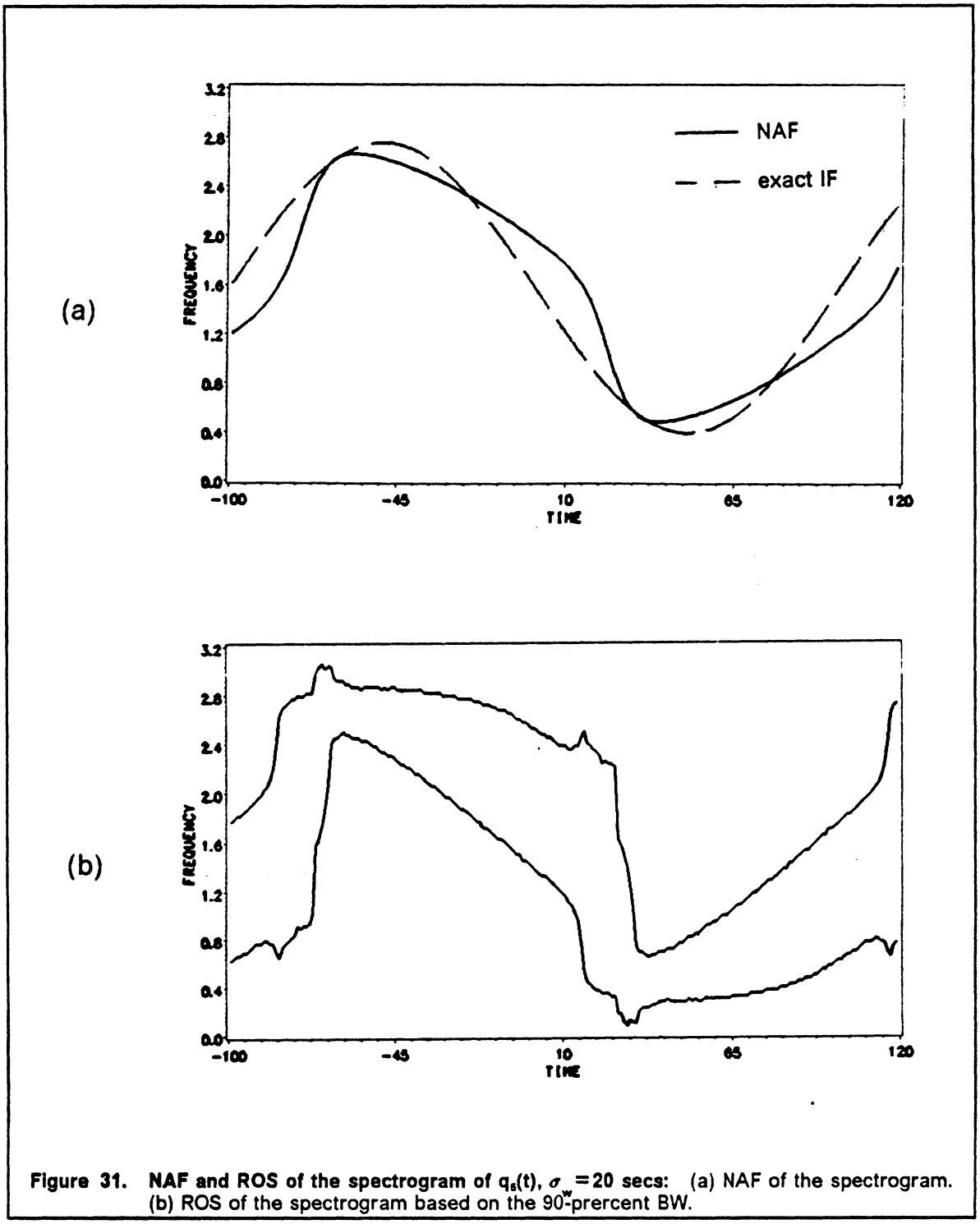

Figure 31. **NAF and ROS of the spectrogram of $q_5(t)$, $\sigma_w = 20$ secs:** (a) NAF of the spectrogram. (b) ROS of the spectrogram based on the 90-prercent BW.

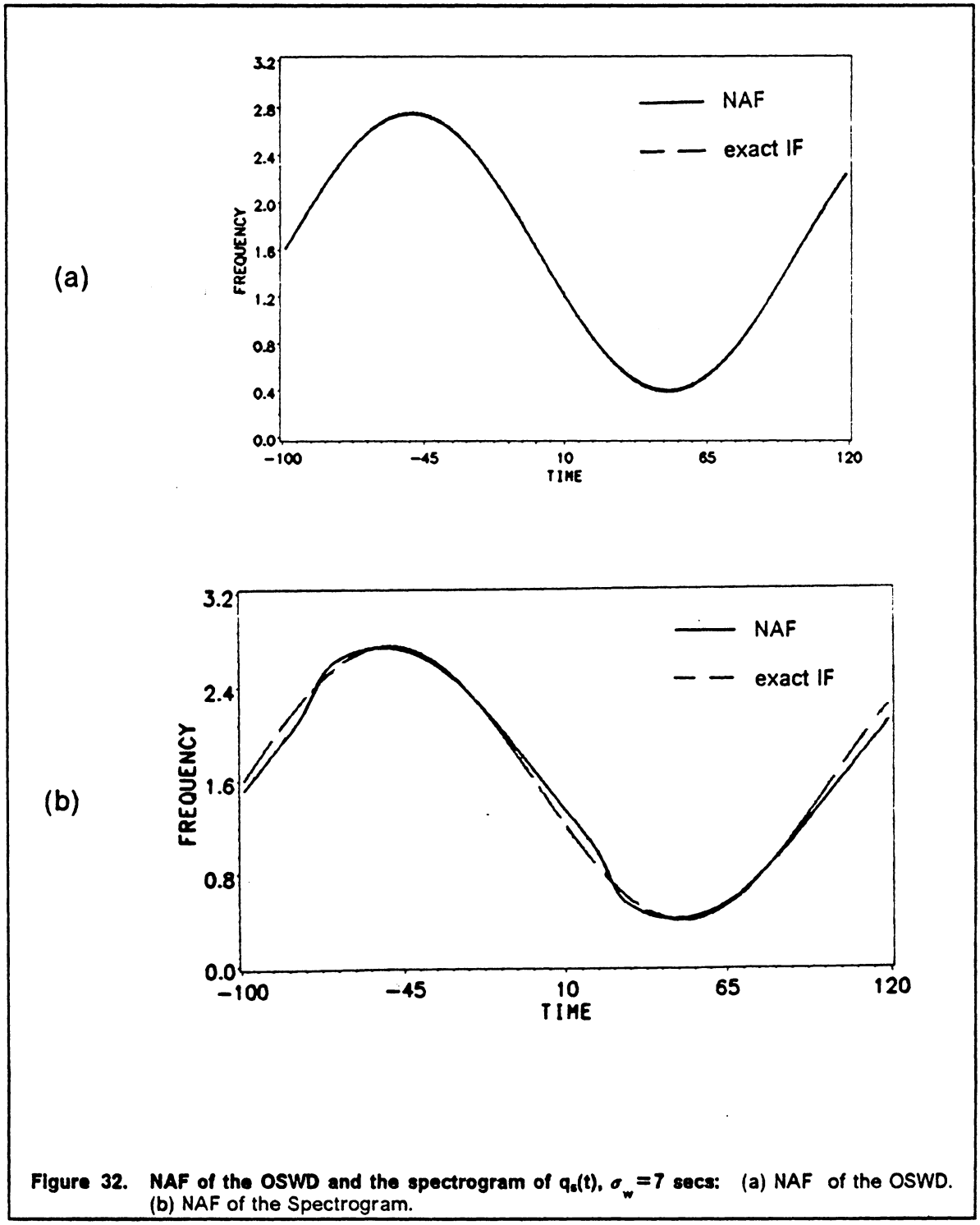

Figure 32. NAF of the OSWD and the spectrogram of $q_s(t)$, $\sigma_w = 7$ secs: (a) NAF of the OSWD. (b) NAF of the Spectrogram.

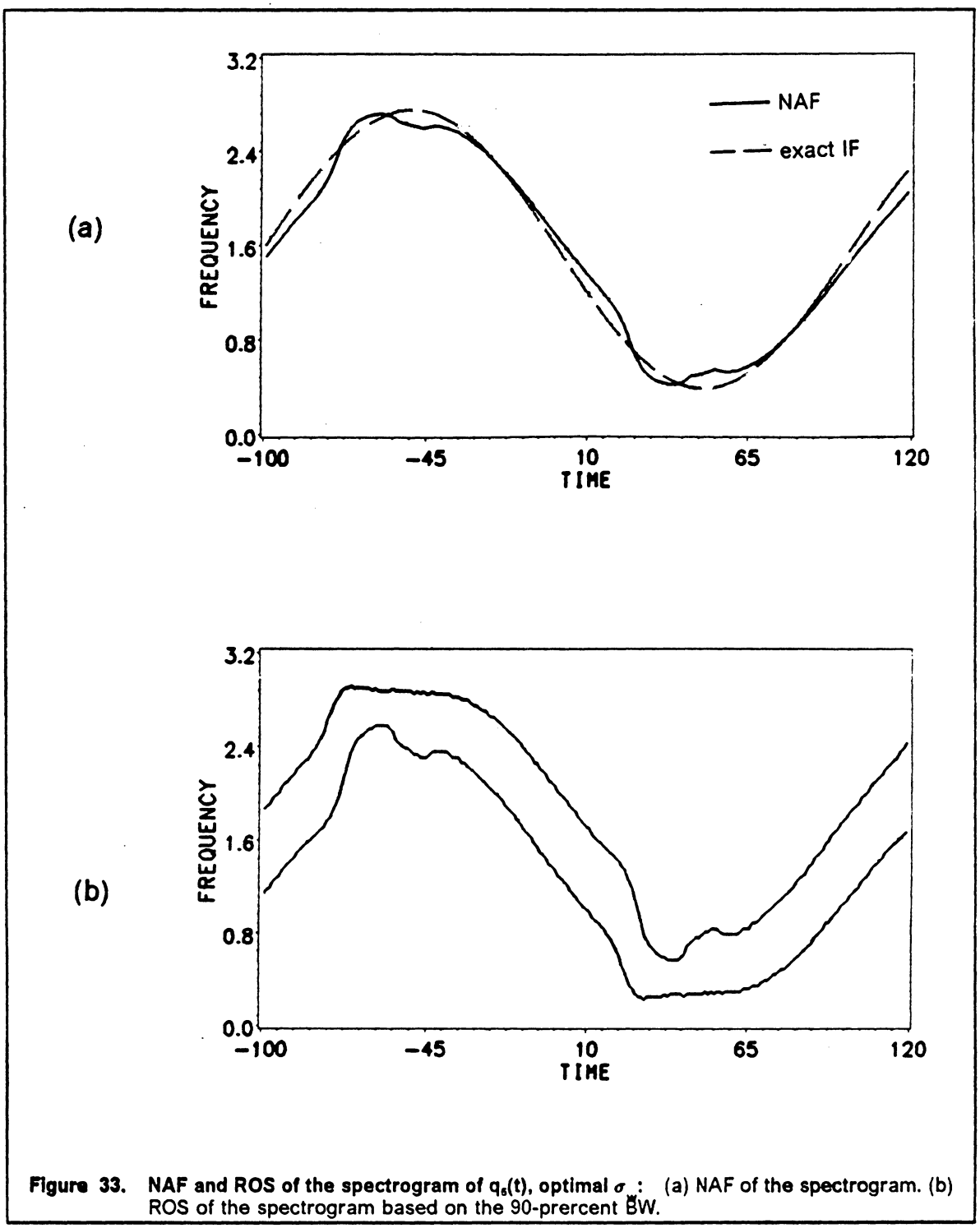

Figure 33. NAF and ROS of the spectrogram of $q_6(t)$, optimal σ : (a) NAF of the spectrogram. (b) ROS of the spectrogram based on the 90-prercent BW.

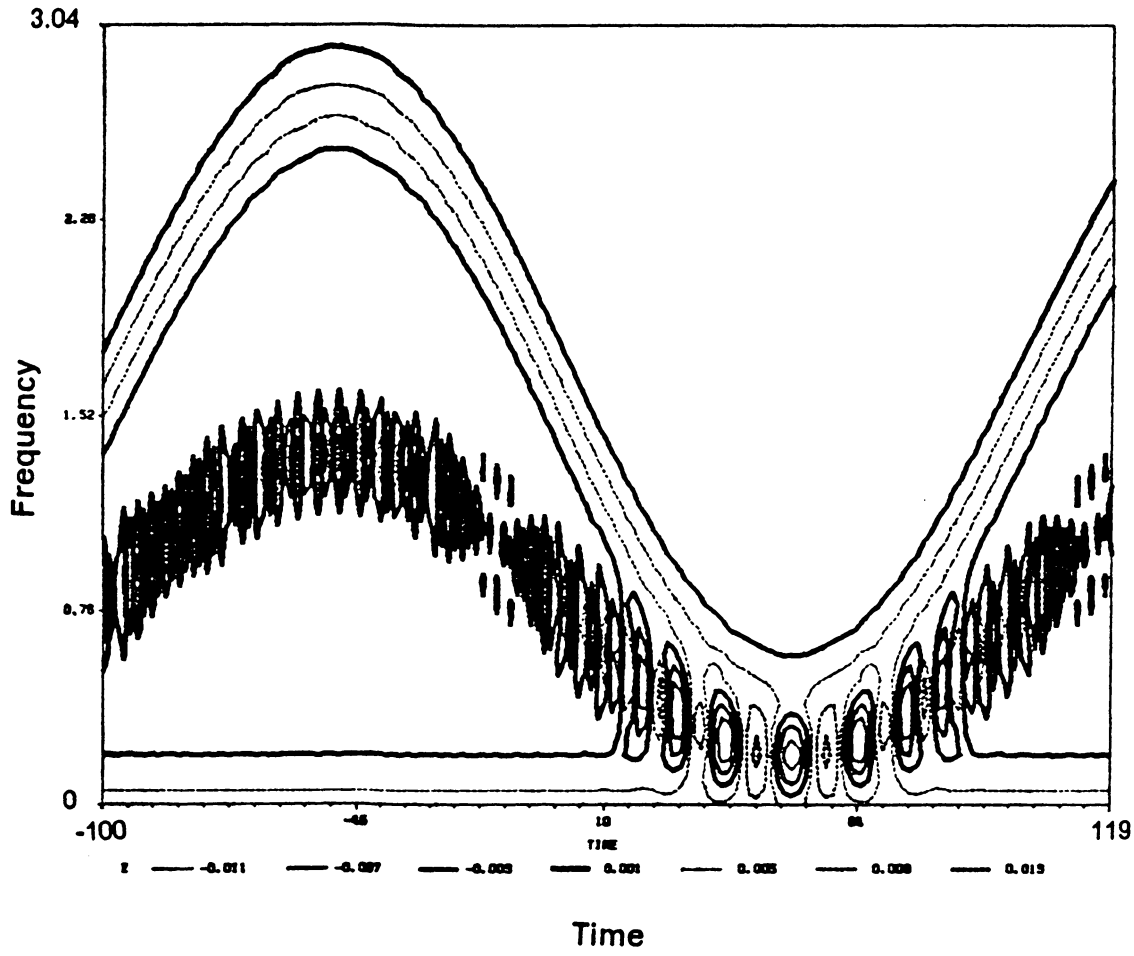

Figure 34. PWD of a biased sinusoid, $\sigma_w = 7$ secs

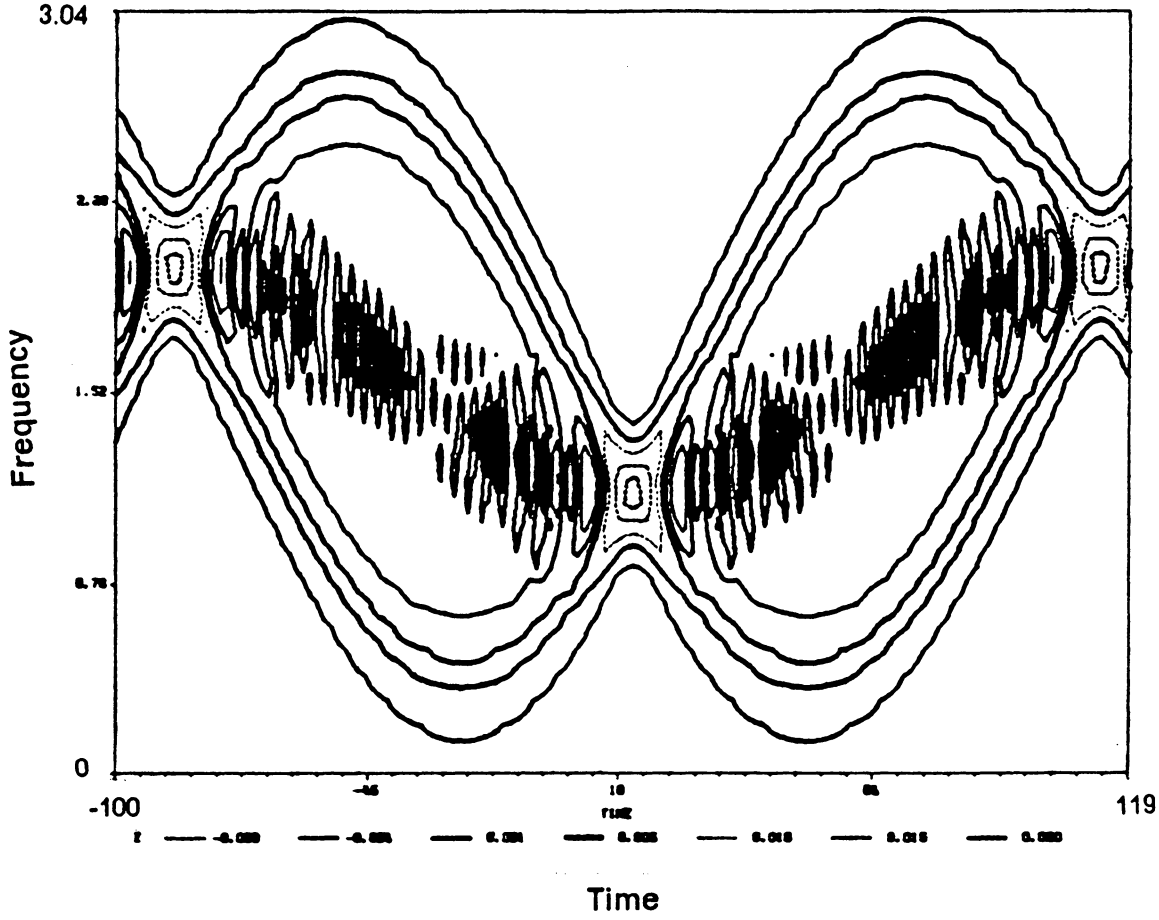

Figure 35. PWD of the sum of two SFM signals, σ_w = 7 secs.

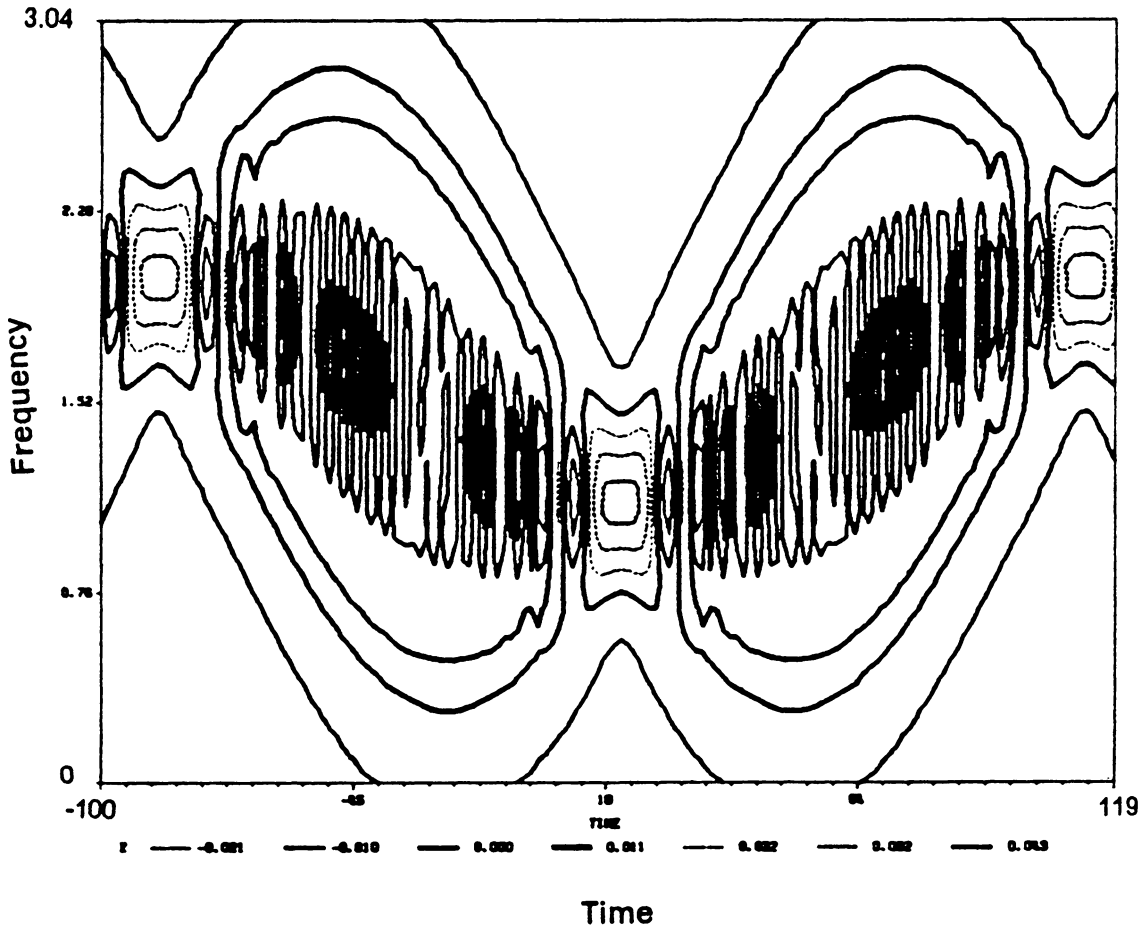

Figure 36. PWD of the sum of two SFM signals, σ_w = 3 secs.

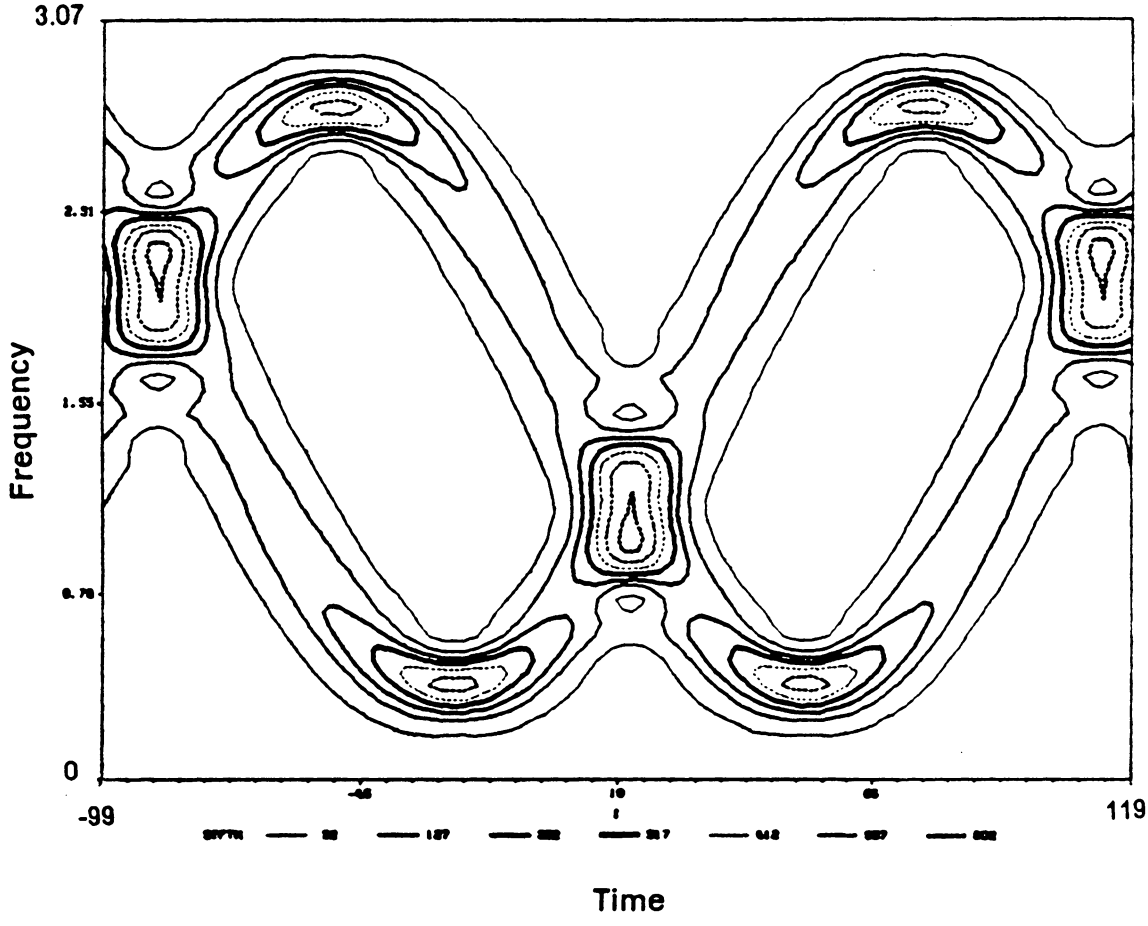

Figure 37. Spectrogram of the sum of two SFM signals, $\sigma_w = 10$ secs..

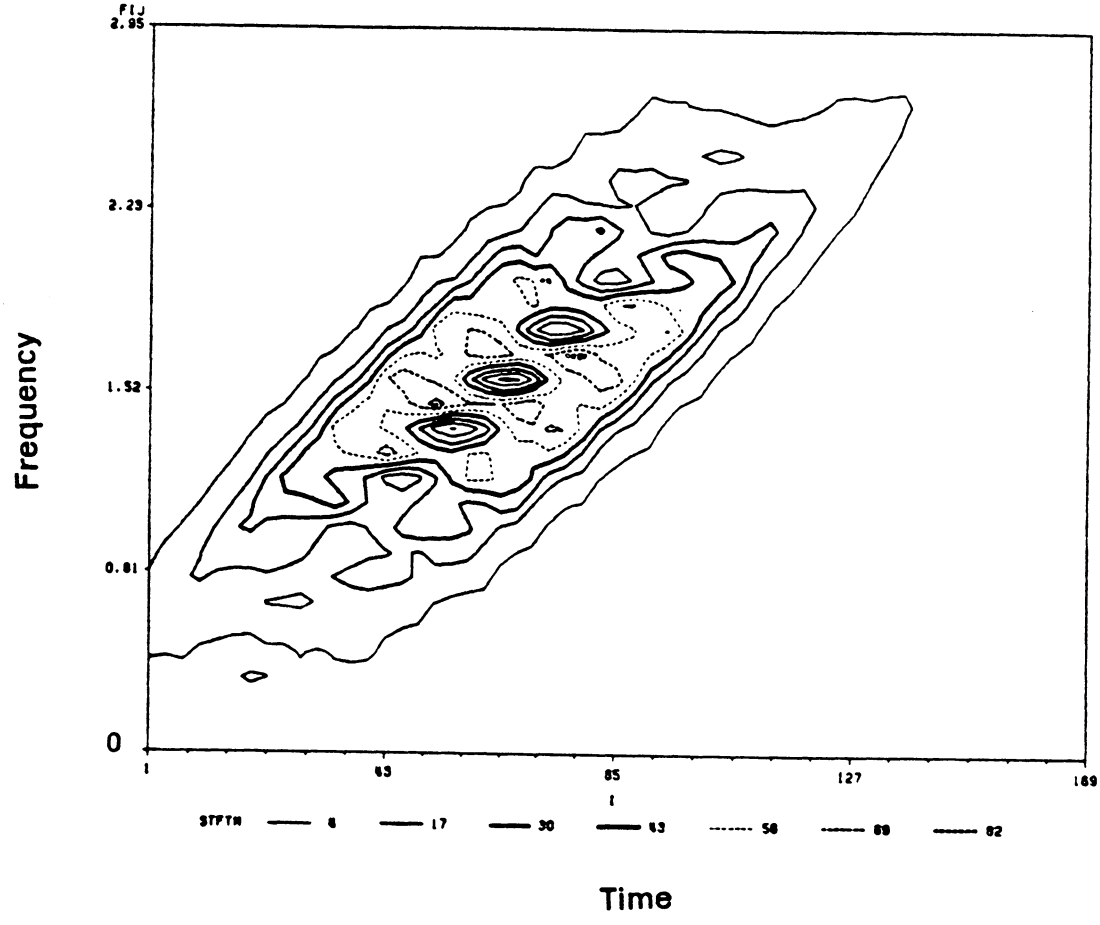

Figure 38. Spectrogram of the sum of two LCSs, $\sigma_w = 14$ secs, S=30 secs.

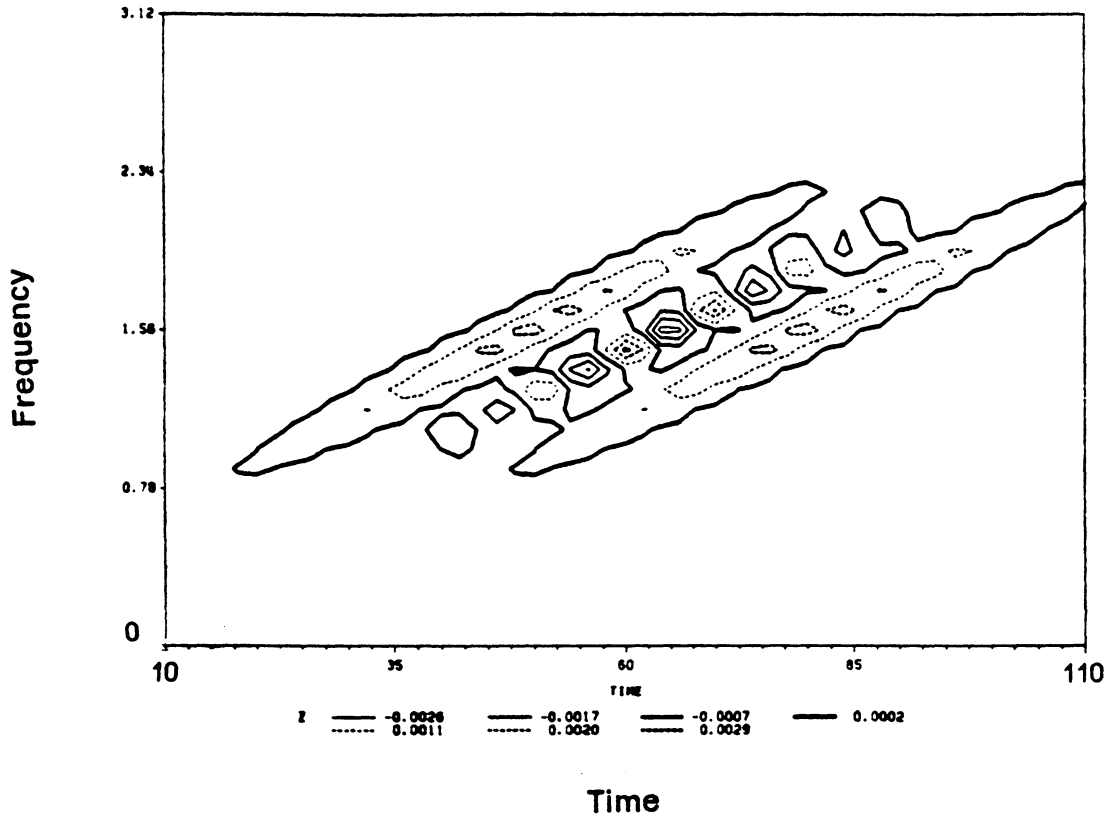

Figure 39. PWD of the sum of two LCSs, $\sigma_w = 14$ secs, S=30 secs.

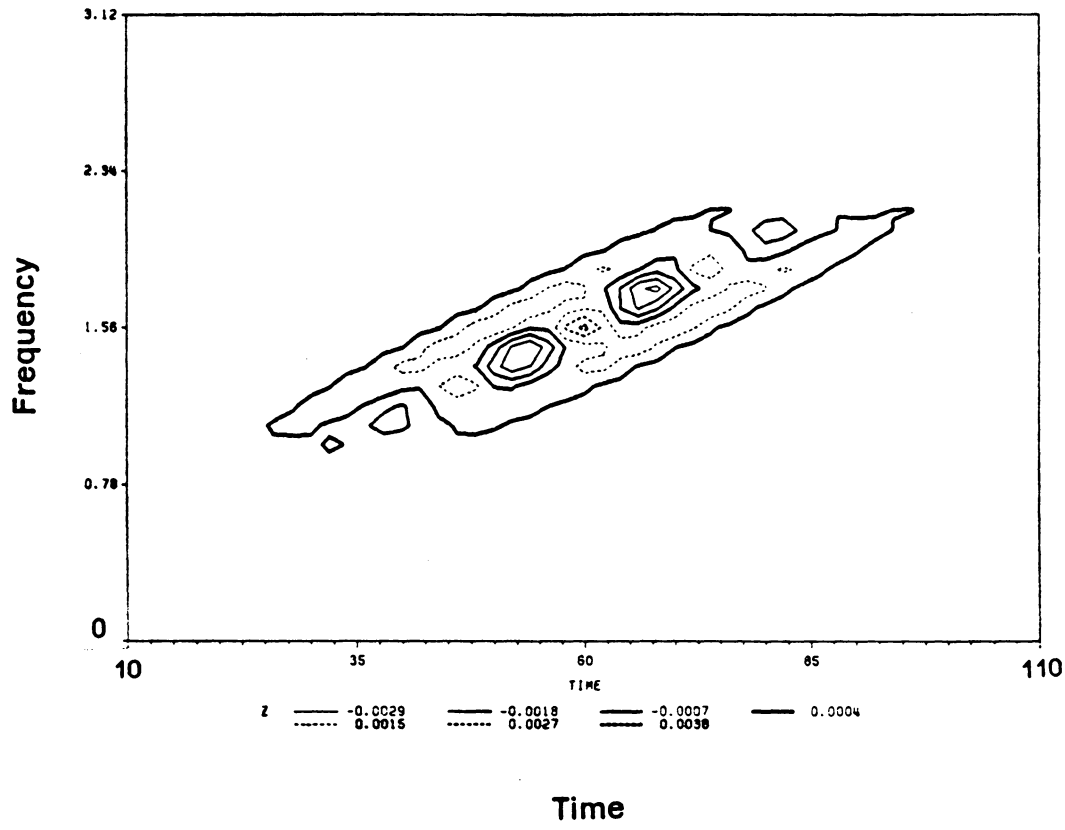

Figure 40. PWD of the sum of two LCSs, $\sigma_w = 14$ secs, S=20 secs.

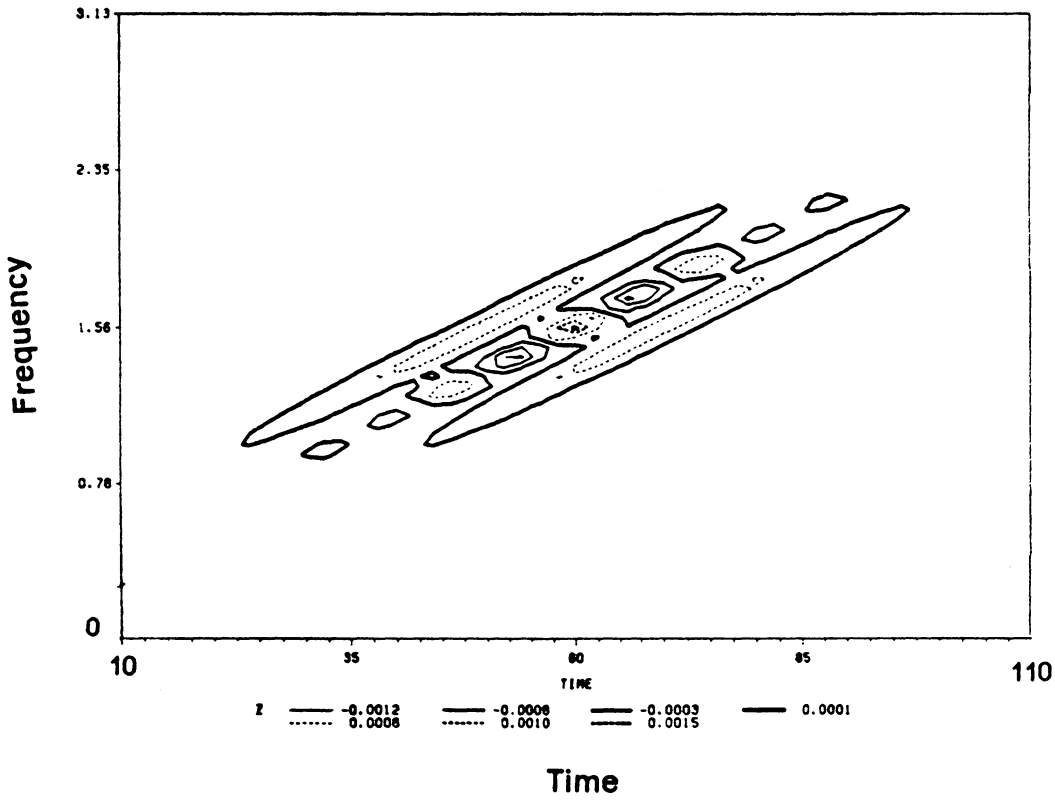

Figure 41. PWD of the sum of two LCSs, σ_w =30 secs, S=20 secs.

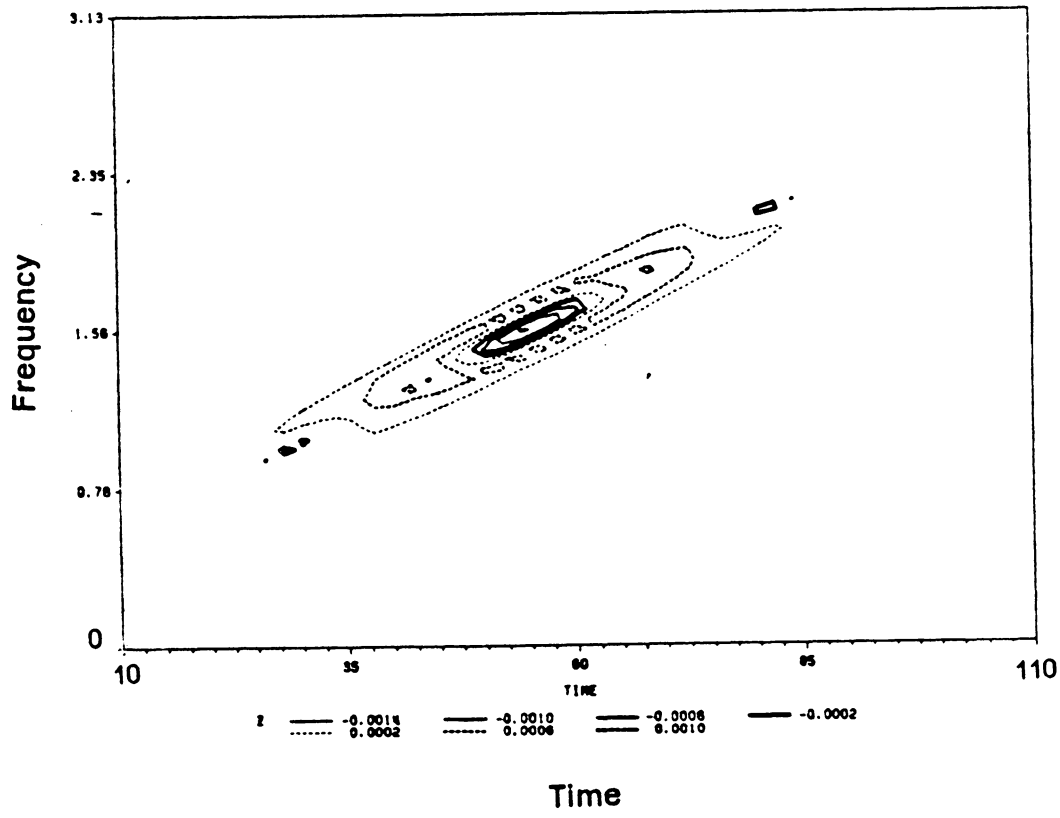

Figure 42. PWD of the sum of two LCSs, σ_w = 30 secs, S = 10 secs.

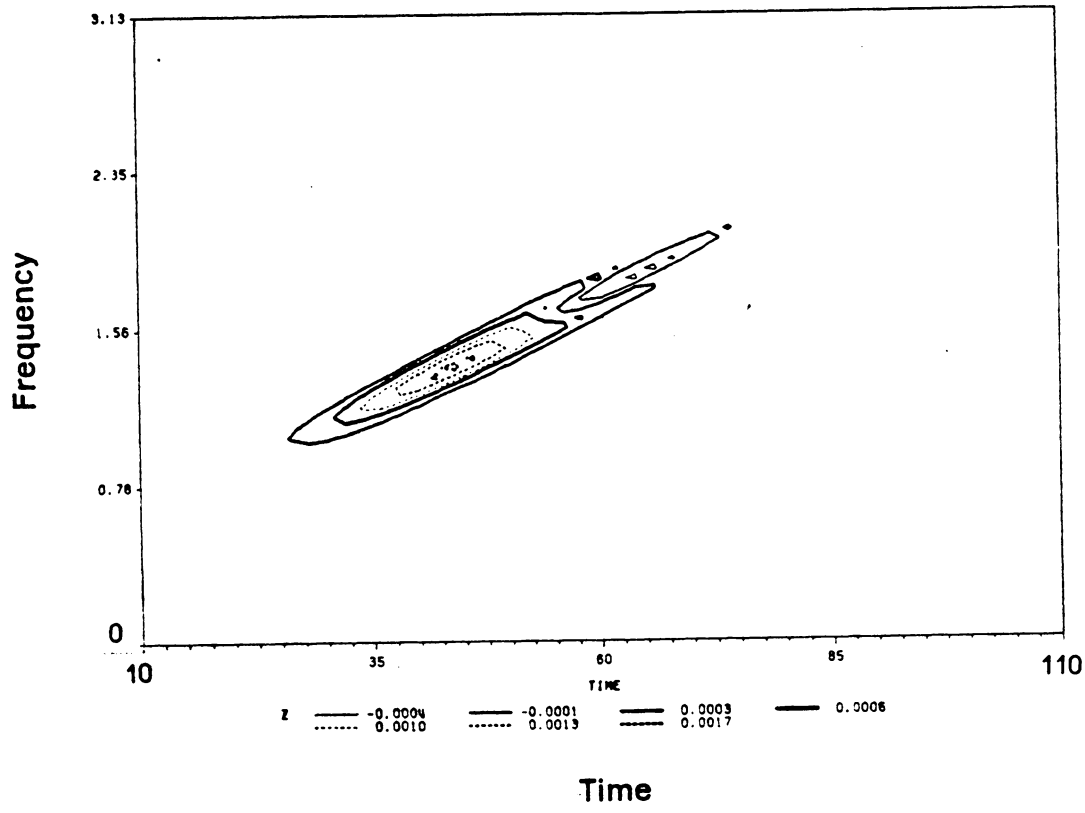

Figure 43. PWD of the sum of two LCSs, σ_w =30 secs, S=5 secs.

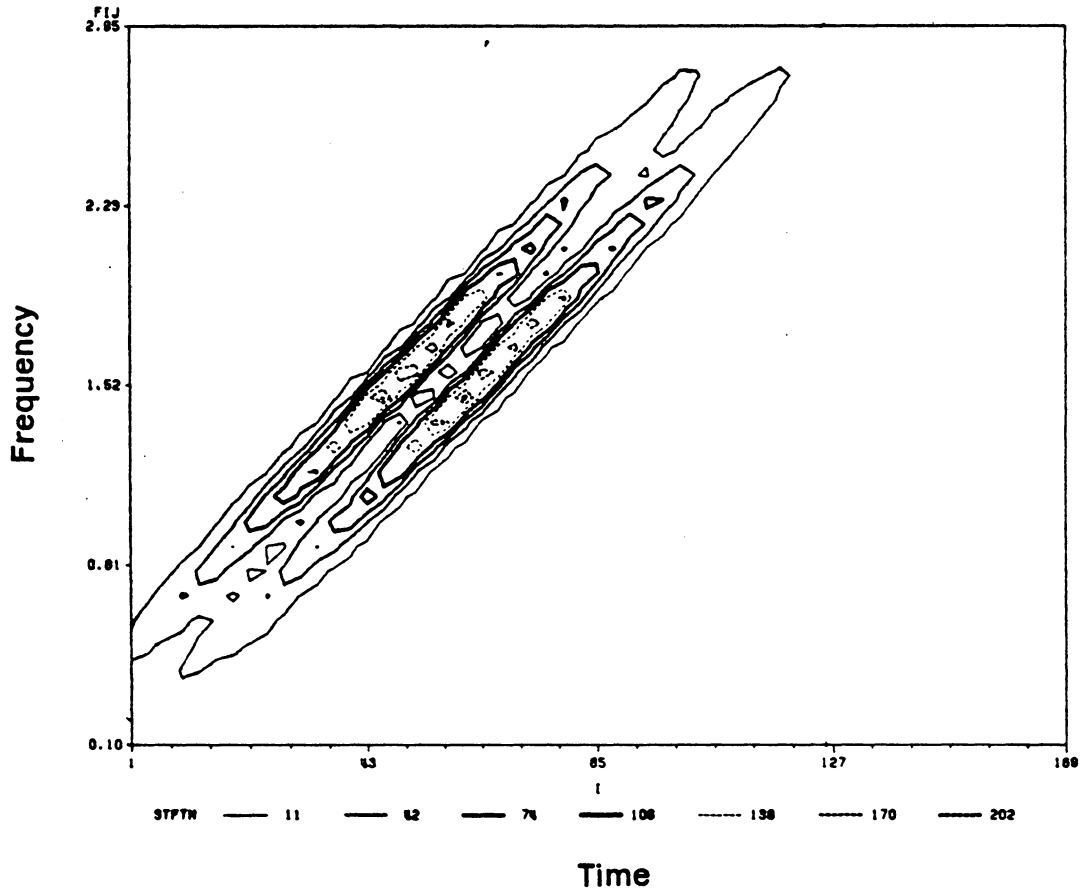

Figure 44. OSWD of the sum of two LCSs, $\sigma_w = 15$ secs, S = 15 secs.

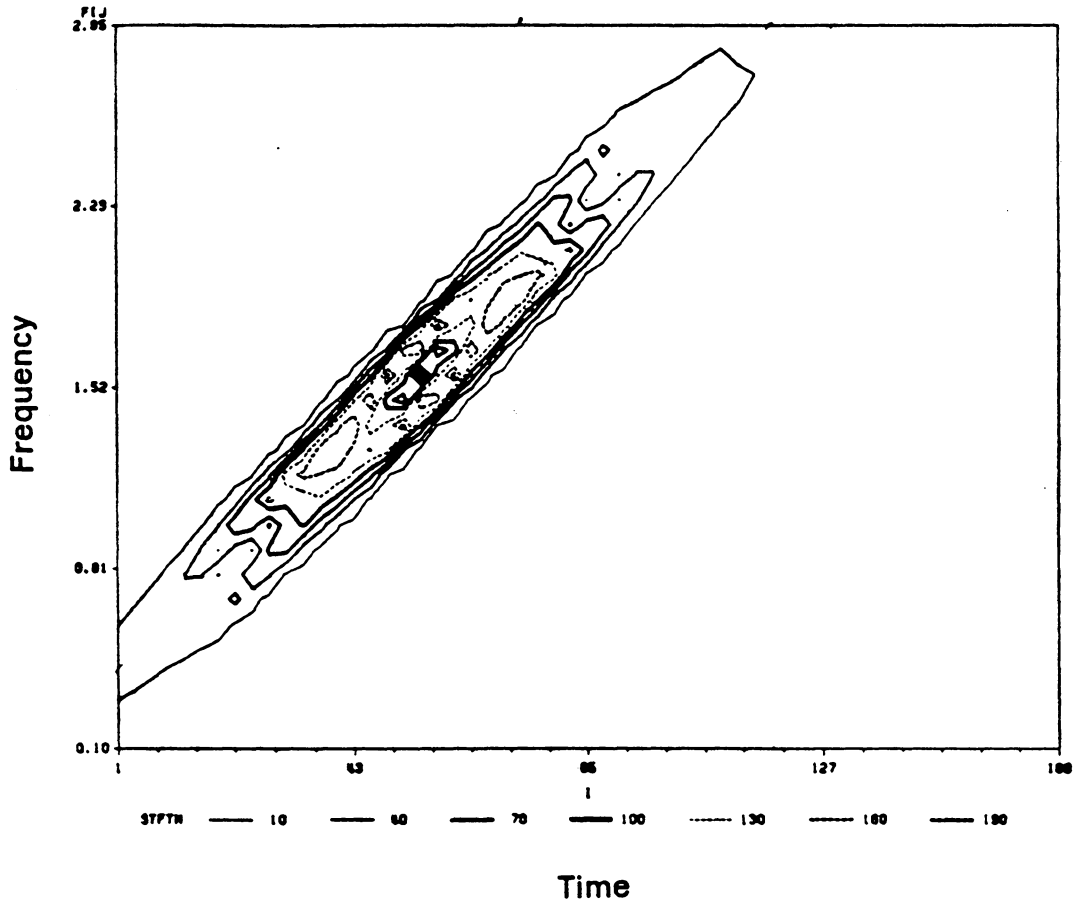

Figure 45. OSWD of the sum of two LCSs, $\sigma_w = 15$ secs, S = 10 secs.

4.0 Filtering of STV signals using linear shift-variant filters

4.1 Introduction

In the previous chapter, we used different MTFRs to analyze a STV signal. The analysis yielded useful information about the signal, basically, a description of the ROS of the signal components in the time-frequency plane. This information, however, does not describe a signal component completely. In this chapter, we investigate the problem of isolating a desired signal component from a noise-corrupted measurement using the information obtained in the analysis. One way to obtain the desired signal component consists of masking a MTFR of the signal and applying an inverse transformation to the resulting MTFR. This approach has been applied to the WD, PWD and the STFT [B5], [Y1] and [H3]. The only information needed is a description of the ROS of the considered MTFR, which can be expressed in terms of the instantaneous frequency and BW of the MTFR under consideration.

As was shown in the previous chapter, the WD, the PWD, or the STFT often do not yield an adequate description of the ROS of a multicomponent signal in the time-frequency plane.

In many cases, the ROS of the OSTFT (or the OSWD) is more adequate. In this chapter, we propose applying the masking function approach to the OSTFT. We present an equivalent time-domain implementation and specification based on the concept of local nonstationarity cancellation (LNC), and resulting in a linear shift-variant (LSV) filter. The proposed LNC filter has a superior performance, achieved at the expense of using additional information about the signal, namely, the derivative of the signal instantaneous frequency.

In the derivation that follows, an analytic STV signal $x(t)$ is properly sampled [M1] with a sampling period T. The sampled signal $x(nT) = a(nT)e^{j\phi(nT)}$ is to be reconstructed in the presence of noise or signal interference. The signal is recovered by the following LSV filtering operation :

$$y(nT) = T \sum_{m=-M}^{M} h(nT,mT)x_i(nT - mT) \tag{4.1.1}$$

where $x_i(nT)$ is the signal at the input of the LSV filter. It consists in general of a desirable signal component $x(nT)$, of an undesirable signal component $x_2(nT)$, and of additive noise $z(nT)$,

$$x_i(nT) = x(nT) + x_2(nT) + z(nT) \tag{4.1.2}$$

In order for the filtering operation to be successful, two requirements have to be satisfied simultaneously.

- First, the filtered desired signal,

$$x_o(nT) = T \sum_{m=-\infty}^{\infty} h(nT,mT)x(nT - mT) \tag{4.1.3}$$

has to approximate $x(nT)$ as much as possible.

- Second, the filtered undesired signals have to be "small". For instance, we require that $E\{|z_o(nT)|^2\}$, the power of the filtered noise

$$z_o(nT) = T \sum_{m=-\infty}^{\infty} h(nT,mT)z(nT - mT) \tag{4.1.4}$$

approximate zero as much as possible.

4.2 Description of linear shift-variant filters

A linear shift-variant (LSV) filter is generally characterized in terms of its system response, also known as Green's function $\bar{h}(nT,mT)$, which represents the output of the system at time nT, due to an impulse at time mT . The relation between the input $x(nT)$ and the output $y(nT)$ of the filter is given by

$$y(nT) = T \sum_{m=-\infty}^{\infty} \bar{h}(nT,mT)x(mT) \tag{4.2.1}$$

The input-output relation in Eq. (4.2.1) can be written in the form

$$\begin{aligned} y(nT) &= T \sum_{m=-\infty}^{\infty} h(nT,nT - mT)x(mT) \\ &= T \sum_{m=-\infty}^{\infty} h(nT,mT)x(nT - mT) \end{aligned} \tag{4.2.2}$$

where $h(nT,mT) = \bar{h}(nT,nT - mT)$, known as the impulse response of the system, denotes the output of the system at time nT, due to an input impulse at time $(nT - mT)$. Therefore, mT represents the time lag between the input and the output [P8].

For linear shift-invariant (LSI) filters, Eq.(4.2.1) and Eq. (4.2.2) reduce to

$$\begin{aligned} y(nT) &= T \sum_{m=-\infty}^{\infty} h(nT - mT)x(mT) \\ &= T \sum_{m=-\infty}^{\infty} \bar{h}(nT - mT)x(mT) \end{aligned} \tag{4.2.3}$$

and $h(nT,mT)$ and $\bar{h}(nT,mT)$ reduce to

$$\bar{h}(nT,mT) = \bar{h}(nT - mT) \tag{4.2.4}$$

$$h(nT,mT) = h(mT) \tag{4.2.5}$$

If the input x(nT) is a complex exponential, $x(nT) = e^{j\omega nT}$, the output becomes

$$y(nT) = H(e^{j\omega T})e^{j\omega nT} \tag{4.2.6}$$

where $H(e^{j\omega T})$ is the Fourier transform of h(nT), and is known as the frequency function of the LSI filter; $H(e^{j\omega T})$ is the eigenvalue of the linear system corresponding to the eigenfunction $e^{j\omega nT}$. Taking the FT of Eq. (4.2.2), we get

$$\begin{aligned} Y(e^{j\omega T}) &= T \sum_{n=-\infty}^{\infty} T \sum_{m=-\infty}^{\infty} h(nT - mT)x(mT)e^{-j\omega mT} \\ &= X(e^{j\omega T})H(e^{j\omega T}) \end{aligned} \tag{4.2.7}$$

where $H(e^{j\omega T})$ is the frequency function (FF) of the filter $h(nT)$.

The convolution in the time domain, as expressed in Eq. (4.2.3), has been transformed to a multiplication in the frequency domain. The formula given in Eq. (4.2.6) can be generalized to LSV filters. In fact, if the input to the LSV filter in Eq. (4.2.2) is a complex sinusoid, $x(nT) = e^{j\omega nT}$, the output will have the form

$$y(nT) = H(nT,e^{j\omega T})e^{j\omega nT} \tag{4.2.8}$$

where $H(nT,e^{j\omega T})$ is referred to as the generalized frequency function (GFF) of the LSV filter, and is defined as a partial FT of the two-dimensional sequence $h(nT,mT)$, with respect to its second argument mT; i.e.,

$$H(nT,e^{j\omega T}) = T\sum_{m=-\infty}^{\infty} h(nT,mT)e^{-j\omega mT} \tag{4.2.9}$$

$$h(nT,mT) = \frac{1}{2\pi}\int_{-\frac{\pi}{T}}^{\frac{\pi}{T}} H(nT,e^{j\omega T})e^{j\omega mT}d\omega \tag{4.2.10}$$

Substituting Eq. (4.2.10) into Eq. (4.2.2) yields

$$\begin{aligned} y(nT) &= T\sum_{m=-\infty}^{\infty} \frac{1}{2\pi}\int_{-\frac{\pi}{T}}^{\frac{\pi}{T}} H(nT,e^{j\omega T})e^{j\omega mT}x(nT-mT)d\omega \\ &= \frac{1}{2\pi}\int_{-\frac{\pi}{T}}^{\frac{\pi}{T}} H(nT,e^{j\omega T})\left[T\sum_{m=-\infty}^{\infty} x(nT-mT)e^{-j\omega(nT-mT)}\right]e^{j\omega nT}d\omega \end{aligned} \tag{4.2.11}$$

or

$$y(nT) = \frac{1}{2\pi}\int_{-\frac{\pi}{T}}^{\frac{\pi}{T}} H(nT,e^{j\omega T})X(e^{j\omega T})e^{j\omega nT}d\omega \tag{4.2.12}$$

The function $H(nT,e^{j\omega T})X(e^{j\omega T}) = Y(e^{j\omega T};nT)$ can be interpreted as the FT of a signal $y(kT;nT)$ which is the output of a LSI filter with a frequency function $H(nT,e^{j\omega T})$ due to an input $x(kT)$. This Frequency Function (FF) is indexed on the time nT. Only one sample out of the sequence $y(kT;nT)$ is needed, namely, the sample when $k = n$. The rest of the sequence can be discarded. As was shown in Eq. (4.2.12), the inverse Fourier transform of $Y(e^{j\omega T};nT)$ needs to be performed for one value of k, namely, for $k = n$. We use the notation

$$y(nT) = y(kT;nT)\big|_{k=n} \tag{4.2.13}$$

to emphasize that $y(nT)$ has been found by picking only one sample out of the sequence $y(kT;nT)$.

4.3 Specification of LSV filters based on masking the STFT

4.3.1 Region of support of the spectrogram

The specification of the LSV filter proposed in [H3] is based on masking the STFT of the signal. We shall call the resulting filter the STFT masking filter. The STFT of the signal $x(nT)$ is defined in Eq. (3.4.1) and is reproduced here for a discrete-time signal $x(mT)$

$$S_x(nT, e^{j\omega}) = T \sum_{m=-\infty}^{\infty} x(mT)w(nT - mT)e^{-j\omega mT} \tag{4.3.1}$$

where $w(nT)$ represents the analysis window. It is normalized such that $w(0) = 1$. The inverse relation is given by

$$w(nT - mT)x(mT) = \frac{1}{2\pi} \int_{-\frac{\pi}{T}}^{\frac{\pi}{T}} S_x(nT, e^{j\omega T})e^{j\omega mT} d\omega \tag{4.3.2}$$

Setting $m = n$, and noting that $w(0) = 1$, we get

$$x(nT) = \frac{1}{2\pi} \int_{-\frac{\pi}{T}}^{\frac{\pi}{T}} S_x(nT, e^{j\omega T})e^{j\omega nT} d\omega \tag{4.3.3}$$

Let $x_i(nT)$ be the input to the LSV filter $h(nT,mT)$. It is natural to assume that although $x(nT)$ is not known, the ROS of its STFT is known. In the case of a monocomponent signal, the ROS of the STFT is defined as the smallest simply connected region of the time-frequency plane where the STFT is nonzero, including the regions inside the ROS having a zero measure (area) where the STFT vanishes. In practice, these isolated islands of zero STFT rarely occur, and can be neglected. Hence, a point in the time-frequency plane is taken to be outside the ROS of the STFT if the value of the spectrogram (STFT magnitude squared) at that point is negligibly small, as compared to the order of magnitude of the spectrogram as a whole.

A useful approximation [H2], [H3] to the ROS of the spectrogram is in terms of the NAF of the spectrogram and its BW. A point $P(nT,e^{j\omega T})$ is taken to belong to the ROS of the spectrogram if

$$|\omega - \Omega_{xs}| \leq \frac{1}{2} B_{sx} \tag{4.3.4}$$

where B_{sx} is any BW of the spectrogram (such as the RMS or the 95-percent BW) centered about the NAF Ω_{xs} of the spectrogram. Both Ω_x and B_{sx} depend on the time nT. To simplify the notation, this dependence will not be shown explicitly.

4.3.2 Masking function

The filtering operation can be carried out by multiplying the STFT $S_{x_i}(nT,e^{j\omega T})$ by the ideal masking function $H_i(nT,e^{j\omega T})$. Since the STFT is linear, the STFT of $x_i(nT) = x(nT) + z(nT)$ is given by

$$S_{x_i}(t, \omega) = S_x(nT,e^{j\omega T}) + S_z(nT,e^{j\omega T}) \tag{4.3.5}$$

and hence,

$$Y(nT,e^{j\omega T}) = H_i(nT,e^{j\omega T})S_{x_i}(nT,e^{j\omega T})$$

$$= H_i(nT,e^{j\omega T})S_x(nT,e^{j\omega T}) + H_i(nT,e^{j\omega T})S_z(nT,e^{j\omega T}) \tag{4.3.6}$$

where the masking function $H_i(nT,e^{j\omega T})$ is defined such that the desired signal will pass through with minimal distortion. This is achieved by letting

$$H_i(nT,e^{j\omega T}) = \begin{cases} 1 & \text{in the ROS of } S_x(nT,\, e^{j\omega T}) \\ 0 & \text{otherwise} \end{cases} \tag{4.3.7}$$

In this case,

$$H_i(nT,e^{j\omega T})S_x(nT,e^{j\omega T}) \simeq S_x(nT,e^{j\omega T}) \tag{4.3.8}$$

Assuming little overlap between the ROS of the desired and undesired signals, we have

$$H_i(nT,e^{j\omega T})S_z(nT,e^{j\omega T}) \simeq 0 \tag{4.3.9}$$

and hence,

$$Y(nT,e^{j\omega T}) \simeq S_x(nT,e^{j\omega T}) \tag{4.3.10}$$

The next step involves an inverse transform of $Y(nT,e^{j\omega T})$ to compute the signal $y(nT)$ approximating the desired signal $x(nT)$,

$$y(nT) = \frac{1}{2\pi}\int_{-\frac{\pi}{T}}^{\frac{\pi}{T}} Y(nT,e^{j\omega T})e^{j\omega nT}d\omega \tag{4.3.11}$$

$$y(nT) = \frac{1}{2\pi}\int_{-\frac{\pi}{T}}^{\frac{\pi}{T}} H_i(nT,e^{j\omega T})S_{x_i}(nT,e^{j\omega T})e^{j\omega nT}d\omega \tag{4.3.12}$$

It should be noted, however, that $Y(nT,e^{j\omega T})$ is rarely a valid STFT. $Y(nT,e^{j\omega T})$ is a valid STFT if there exists a signal y(nT) such that its STFT $S_y(nT, e^{j\omega T})$ is exactly equal to $Y(nT,e^{j\omega T})$. This validity problem was studied in [S1]. The signal y(nT) can be interpreted as the inverse transform of a valid STFT approximating $Y(nT,e^{j\omega T})$.

An equivalent time-domain implementation can be derived by assuming that $H_i(nT,e^{j\omega T})$ is actually a GFF related to a LSV filter impulse response $h_i(nT,mT)$ via Eq. (4.2-10). Note that at a given time nT, $H_i(nT, e^{j\omega T})$ represents an ideal bandpass filter having an impulse response

$$h_i(nT,mT) = g_i^B(mT;nT) \tag{4.3.13}$$

where $g_i^B(mT;nT)$ is the impulse response of an ideal LSI bandpass filter whose passband is found from the ROS of the STFT. This ROS was described in Eq. (4.3.4) in terms of the interval $\left(\Omega_{sx} - \frac{1}{2}B_{sx}, \Omega_{sx} + \frac{1}{2}B_{sx}\right)$. Substituting Eq. (4.2.9) in Eq. (4.3.12), and rearranging terms gives

$$y(nT) = T \sum_{m=-\infty}^{\infty} h_i(nT,mT)\left[\frac{1}{2\pi}\int_{-\frac{\pi}{T}}^{\frac{\pi}{T}} S_{x_i}(nT,e^{j\omega T})e^{j\omega(nT-mT)}d\omega\right] \tag{4.3.14}$$

Using the definition of the STFT in the above equation gives

$$\begin{aligned} y(nT) &= T \sum_{m=-\infty}^{\infty} w(mT)h_i(nT,mT)x(nT-mT) \\ &= T \sum_{m=-\infty}^{\infty} h(nT,mT)x(nT-mT) \end{aligned} \tag{4.3.15}$$

where the window $w(mT)$ is the same analysis window used to compute the STFT.

4.4 Specification of LSV filters based on local nonstationarity cancellation

The filter $H_i(nT,e^{j\omega T})$ specified in Eq. (4.3.7) is defined using the ROS of the STFT $S_x(nT,e^{j\omega T})$. It modifies the magnitude of $S_{x_i}(nT, e^{j\omega T})$ only, and depends only on the instantaneous frequency and the BW of the STFT at the time nT.

When deriving Eq. (4.3.15), the window $w(mT)$ was not assumed to be real or symmetric. Therefore, Eq. (4.3.15) holds also for the complex window

$$v(mT; nT) = v(\tau; t)|_{\tau=mT,\ t=nT} \tag{4.4.1}$$

where $v(\tau; t)$ was defined in Eq. (3.5.10) and used to compute the OSWD and the OSTFT. It was shown in Section 3.2.2 that the BW of the OSWD is smaller than the BW of the spectrogram. Therefore, it is expected that the filter based on masking the OSTFT will have a smaller BW, and hence, will suppress more noise than the filter based on masking the STFT.

In the following development, we seek to establish the superior performance of the proposed filter. First, we show an alternative development of the filter in the time-domain. Next, we analyze the filter robustness and performance in suppressing random noise, and separating different signal components.

The signal is assumed to be a STV signal with quadratic phase. It was defined in Section 3.5.1.2, and its discrete-time version is given by

$$x(nT) = a(nT)e^{j\phi(nT)} \tag{4.4.2}$$

$$\phi(nT + mT) \simeq \phi(nT) + \Omega_x mT + \frac{1}{2}\alpha_x m^2 T^2 \tag{4.4.3}$$

where Eq. (4.4.3) is valid for $mT \leq \tau_{max}$. Both Ω_x and α_x are dependent on nT.

4.4.1 Theoretical development

We seek to specify the LSV filter $h(nT,mT)$ using Ω_x, α_x and B_s, all assumed to be available. Let $h_i(nT,mT)$ be an ideal filter having the form

$$h_i(nT,mT) = g_i(mT;nT)\exp(j\nu mT + j\beta m^2T^2) \tag{4.4.4}$$

where ν and β are two parameters dependent on time nT and $g_i(mT)$ is an ideal low pass filter whose bandwidth B_{g_i} is also a function of time nT. This time-dependence is not shown explicitly. Note the following :

- $g_i(mT;nT)e^{j\nu mT}$ is an ideal bandpass filter centered about the frequency ν, and having a BW of $2B_{g_i}$.
- By setting $\beta = 0$, we regain the filter based on masking the STFT and considered in Section 4.3.2.

The FT of $g_i(mT;nT)$ is given by

$$G_i(e^{j\omega T}) = \begin{cases} 1 & \text{if } |\omega| < B_{g_i} \\ 0 & \text{otherwise} \end{cases} \tag{4.4.5}$$

and hence,

$$g_i(mT;nT) = \frac{1}{\pi} \quad \frac{\sin B_{g_i}mT}{mT} \tag{4.4.6}$$

Clearly, $g(mT;nT)$ decays as $|mT| \to \infty$. In practice, a FIR implementation is obtained by multiplying the ideal filter by a window $w(mT)$ of length $2M + 1$ points. Standard windows, such as the Hamming or the Gaussian windows, can be used. We shall assume that $w(0) = 1$, and $w(-mT) = w(mT)$. Define the FIR LSV filters

$$g(mT;nT) = w(mT)g_i(mT;nT)$$
$$h(nT,mT) = w(mT)h_i(nT,mT) \tag{4.4.7}$$

Substituting Eq. (4.4.4) and Eq. (4.4.7) in Eq. (4.2.2) gives

$$y(nT) = T\sum_{m=-\infty}^{\infty} w(mT)g_i(mT)e^{j\nu mT+j\beta m^2T^2}x(nT-mT) \tag{4.4.8}$$

Note that since $w(mT) = 0$ for $|m| > M$, we are allowed to extend the limits of the summation from $-\infty$ to ∞.

If $MT < \tau_{max}$, the Taylor series expansion in Eq. (4.4.3) can be used to obtain:

$$x(nT-mT) \simeq a(nT-mT)e^{j\phi(nT)-j\Omega_x mT+\frac{j}{2}\alpha_x m^2T^2}, \quad mT \le \tau_{\max} \tag{4.4.9}$$

Using the above equation, Eq. (4.4.8) becomes

$$y(nT) \simeq e^{j\phi(nT)}T\sum_{m=-\infty}^{\infty} w(mT)g_i(mT;nT)a(nT-mT)e^{j(\nu-\Omega_x)mT+j(\beta+\frac{1}{2}\alpha_x)m^2T^2} \tag{4.4.10}$$

Note that $y(nT)$ can be thought of as one sample of the sequence

$$y(kT;nT) \simeq e^{j\phi(nT)}T\sum_{m=-\infty}^{\infty} w(nT-kT+mT)a(kT-mT)g_i(mT;nT)e^{j(\nu-\Omega_x)mT+j(\beta+\frac{1}{2}\alpha_x)m^2T^2} \tag{4.4.11}$$

obtained by setting $k = n$. To recover $y(nT)$, we simply use $y(nT) = y(kT;nT)|_{k=n}$

Choose the parameters ν and β to reduce the phase terms in Eq. (4.4.11) to zero; i.e., let

$$\nu = \Omega_x \quad \text{and} \quad \beta = -\frac{1}{2}\alpha_x \tag{4.4.12}$$

This has the effect of locally cancelling the nonstationarity introduced by the quadratic phase term $e^{\frac{j}{2}\alpha_x(nT)m^2T^2}$. For the choice of ν and β in Eq. (4.4.12), Eq. (4.4.11) becomes

$$y(kT;nT) \simeq e^{j\phi(nT)T} \sum_{m=-\infty}^{\infty} w(nT - kT + mT)a(kT - mT)g_i(mT;nT) \tag{4.4.13}$$

The above sum represents the convolution in kT of the ideal filter response $g_i(kT;nT)$ and of the signal

$$a_w(kT;nT) = w(nT - kT)a(kT) \tag{4.4.14}$$

An equivalent relation in the frequency domain is given by

$$Y(e^{j\omega T};nT) \simeq e^{j\phi(nT)} A_w(e^{j\omega T};nT)G_i(e^{j\omega T};nT) \tag{4.4.15}$$

where $A_w(e^{j\omega T};nT)$ and $G_i(e^{j\omega T};nT)$ are the FTs of $a_w(kT;nT)$ and $g_i(kT;nT)$ respectively. The signal $a_w(kT;nT)$ is a lowpass signal whose BW B_{aw} is equal to half the BW of the OSWD of the signal. This BW was approximated in Eq. (3.5.30)

$$B_{aw} \simeq \frac{1}{2}(\text{BW of the OSWD}) \tilde{<} B_a + B_w \tag{4.4.16}$$

Therefore, the filter BW is set equal to

$$B_{g_i} = \frac{1}{2}(\text{BW of OSWD of desired signal}) \tag{4.4.17}$$

In this case, $a_w(kT;nT)$ falls within the passband of $g_i(kT;nT)$, and hence,

$$A_w(e^{j\omega T};nT)G_i(e^{j\omega T};nT) \simeq A_w(e^{j\omega T};nT)$$

In the time domain, this is equivalent to

$$T \sum_{m=-\infty}^{\infty} w(nT - kT + mT)a(kT - mT)g_i(mT;nT) \simeq w(nT - kT)a(kT) \tag{4.4.19}$$

For $k = n$, Eq. (4.4.13) reduces to

$$y(nT) \simeq w(0)a(nT)e^{j\phi(nT)} = a(nT)e^{j\phi(nT)} \tag{4.4.20}$$

The output of the LNC filter is approximately equal to the desired signal. The error of the approximation results from using a nonideal FIR filter, and from truncating the Taylor series of the phase in Eq. (4.4.3).

In summary, the LNC filter is given by

$$\begin{aligned} h(nT,mT) &= w(mT)g_i(mT;nT)e^{j\Omega_x mT - \frac{j}{2}\alpha_x m^2T^2} \\ B_{g_i} &= \frac{1}{2}B_{aw} \simeq B_a + B_w \end{aligned} \tag{4.4.21}$$

4.4.2 Sensitivity of the local nonstationarity cancellation filter

It is of interest to study the sensitivity of the proposed filter to errors in estimating the parameters Ω_x and α_x. Let

$$\begin{aligned} \nu &= Estimate\{\Omega_x\} = \Omega_x + \delta_\Omega \\ \beta &= -\frac{1}{2}Estimate\{\alpha_x\} = -\frac{1}{2}\alpha_x + \delta_\alpha \end{aligned} \tag{4.4.22}$$

where δ_Ω and δ_α are the estimation errors corresponding to Ω_x and α_x. Note that all of the above quantities depend on time nT.

Let $\hat{y}(nT)$ denote the output of the filter when the estimates in Eq. (4.4.22) are used. Substituting Eq. (4.4.22) in Eq. (4.4.10) gives

$$\hat{y}(nT) \simeq e^{j\phi(nT)}T \sum_{m=-\infty}^{\infty} w(mT)a(nT - mT)g_i(mT;nT)e^{j\delta_\Omega mT + j\delta_\alpha m^2T^2} \tag{4.4.23}$$

Substituting $m^2T^2 = (n-m)^2T^2 - n^2T^2 + 2nTmT$ in Eq. (4.4.23), and rearranging terms yields

$$\hat{y}(nT) \simeq e^{j\phi(nT)-j\delta_\alpha n^2T^2} \cdot T \sum_{m=-\infty}^{\infty} \left[g_i(mT)e^{j(\delta_\Omega+2\delta_\alpha nT)mT}\right] \cdot \left[w(mT)a(nT-mT)e^{j\delta_\alpha(n-m)^2T^2}\right] \tag{4.4.24}$$

Again, $\hat{y}(nT)$ can be obtained by sampling the sequence $\hat{y}(kT;nT)$ at $k = n$, where the sequence $\hat{y}(kT;nT)$ is given by the convolution

$$\hat{y}(kT;nT) \simeq e^{j\phi(nT)-j\delta_\alpha n^2T^2} \cdot \left[g_i(kT)e^{j(\delta_\Omega+2\delta_\alpha nT)kT}\right] \ *_{kT} \ \left[w(nT-kT)a(kT)e^{j\delta_\alpha k^2T^2}\right] \tag{4.4.25}$$

where the symbol $*_{kT}$ denotes convolution with respect to kT. Fourier transforming the above equation with repsect to the time index kT, we get

$$\hat{Y}(e^{j\omega T};nT) \simeq e^{j\phi(nT)-j\delta_\alpha n^2T^2} G^\delta(e^{j\omega T};nT)A^\delta(e^{j\omega T};nT) \tag{4.4.26}$$

where $G^\delta(e^{j\omega T};nT)$ and $A^\delta(e^{j\omega T};nT)$ are the FTs of

$$\begin{aligned} g^\delta(kT;nT) &= g_i(kT)e^{j(\delta_\Omega+2\delta_\alpha nT)kT} \\ a^\delta(kT;nT) &= w(nT-kT)a(kT)e^{j\delta_\alpha k^2T^2} \end{aligned} \tag{4.4.27}$$

Assuming a Gaussian window $w(kT) = e^{j\zeta k^2T^2}$, the signal $w(nT-kT)e^{j\delta_\alpha k^2T^2}$ becomes a linear chirp signal whose FT is centered at $2\delta_\alpha nT$ and whose BW is given by $\sqrt{\zeta + \frac{\delta_\alpha^2}{\zeta}}$. Therefore, the FT of the signal $a^\delta(kT;nT)$ is centered at $2\delta_\alpha nT$ and has a bandwidth $2B_a^\delta$ where

$$B_a^\delta \lesssim B_a + \sqrt{\zeta + \frac{\delta_\alpha^2}{\zeta}} \tag{4.4.28}$$

The filter $G^\delta(e^{j\omega T};nT)$ is an ideal bandpass filter centered at $\delta_\Omega + 2\delta_\alpha nT$ and having a BW of $B_{g_i}^\delta$. If the BW $B_{g_i}^\delta$ is chosen such that

$$B_{g_i}^\delta \geq B_a^\delta + \delta_\Omega \tag{4.4.29}$$

then the frequency support of the signal $a^{\delta}(kT;nT)$ falls within the passband of the ideal bandpass filter $g^{\delta}(kT;nT)$. In this case,

$$G^{\delta}(e^{j\omega T};nT)A^{\delta}(e^{j\omega T};nT) \simeq A^{\delta}(e^{j\omega T};nT) \tag{4.4.30}$$

Therefore, Eq. (4.4.25) reduces to

$$\hat{y}(kT;nT) \simeq e^{j\phi(nT)-j\delta_{\alpha}n^2T^2}w(nT-kT)a(kT)e^{j\delta_{\alpha}k^2T^2} \tag{4.4.31}$$

The output of the LSV filter is obtained by sampling $\hat{y}(kT;nT)$ at $k=n$; i.e.,

$$\hat{y}(nT) = \hat{y}(kT;nT)\big|_{k=n} \simeq a(nT)e^{j\phi(nT)} \tag{4.4.32}$$

The output of the filter is again approximately equal to the desired signal. The error of the approximation results from using a nonideal FIR filter and from truncating the Taylor series of the signal phase.

In summary, the effect of the errors present in the estimates of the paramters Ω_x and α_x can be accounted for by using a larger filter BW. In particular, note that the STFT masking filter is obtained by setting $\beta = 0$, resulting in the error $\delta_{\alpha} = -\frac{\alpha_x}{2}$. In this case, Eq. (4.4.29) becomes

$$B_{g_i}^{\delta} = B_a + \sqrt{\zeta + \frac{\delta_{\alpha}^2}{\zeta}} = B_a + \sqrt{\zeta + \frac{\alpha_x^2}{4\zeta}} \tag{4.4.33}$$

This shows that the STFT masking filter requires a larger BW.

4.5 *Suppression of unwanted signals*

We have shown that the LSV filter specified in Eq. (4.4.21) can successfully pass the desired signal with minimum distortion. In the following discussion it will be shown that this filter effectively reduces the undesired signals under some assumptions. We consider two

cases. In the first case, the undesired signal $z(nT)$ is assumed to be a zero mean white noise (ZMWN) process. In the second case, the undesired signal $x_2(t)$ is assumed to be a time varying signal having a structure similar to that of the desirable signal.

4.5.1.1 Case 1 : White noise

Let $z(nT)$ be the analytic part of a ZMWN process. The autocorrelation function of z(nT) is given by $R_z(nT,mT) = E\{z(nT)z^*(nT+mT)\} = p(nT)\delta(mT)$ where $p(nT) = E\{|z(nT)|^2\}$. If $z(nT)$ is stationary, then $p(nT) = P_z$. Denote by $z_o(nT)$ the output of the LNC filter corresponding to the input $z(nT)$.

$$z_o(nT) = T\sum_{m=-\infty}^{\infty} w(mT)g_i(mT)\exp(jvmT + j\beta m^2T^2)z(nT-mT) \tag{4.5.1}$$

Substituting $m^2T^2 = (nT-mT)^2 + 2nTmT - n^2T^2$ in Eq. (4.5.1), and rearranging terms, gives

$$\begin{aligned} z_o(nT) &= e^{-j\beta n^2T^2}T\sum_{-\infty}^{\infty}[g(mT;nT)e^{j(v+2\beta nT)mT}][z(nT-mT)e^{j\beta(nT-mT)^2}] \\ &= e^{-j\beta n^2T^2}T\sum_{m=-\infty}^{\infty} g_2(mT;nT)z_2(nT-mT) \end{aligned} \tag{4.5.2}$$

where

$$\begin{aligned} g_2(mT;nT) &= w(mT)g_i(mT;nT)e^{j(v+2\beta nT)mT} \\ z_2 &= z(nT)e^{j\beta n^2T^2} \end{aligned} \tag{4.5.3}$$

Note that $g_2(mT;nT)$ represents the impulse response of a bandpass filter centered at the frequency $(v+2\beta nT)$, and having a BW $2B_{g_2} = 2B_{g_i}$ where B_{g_i} is defined in Eq. (4.4.17). Moreover, the summation in Eq. (4.5.2) can be interpreted as a convolution, and hence $z_o(nT)$ can be expressed as

$$z_o(nT) = e^{-j\beta n^2T^2} z_3(kT;nT)\big|_{k=n}$$
$$z_3(kT;nT) = [g_2(kT) \ {}^*_{kT} \ z_2(kT)] \tag{4.5.4}$$

The autocorrelation function of $z_2(nT)$ is given by

$$\begin{aligned} R_2(nT, mT) &= E\{z_2(nT)z_2^*(nT+mT)\} \\ &= \exp(-j\beta(2nTmT + m^2T^2))E\{z(nT)z^*(nT+mT)\} \\ &= \exp(-j\beta(2nTmT + m^2T^2))p(nT)\delta(mT) \\ &= p(nT)\delta(mT) \end{aligned} \tag{4.5.5}$$

Hence, $z_2(nT)$ is a ZMWN process. Assume that the input noise $z(nT)$ is stationary; i.e., let $p(nT) = P_z$. The power spectrums of $z(nT)$ and $z_2(nT)$ are given by $P_{z_2}(e^{j\omega T}) = P_z(e^{j\omega T}) = P_z$. At a given instant nT, the filter $g_2(mT;nT)$ is shift-invariant, and the power spectrum of $z_3(kT;nT)$ is [P1]

$$P_{z_3}(e^{j\omega T};nT) = |G_2(e^{j\omega T};nT)|^2 P_{z_2}(e^{j\omega T}) \tag{4.5.6}$$

where $P_{z_2}(e^{j\omega T}) = P_z$ for the stationary input noise $z(nT)$. The average power of the noise process $z_3(kT;nT)$ is given by [P1]

$$\begin{aligned} E\{|z_3(kT;nT)|^2\} &= \frac{1}{2\pi}\int_{-\frac{\pi}{T}}^{\frac{\pi}{T}} P_{z_3}(e^{j\omega T};nT)d\omega \\ &= \frac{1}{2\pi}\int_{-\frac{\pi}{T}}^{\frac{\pi}{T}} |G_2(e^{j\omega T};nT)|^2 P_z d\omega \\ &= \frac{1}{2\pi}\int_{(\nu+2\beta nT-B_{g_i})}^{(\nu+2\beta nT+B_{g_i})} P_z d\omega \\ &= \frac{2B_{g_i}}{2\pi} P_z \end{aligned} \tag{4.5.7}$$

Clearly,

$$E\{|z_o(nT)|^2\} = E\{|z_3(nT;nT)|^2\} = \frac{2B_{g_i}}{2\pi} P_z \tag{4.5.8}$$

Hence, the average output noise power is proportional to the LNC filter BW B_{g_i}. Note that B_{g_i} was chosen to be half the BW of the OSWD of the desired signal (see Eq. (4.4.17)).

The STFT masking filter can be obtained from the LNC filter by letting $\beta = 0$ and setting the filter BW B_{g_i} to half the BW of the spectrogram of the desired signal. In this case, the above result shows that the average noise power at the output of the STFT masking filter is proportional to the BW of the spectrogram. Since the BW of the OSWD can be much smaller than that of the spectrogram, the LNC filter can perform much better than the STFT masking filter.

4.5.1.2 Case 2 : Multicomponent signals

Let the input signal $x_i(nT)$ to the LSV filter be composed of two STV signals

$$x_i(nT) = x(nT) + x_2(nT) \tag{4.5.9}$$

where $x_2(nT)$ is an undesirable time-varying signal having a structure similar to that of $x(nT)$. Let

$$x_2(nT + mT) = a_2(nT + mT)e^{j\phi_2(nT)+j\Omega_{x2}mT+j\frac{1}{2}\alpha_{x2}m^2T^2} \tag{4.5.10}$$

Consider $y_2(nT)$ the output of the LNC filter defined in Eq. (4.4.17), due to the input signal $x_2(nT)$,

$$\begin{aligned} y_2(nT) &= T\sum_{-\infty}^{\infty} h(nT,mT)x_2(nT - mT) \\ &= e^{j\phi_2(nT)}.T\sum_{-\infty}^{\infty} w(mT)g_i(mT;nT)a_2(nT - mT)e^{j\Delta_\Omega mT+j\Delta_\alpha m^2T^2} \end{aligned} \tag{4.5.11}$$

where

$$\Delta_\Omega = \Omega_x - \Omega_{x2}\,, \quad \text{and} \quad \Delta_\alpha = -\frac{\alpha_x}{2} + \frac{\alpha_{x2}}{2} \tag{4.5.12}$$

Note that Eq. (4.5.11) is very similar to Eq. (4.4.23). We think of $y_2(nT)$ as one sample of the sequence

$$y_2(kT;nT) \simeq e^{j\phi_2(nT) - j\Delta_\alpha n^2T^2}\left[g_i(kT)e^{j(\Delta_\Omega + 2\Delta_\alpha nT)kT}\right] *_{kT}\left[w(nT-kT)a(kT)e^{j\Delta_\alpha k^2T^2}\right] \tag{4.5.13}$$

Using arguments similar to those presented in Section 4.4.2, one can show that

$$Y_2(e^{j\omega T};nT) \simeq e^{j\phi_2(nT) - j\Delta_\alpha n^2T^2} G^\Delta(e^{j\omega T};nT)A^\Delta(e^{j\omega T};nT) \tag{4.5.14}$$

where $G^\Delta(e^{j\omega T};nT)$ and $A^\Delta(e^{j\omega T};nT)$ are the FTs of

$$\begin{aligned} g^\Delta(kT;nT) &= g_i(kT)e^{j(\Delta_\Omega + 2\Delta_\alpha nT)kT} \\ a^\Delta(kT;nT) &= w(nT-kT)a_2(kT)e^{j\Delta_\alpha k^2T^2} \end{aligned} \tag{4.5.15}$$

Assuming a Gaussian window $w(kT) = e^{j\zeta k^2T^2}$, the signal $w(nT-kT)e^{j\Delta_\alpha k^2T^2}$ becomes a linear chirp signal whose FT is centered at $2\Delta_\alpha nT$ and whose BW is given by $2\sqrt{\zeta + \frac{\Delta_\alpha^2}{\zeta}}$ Therefore, the FT of the signal $a^\Delta(kT;nT)$ is centered at $2\Delta_\alpha nT$ and has a bandwidth $2B_a^\Delta$, where

$$B_a^\Delta \tilde{<} = B_{a2} + \sqrt{\zeta + \frac{\Delta_\alpha^2}{\zeta}} \tag{4.5.16}$$

The filter $G^\Delta(e^{j\omega T};nT)$ is an ideal bandpass filter centered at $2\Delta_\alpha nT + \Delta_\Omega$, and having a bandwidth $2B_{g_i}^\Delta$, where

$$B_{g_i}^\Delta = B_{g_i} \tilde{<} B_a + B_w \tag{4.5.17}$$

The two signals are separable if $G^\Delta(e^{j\omega T};nT)A^\Delta(e^{j\omega T};nT) = 0$. This is true if the condition

$$\Delta_\Omega \geq B_{g_i}^\Delta + B_a^\Delta \tag{4.5.18}$$

is satisfied. In this case, the frequency support of the signal $a^{\Delta}(kT;nT)$ falls completely outside the passband of the ideal bandpass filter $g^{\Delta}(kT;nT)$.

In summary, the two signal components are separable if

$$\Delta_{\Omega} \geq B_{g_l} + B_a^{\Delta} \simeq B_a + B_{a_2} + \sqrt{\zeta + \frac{\Delta_{\alpha}^2}{\zeta}} + \sqrt{\zeta} \tag{4.5.19}$$

where the fact that $B_w = \sqrt{\zeta}$ has been used.

Case of parallel components

Assume the two signal components $x(nT)$ and $x_2(nT)$ are "parallel" in the time-frequency plane; i.e., let $\alpha_{x_2} = \alpha_x$, and $\Delta_{\alpha} = 0$. The two signals are separable if

$$\Delta_{\Omega} \geq B_a + B_{a_2} + 2\sqrt{\zeta} \tag{4.5.20}$$

Clearly, increasing σ_w reduces ζ and hence improves separability. In fact, if σ_w is large enough so that $\sqrt{\zeta} \ll B_a + B_{a_2}$, then the above equation becomes $\Delta_{\Omega} \geq B_a + B_{a_2}$. Hence, the two components are separable if the difference between their instantaneous frequencies is at least equal to the sum of the BWs of the envelope of each component. This is the best achievable result because it holds when the signals to be separated are time-invariant; i.e., when $\alpha_{x2} = \alpha_x = 0$.

4.6 Numerical examples

In this section, we illustrate the use of LSV filters in filtering a STV signal in the presence of noise, and in decomposing a STV signal into the sum of closely spaced parallel components. We shall compare the performance of the STFT masking and the LNC filters. The simulations will show that the LNC filter is superior.

4.6.1 Filtering of a linearly frequency modulated signal in the presence of white noise

The objective of this experiment is to filter the linearly frequency modulated (LFM) signal $x_r(t) = \cos \mu t^2$, for $20 \leq t \leq 180$ secs and $\mu = 0.002\pi$ rad sec^{-2} . The corresponding analytic signal can be approximated by $x(t) = e^{j\mu t^2}$, where $20 \leq t \leq 180$. Hence, the signal instantaneous frequency is approximately

$$\Omega_x(t) = 2\mu t = 0.004\pi t \tag{4.6.1}$$

An acceptable sampling period is given by $T = 1$ sec. The portion of the signal, extending over the time interval $50 \leq nT \leq 150$ secs, shall be filtered from the noise-corrupted measured signal $x_n(nT) = x_r(nT) + z_r(nT)$ where $z_r(nT)$ is a real ZMWN having a power density P_{win}.

To analyze the desired signal, the spectrogram and the OSWD are computed using a 45-point (M = 22) Hamming window. These MTFRs are shown on Fig. 46. The BW given by the spectrogram is uniform for all times and can be read to be approximately $0.63 \simeq 0.1(2\pi)$ rad/sec. The BW of the OSWD is approximately given by $0.31 \simeq 0.05(2\pi)$ rad/sec.

4.6.1.1 STFT masking filter

First, we use the STFT masking filter defined in Section 4.3. The STFT masking function is given by

$$H_1(nT, e^{j\omega T}) = \begin{cases} 1 & \text{if } |\omega - 2\mu\pi t| < \dfrac{B_h}{2} \\ 0 & \text{otherwise} \end{cases} \tag{4.6.2}$$

where B_h is the filter BW. Equivalently,

$$h_1(nT,mT) = \frac{w(mT)}{\pi mT}\left[\sin(2\mu nT - \frac{B_h}{2})mT - \sin(2\mu nT + \frac{B_h}{2})\right] \tag{4.6.3}$$

We shall use a Kaiser window $w(mT)$ of $(2M + 1) = 55$ points and a bandstop attenuation of 30 dB.

To measure the performance of the filter we define the Noise Rejection Ratio (NRR) as the ratio of the power of the input noise $z_r(nT)$ to the power of the output noise $y_r(nT) - x_r(nT)$.

$$NRR = \frac{\sum_{n=50}^{150} (z_r(nT))^2}{\sum_{n=50}^{150} (y_r(nT) - x_r(nT))^2} \tag{4.6.4}$$

where $y_r(nT)$ represents the output of the STFT masking filter.

In Fig. 47, the noise rejection ratio for different input noise powers P_{win} and different filter Bandwidths B_h is shown. Clearly, in the case of high input signal to noise ratio, the best performance of the STFT masking filter is achieved when the BW of the spectrogram of the desired signal ($\simeq 0.1(2\pi)$) is used as the BW of the filter. It should be noted, however, that there is little or no noise rejection. This is so because the filter cannot pass the signal without distortion unless the filter BW is excessively large; i.e., when almost all the noise is passed.

In the case of low input signal to noise ratio, the output noise power can be made small if the filter BW is narrow enough, since in this case most of the noise power is suppressed; the overall output noise power may not be negligible since the filtering introduces significant signal distortion. The theoretical justification for using a narrow filter BW has been provided in [H3], and is related to the theory of time-varying Wiener filters [O3].

Figure 48 illustrates the performance of the filter when the input noise power is $P_{win} = 0$ dB, and $B_h = 0.045(2\pi)$ rad/sec. The original and filtered signals as well as the original and noise-corrupted signals are compared.

4.6.1.2 LNC filter

To use the LNC filter, one needs to compute the analytic version of the measured signal. To compute Hilbert transforms, we design a FIR Hilbert transformer by the window method using a Hamming window of 61 points. Using this transformer, the analytic part $x_i(nT)$ of the real noise-corrupted measured signal $x_{ri}(nT)$ is computed. The signal $x_i(nT)$ is fed into the LNC filter defined in Eq. (4.4.21),

$$h_2(nT,mT) = \frac{w(mT)}{\pi mT} \sin\frac{B_h mT}{2} e^{j2\mu nTmT - j\mu m^2T^2} \tag{4.6.5}$$

where $w(mT)$ is a Kaiser window of length $2M + 1 = 55$ points, and a stopband attenuation of 30 dB. Note that $\frac{1}{\pi mT} \sin\frac{B_h mT}{2} e^{j2\mu nTmT}$ is a bandpass filter having a BW B_h, and center frequency $2\mu nT$.

To assess the performance of the LNC filter, the NRR defined in Eq. (4.6.5) is used. The signal $y_r(nT) = Re\ y(nT)$ represents the real part of the output of the LNC filter. Fig. 49 shows the resulting NRR for different input noise powers and filter BWs. Clearly, this filter performs better than the previous one. In the case of high SNR , the LNC filter performs best when its BW B_h is equal to the BW of the OSWD.

Figure 50 illustrates the performance of the filter when the input noise power is $P_{win} = 0$ dB, for the optimal BW $B_h = 0.025(2\pi)$. The original and filtered signals as well as the original and noise-corrupted signals are compared.

4.6.1.3 *Sensitivity of the LNC filter*

To illustrate the sensitivity of the LNC filter to errors in the estimation of its defining parameters, we conduct the following experiment. Consider the signal $x_r(nT) = \cos(\nu nT + \mu n^2T^2)$, $20 \leq nT \leq 180$, considered in the previous section ($\mu = 0.002\pi$ and $\nu = 0$). Assume that the signal is known to be a linear chirp signal, but its parameters ν and μ are unknown and need to be determined in order to specify the LNC filter. To achieve this, we compute the spectrogram of the noise-corrupted signal $x_{ri}(nT) = x_r(nT) + z_r(nT)$, where $z_r(nT)$ is a real zero-mean white Gaussian noise of power density $P_{win} = 0$ dB. The NAF of the spectrogram is used to obtain an initial estimate $\overline{\Omega}(nT)$ of the instantaneous frequency of the desired signal. Using least square techniques, a straight line was fitted to the curve $\overline{\Omega}(nT)$ to obtain the approximation $\overline{\Omega}(nT) \simeq 2\hat{\mu}nT + \hat{\nu}$ where $\hat{\mu} = 0.00193\pi$ and $\hat{\nu} = 1.38 \times 10^{-4}\pi$.

Let us compare the performance of the LNC filter when the exact and estimated values of parameters ν and μ are used. The LNC filter is given by

$$h_2(nT,mT) = \frac{w(mT)}{\pi mT} \sin(\frac{B_h}{2} mT) e^{j\nu nT + j2\mu nT - j\mu m^2T^2} \tag{4.6.6}$$

First, we use the exact values of μ and ν to define the above LNC filter. This filter is used to filter $x_i(nT)$, the analytic version of $x_{ir}(nT)$. Since this is a case of low signal to noise ratio, we determine the optimal filter BW experimentally. It is given by $B_h = 0.031(2\pi)$, and the corresponding NRR is 12.46 dB. In contrast, using the estimates $\hat{\mu}$ and $\hat{\nu}$ yields a NRR of 11.8 dB, for the same BW $B_h = 0.031(2\pi)$. This is a reasonable degradation in performance. Note that if we use a larger BW, namely $B_h = 0.034(2\pi)$, the NRR can be improved to 11.93 dB. This is in agreement with the results of Section 4.4.2.

4.6.2 Separation of parallel linearly frequency modulated signals in the presence of noise

Next, we investigate the ability of the filter to separate closely-spaced linearly frequency modulated signals. Consider the two signals

$$x_r(nT) = \cos(\mu n^2 T^2) \ , \qquad 20 \leq nT \leq 180 \tag{4.6.7}$$

$$x_{r2}(nT) = \cos(\mu n^2 T^2 + 2\pi(0.1)nT) \ , \qquad 20 \leq nT \leq 180 \tag{4.6.8}$$

where $\mu = 0.002\pi$. Clearly, $x_2(nT)$ is a linearly frequency modulated signal similar to $x(nT)$ and parallel to it. We seek to isolate the signal component $x(nT)$ using the noise-corrupted measured signal

$$x_{ri}(nT) = x_r(nT) + x_{r2}(nT) + z_r(nT) \tag{4.6.9}$$

The desired signal $x_r(nT)$ is the same signal considered in the previous section. We shall use the STFT masking filter specified in Eq. (4.6.3) and the LNC filter specified in Eq. (4.6.5) to filter the desired signal.

To assess the performance of the filters, we modify the NRR defined in Eq. (4.6.4) such that the undesirable signal $x_2(nT)$ contributes to the input noise power; i.e.,

$$NRR = \frac{\sum_{n=50}^{150} (z_r(nT) + x_{r2}(nT))^2}{\sum_{n=50}^{150} (y_r(nT) - x_r(nT))^2} \tag{4.6.10}$$

where $y_r(nT)$ represents the real part of the signal at the output of the filters.

Fig. 51 illustrates the performance of the STFT masking filter and shows the resulting NRR for different filter BWs and input noise powers P_{win}. The NRR obtained through the LNC filter is shown on Fig. 53.

The performance of the STFT masking filter and the LNC filter for an input noise power of -10 dB is shown on Fig. 52 and Fig. 54. respectively. The BW of the STFT masking filter used to obtain Fig. 52 is $B_h = 0.095(2\pi)$ rad/sec. This BW should give the best performance for the specified input noise power as can be seen from Fig. 51. The resulting NRR is 11.5 dB.

The BW of the LNC filter used to obtain Fig. 54 is given by $B_h = 0.035(2\pi)$ rad/sec. This BW should give the best performance as can be seen from Fig. 53. The resulting NRR is 17.5 dB. The LNC filter performs better by 6 dB.

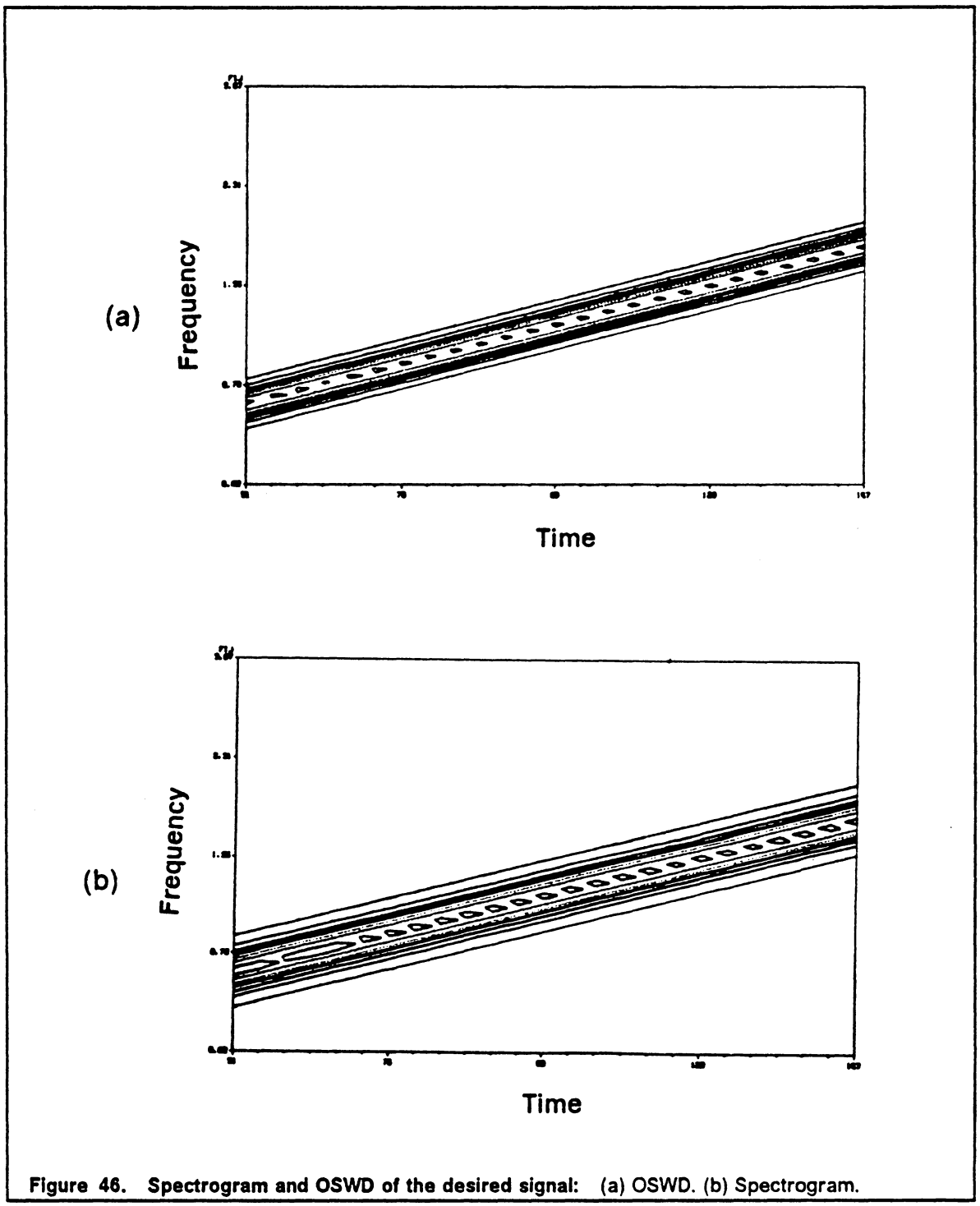

Figure 46. Spectrogram and OSWD of the desired signal: (a) OSWD. (b) Spectrogram.

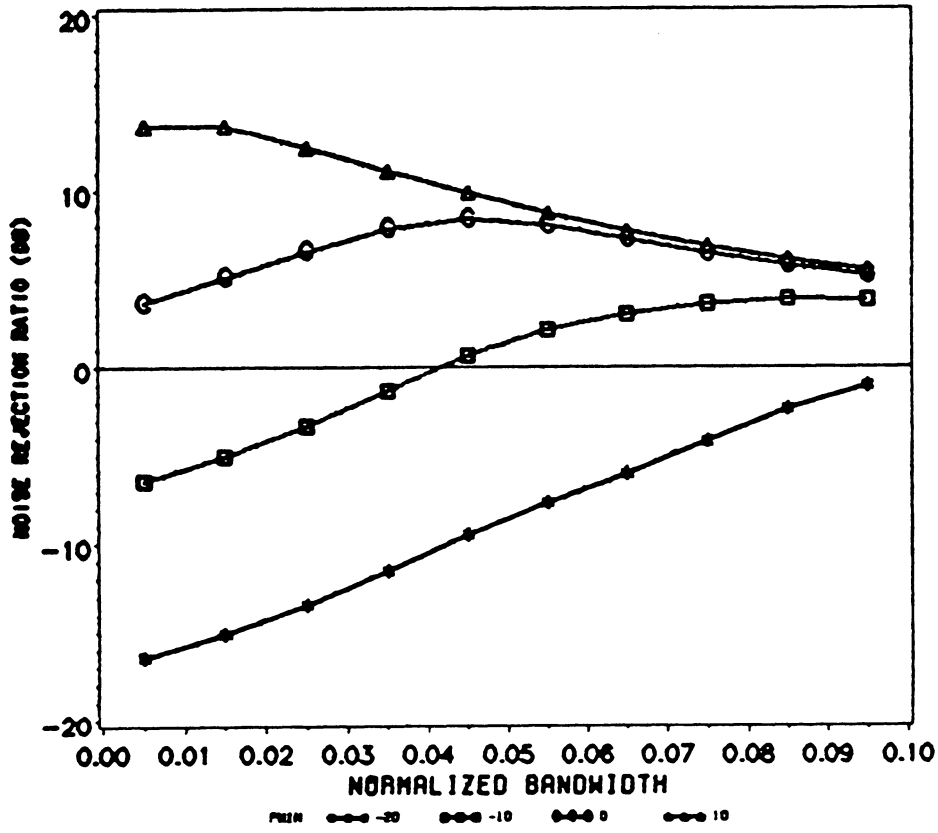

Figure 47. Suppression of white noise by the STFT masking filter: NRR is shown for different input noise powers and different filter BWs.

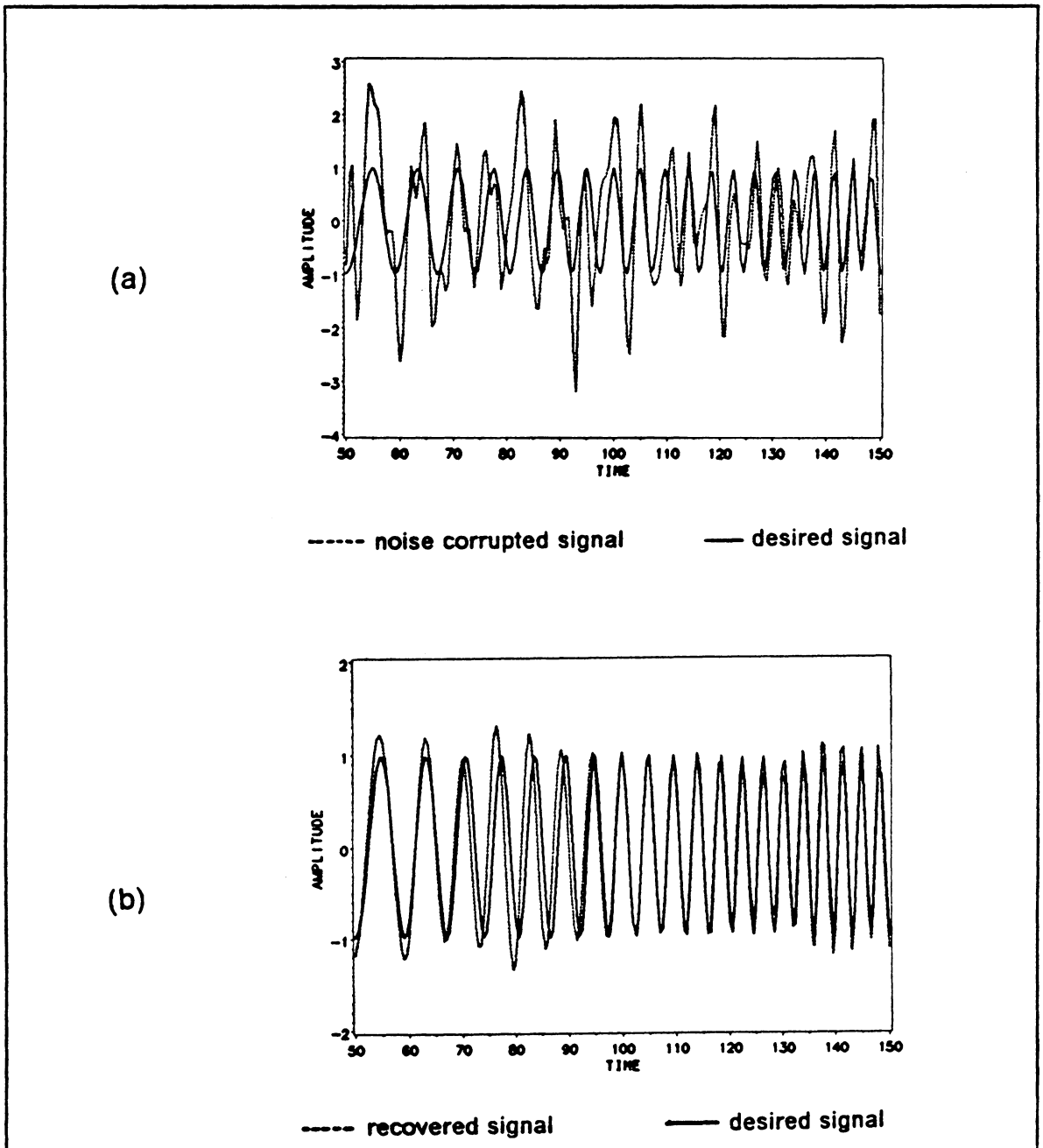

Figure 48. **Typical performance of the STFT masking filter in suppressing white noise:** $P_{win} = 0$ dB, $B_h = 0.045(2\pi)$ rad/sec, NRR = 8 dB. (a) noise-corrupted signal is compared to the desired signal. (b) filtered signal is compared to desired signal.

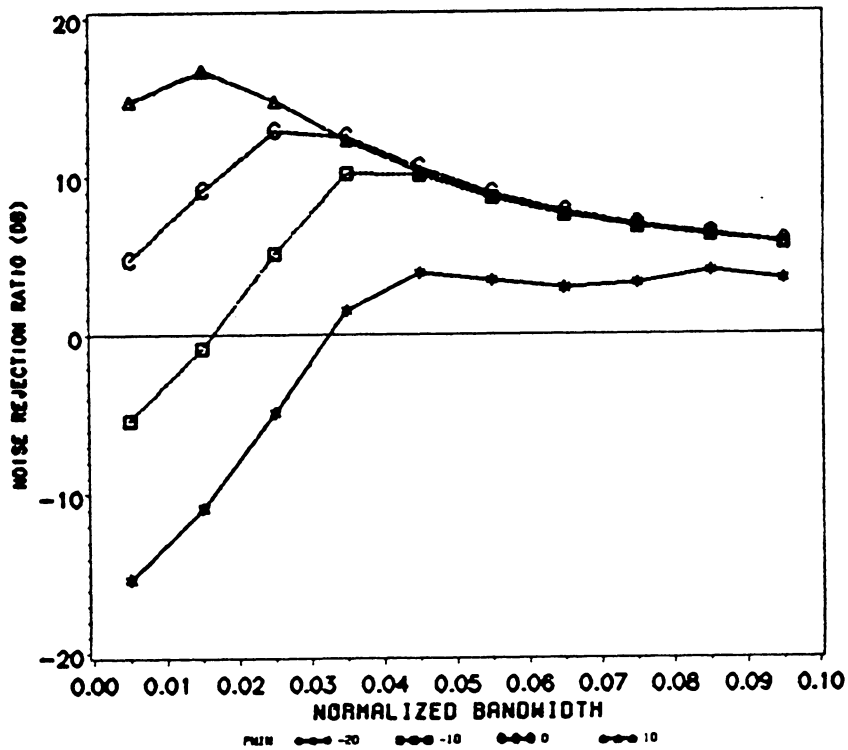

Figure 49. Suppression of white noise by the LNC filter: NRR is shown for different input noise powers and different filter BWs.

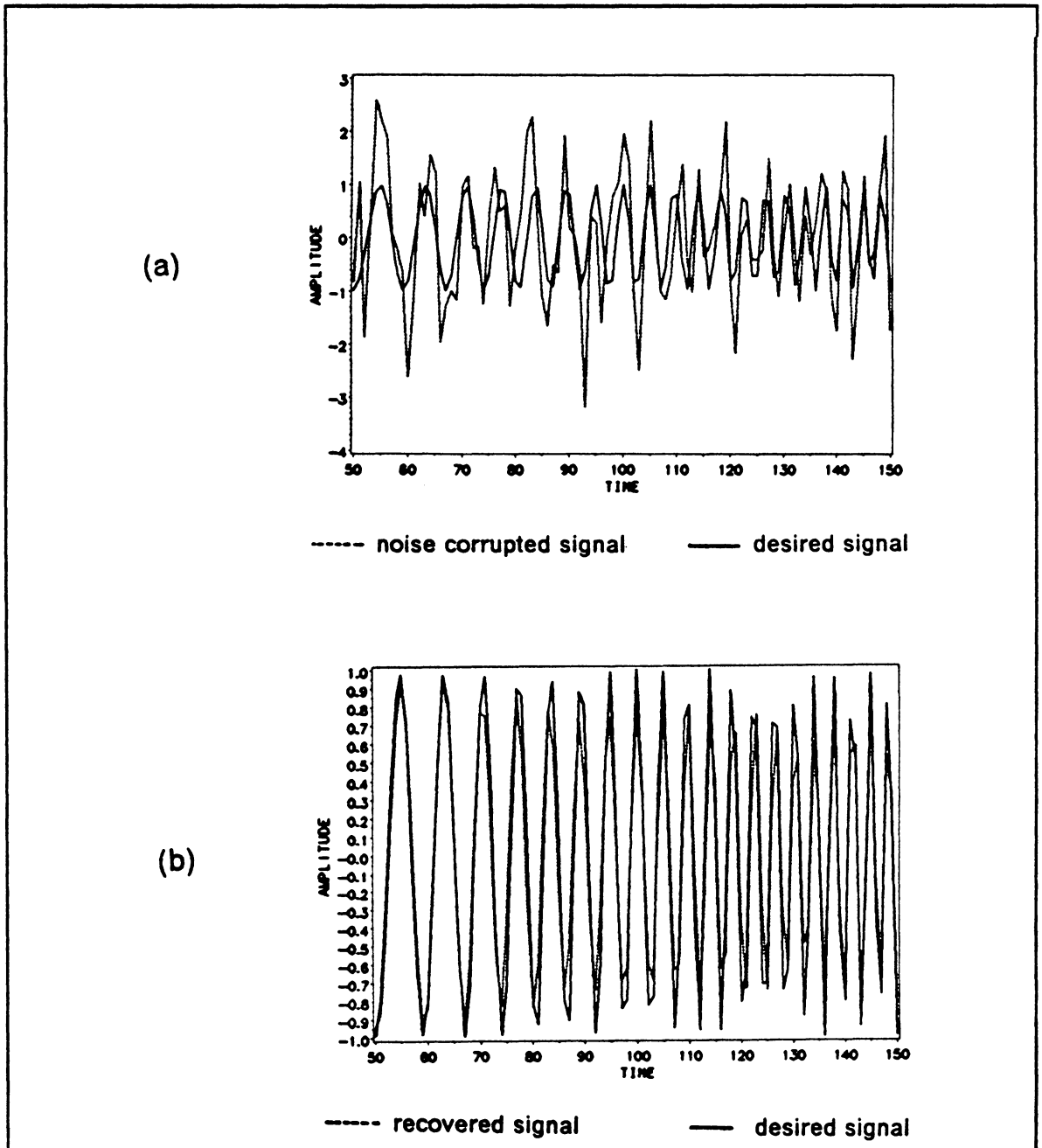

Figure 50. **Typical performance of the LNC filter in suppressing white noise:** $P_{win} = 0$ dB, $B_h = 0.025(2\pi)$ rad/sec, NRR = 13 dB. (a) noise-corrupted signal is compared to the desired signal. (b) filtered signal is compared to desired signal.

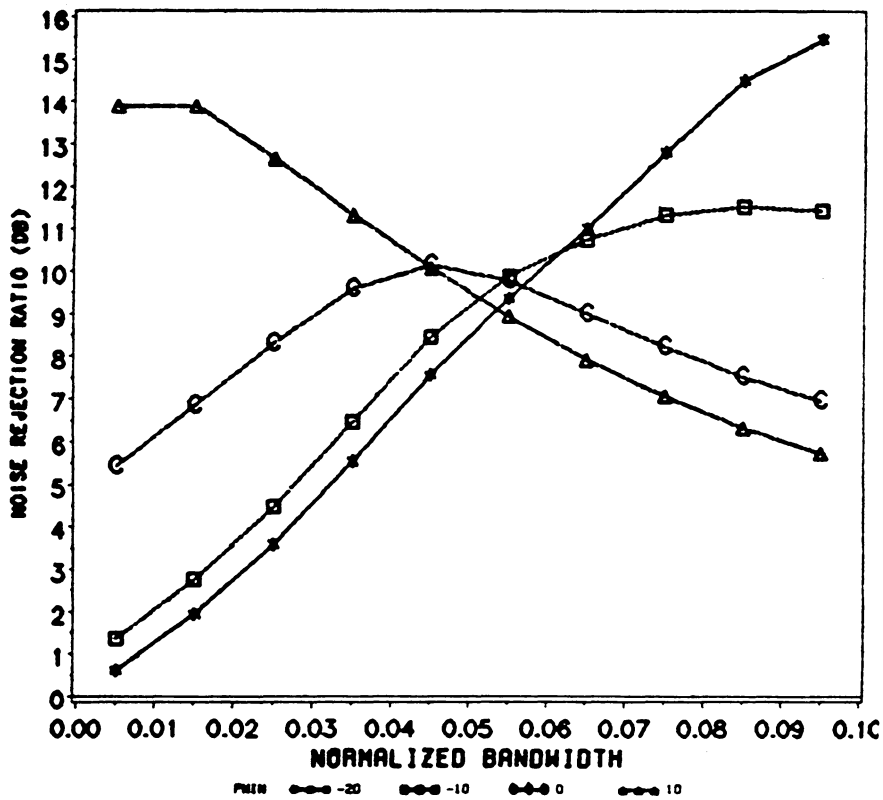

Figure 51. **Separation of linearly frequency modulated signals by STFT masking filter:** NRR is shown for different input noise powers and different filter BWs.

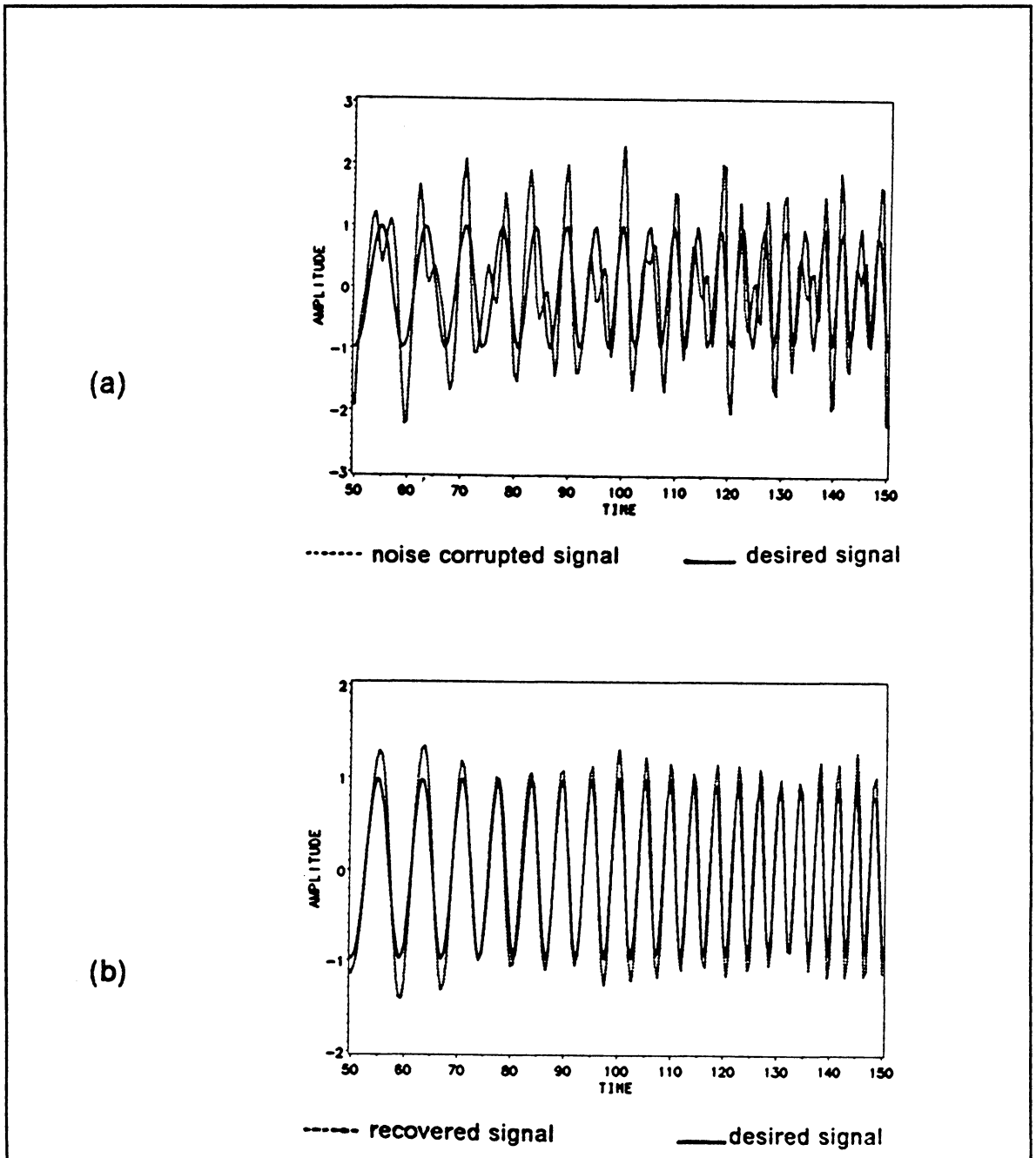

Figure 52. **Typical performance of the STFT masking filter in separating linearly frequency modulated signals:** P_{win} = -10 dB, $B_h = 0.095(2\pi)$ rad/sec, NRR = 11.5 dB. (a) noise-corrupted signal is compared to the desired signal. (b) filtered signal is compared to desired signal.

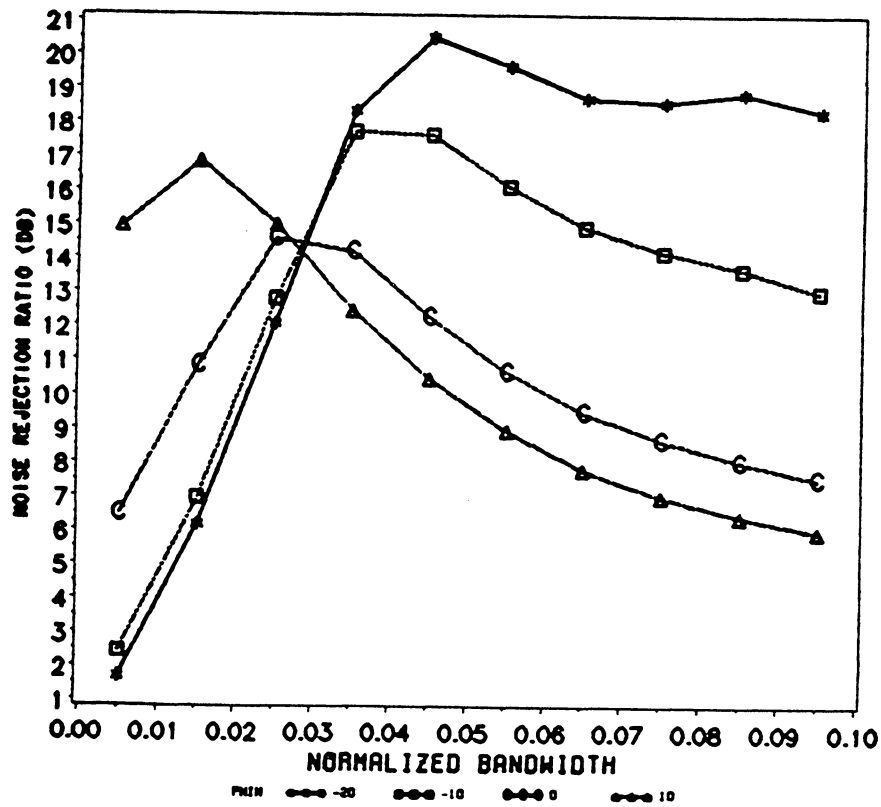

Figure 53. Separation of linearly frequency modulated signals by LNC filter.: NRR is shown for different input noise powers and different filter BWs.

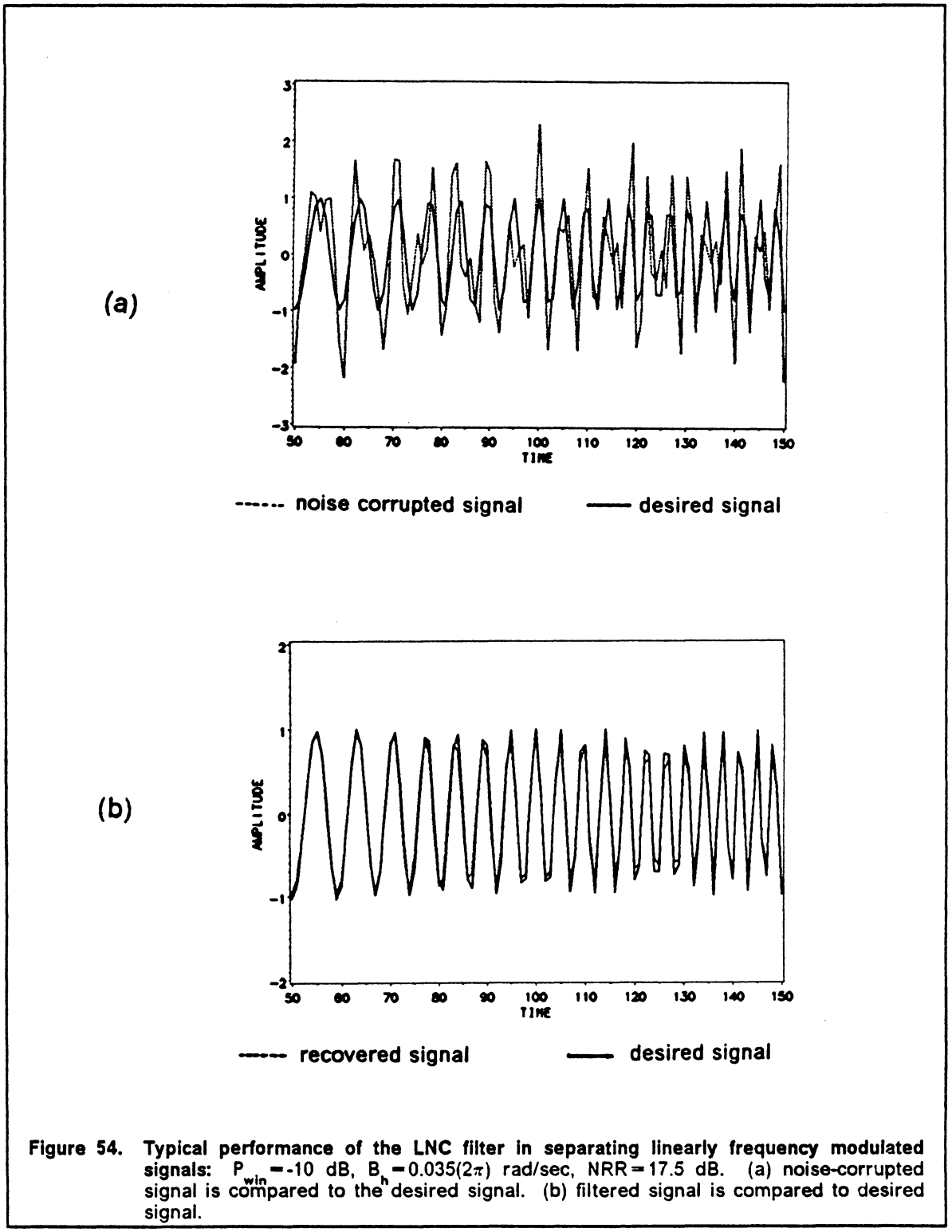

Figure 54. **Typical performance of the LNC filter in separating linearly frequency modulated signals:** $P_{win} = -10$ dB, $B_h = 0.035(2\pi)$ rad/sec, NRR = 17.5 dB. (a) noise-corrupted signal is compared to the desired signal. (b) filtered signal is compared to desired signal.

5.0 Conclusions

In this thesis we proposed a characterization of slowly time-varying signals formulated using short-time techniques. It is based on the idea that slowly time-varying signals are sophisticated but that windowing these signals results in less sophisticated signals, i.e., signals with smaller time-bandwidth or even elementary signals. This discussion has used and shown the relevance of modulation theory concepts, such as amplitude and frequency modulation. Two classical examples of time-varying signals, the linear chirp signal and the sinusoidally frequency modulated signals, were shown to have a reduced BW when windowed by a real Gaussian window. Chapter 3 further consolidated this idea by showing that, if a larger class of windows is considered (such as the complex window of the OSWD), the BW of the windowed signal can be reduced even more.

Chapter 3 considered the analysis of STV signals using MTFRs. A comparison of the different competing MTFRs showed that cross-terms, both internal and external, can present severe problems in the case of WD. The PWD suffers from the existence of internal cross-terms, but to a lesser degree. The cross-terms of the PWD cannot be eliminated unless very short windows are used, in which case the spectrogram and the OSWD become sharper. Our simulations show that the performance of the OSWD is the most acceptable one.

We also showed that generalized or extended short-time techniques (such as the OSWD) yield positive spectral representations of the signal which are at least as sharp as the PWD, but are free of cross-terms.

Another contribution of this thesis was to show that, although the OSWD was first derived and proven to be optimal in the case of constant amplitude signals, its advantages are not lost if the signals are amplitude modulated. These advantages include the OSWD minimal BW and the OSWD capability of yielding an exact value of the instantaneous frequency. In contrast, the NAF of the spectrogram can be a severely biased estimate of the instantaneous frequency of an amplitude modulated signal. The spectrogram usually has an unduly large BW. For a linear chirp signal, in which case the PWD does not have any cross-terms, the OSWD has the same BW as the PWD. Simulations have also shown that the OSWD is superior in separating parallel and closely spaced signal components.

The improvement achieved in using the OSWD is at the expense of calculating the analytic version of the signal, and of using additional information, namely, the derivative of the instantaneous frequency. This additional information, however, is not prohibitively diffcult to obtain. In fact, the derivative of the instantaneous frequency is also needed if one decides to compute the STFT with Storey's optimal length window. The problem of estimating the derivative of the instantaneous frequency, while the instantaneous frequency is not exactly known, has been addressed briefly but remains to be investigated fully.

Chapter 4 considered a LSV filter that is equivalent to masking the OSTFT (the STFT whose magnitude squared equals the OSWD). Unlike the derivation of the OSWD, which is based on the concept of minimum BW, and is formulated in the frequency domain, the filter was designed in the time-domain, using the concept of local nonstationarity cancellation. Note that although masking the OSWD and LNC filtering are equivalent, their interpretations are different, and the results proven in Chapters 3 and 4 are complementary. Seemingly, the time-domain formulation is more tractable, and several interesting results are found. The effect of errors in the estimates of the instantaneous frequency and its derivative is studied. It was shown that the effect of these errors can be alleviated by using a larger filter BW.

Conditions were derived under which two signal components can be separated without error. In case the slopes of the instantaneous frequencies of the two signal components are equal, the two components are separable if the difference between their instantaneous frequencies is larger than the sum of the BWs of the component signal envelopes. This is the best achievable result because it holds in the time invariant case. Moreover, the importance of having a minimum BW for the OSWD is motivated in Section 4.5.1.1. In case the signal is corrupted with noise, the LSV filter should have a minimum BW since the amount of noise or undesired signal component energy that can be suppressed, increases when the filter BW decreases.

6.0 References

[A1] J.C. Andrieux, M. Feix, G.Mourgues, P. Bertrand, B. Izrar, and T. Nguyen, 'Optimum Smoothing of the Wigner-Ville Distribution', *IEEE Trans. on Acoustics, Speech and Signal Processing*, Vol. ASSP-35, No. 6, pp.764-769, June 1987

[B1] B. Bouachache, P. Flandrin, 'Wigner-Ville analysis of nonstationary signals', Proc. ICASSP-82, Paris, France 1982, pp. 1329-1332

[B2] B. Bouachache, 'Wigner analysis of time-varying signals. An application in seismic prospecting', Proceed. EUSIPCO-83, Germany, pp. 703-706, 1983

[B3] E. Bedrosian, 'A product theorem for Hilbert transforms', *Proc. IEEE*, USA, Vol. 51, pp. 868-869, 1963

[B4] C. Berthomier, N. Cornilleau-Wherlin, 'Application de la notion de signal analytique et de la frequence instantanee d'un signal', *Ann. de telecomm.*, Vol.30, No. 7, pp.1-7, 1975

[B5] G.F. Boudreaux-Bartels, T.W. Parks, 'Time-varying filtering and signal estimation using Wigner distribution synthesis techniques', *IEEE Trans. on Acoustics, Speech and Signal Processing*, Vol. ASSP-34, pp.442-451, June 1986

[B6] G.F. Boudreaux-Bartels, T.W Parks, 'Wigner distribution analysis of acoustics well logs', private communication, 1987

[C1] T.A.C.M. Claasen, W.F. Mecklenbrauker, 'The Wigner Distribution-- A tool for time-frequency signal analysis, Part-I: Continuous-time signals', *Philips journal of research*, 35, No. 3, pp.217-250, 1980

[C2] T.A.C.M. Claasen, W.F. Mecklenbrauker, 'The Wigner Distribution-- A tool for time-frequency signal analysis, Part-II: Discrete-time signals', *Philips journal of research*, 35, No. 4/5, pp.276-300, 1980

[C3] T.A.C.M. Claasen, W.F. Mecklenbrauker, 'The Wigner Distribution-- A tool for time-frequency signal analysis, Part-III: Relation with other time-frequency signal transformations', *Philips journal of research*, 35, No. 6, pp.372-389, 1980

[C4] T.A.C.M. Claasen, W.F. Mecklenbrauker, 'On stationary linear time-varying systems', *IEEE Trans. on Circuits and Systems*, Vol. CAS-29, No. 3, pp.169-184, March 1984

[C5] G.K.C. Clarke, 'Time-varying deconvolution filters', *Geophysics* , Vol. 33, No. 6, pp. 936-944, Dec. 1968

[G1] R. Gendrin, P. Robert, 'Temps de groupe et largeur de bande des signaux modules simultanement en frequence et amplitude', *Ann. de Telecomm.*, Vol. 37, No. 7-8, 1982

[G2] R. Gendrin, C. de Villedary, 'Unambiguous determination of fine structures in multicomponent time-varying signals', *Ann. de Telecomm.*, Vol. 34, No. 3-4, pp. 122-130, 1979

[G3] L.J. Griffiths, 'Rapid measurement of digital instantaneous frequency', *IEEE Trans. on Acoustics, Speech and Signal Processing*, Vol. ASSP-23, p.207-222, 1975

[H1] N.C. Huang, J.K. Aggarwal, 'Synthesis and implementation of recursive linear shift-variant digital filters', *IEEE Trans. on Circuits and Systems* , Vol. CAS-30, pp.29-36, 1983

[H2] N.C. Huang, J.K. Aggarwal, 'A comparison between time- and frequency- domain techniques for time varying filtering', ICASSP-1982, Paris, France, pp.1341-1344

[H3] N.C. Huang, J.K. Aggarwal, 'Frequency domain considerations of LSV digital filters', Vol. CAS-28, No. 4, pp.279-287, April 1981

[H4] N.C. Huang, J.K. Aggarwal, 'On linear shift-variant digital filters', *IEEE Trans. on Circuits and Systems*, Vol. CAS-27, No. 8, pp.672-680, August 1980

[J1] L.W. Johnson, D.R. Riess, **Numerical analysis**, 2nd edition, Addison-Wesley, 1982

[K1] K. Kodera, R. Gendrin, C. de Villedary, ' Analysis of time-varying signals with small BT values', *IEEE Trans. on Acoustics, Speech and Signal Processing*, Vol. ASSP-26, No. 1, pp.64-76, Feb. 1978

[K2] K. Kodera, C. de Villedary, G. Gendrin, 'A new method for the numerical analysis of non-stationary signals', *Physics of the earth and planetary interiors*, Vol. 12, pp. 142-150, 1976

[L1] W. Li, 'Wigner distribution method equivalent to dechirp method for detecting a chirp signal', *IEEE Trans. on Acoustics, Speech and Signal Processing*, Vol. ASSP-35, No. 8, pp. 1210-1211, August 1987

[M1] A.I. Mees, **Dynamics of feedback systems**, John Wiley, New York, 1981

[M2] D. Munson, 'Minimum sampling rates for linear time-varying discrete time systems', *IEEE Trans. on Acoustics, Speech and Signal Processing* Vol. ASSP-33, No. 6, December 1985

[N1] A.H. Nayfeh, **Introduction to perturbation techniques**, John Wiley, New York, 1981

[O1] A.V. Oppenheim, W. Mecklenbrauker, R. Mersereau, ' Variable cutoff linear phase digital filters', *IEEE Trans. on Circuits and Systems*, Vol. CAS-23, No. 4, pp.199-203, April 1976

[O2] A.V. Oppenheim, R.W. Schafer, **Digital signal processing**, Prentice-Hall, 1975

[O3] S. Orfanidis, **Optimum signal processing : An introduction**, McMillan, New York, 1985

[P1] A. Papoulis, **Probability, random variables, and stochastic processes**, McGraw Hill, New York, 1984

[P2] A. Papoulis, **Signal Analysis**, McGraw Hill, 1977

[P4] S. Park, J.K. Aggarwal, 'Recursive synthesis of linear time-variant digital filters via Chebyshev approximation', *IEEE Trans. on Circuits and Systems* , Vol. CAS-32, No. 3, pp.245-250, March 1985

[P5] S. Park, J.K. Aggarwal, 'A simple form synthesis of a linear time-varaint digital filter via spectral decomposition of its impulse response', Journ. Franklin Institute, Vol. 318, No. 3, pp.151-164, 1984

[P6] B. Picinbono, W. Martin, 'Representations des signaux par amplitude et phase instantanees', *Ann. de Telecomm.*, Vol. 38, No. 5-6, pp. 179-190, 1983

[P7] M.R. Portnoff, 'Short-time Fourier analysis of sampled speech' *IEEE Trans. on Acoustics, Speech and Signal Processing*, Vol. ASSP-29, No.3, pp. 364-373, 1981

[P8] M.R. Portnoff, 'Time Frequency Representation of Digital Signals Based on Short Time Fourier Analysis', *IEEE Trans. on Acoustics, Speech and Signal Processing*, Vol. ASSP-28, No. 1, Feb 1980

[R1] L.R. Rabiner, B. Gold, **Theory and practice of digital signal processing**, Prentice-Hall,1974

[R2] S.O. Rice, 'Envelopes of narrowband signals', *Proceedings of the IEEE*, Vol. 70, No. 7, pp 692-699, July 1982

[S1] B.E. Saleh, N.S. Subotic, 'Time-Variant Filtering in the Mixed Time Frequency Domain', *IEEE Trans. on Acoustics, Speech and Signal Processing*, Vol. ASSP-33, No. 6, pp 1479-1485, December 1985

[S2] L.R.O. Storey, ' Investigation of whistling atmospherics'. *Phil. Trans. Roy. Soc.*, A246, pp.113-114, 1953

[S3] F.G. Stremler, **Introduction to Communication Systems**, 2nd edition, Addison-Wesley Publishing Company, 1982

[V1] Voelker H.B., 'Toward a unified theory of modulation, Part I : phase-envelope relationships', *Proceedings of the IEEE*, Vol 54, No. 3, March 1966

[Y1] K.-B. Yu, S. Cheng, 'Signal synthesis from Wigner distribution', ICASSP, pp.1037-1040, Tampa, Florida, June 26-27,1985

[Z1] L. Zadeh, 'Time varying networks : part I', *Proceedings of the IRE*, Vol. 49, pp.1488-1503, 1961

The vita has been removed from the scanned document